PHOTOSENSITIZERS FOR TUMOR FLUORESCENCE AND PHOTODYNAMIC THERAPY OF CANCER

PROEFSCHRIFT

TER VERKRIJGING VAN DE GRAAD VAN DOCTOR
AAN DE ERASMUS UNIVERSITEIT ROTTERDAM
OP GEZAG VAN DE RECTOR MAGNIFICUS
PROF. DR. C.J. RIJNVOS
EN VOLGENS BESLUIT VAN HET COLLEGE VAN DECANEN.
DE OPENBARE VERDEDIGING ZAL PLAATSVINDEN OP
DONDERDAG 6 MEI 1993 OM 13^{30} UUR

DOOR

Henricus Leonardus Louis Marie van Leengoed
Geboren 12 December 1956 te Roosendaal

PROMOTIE-COMMISSIE

Promotor:	Prof. Dr. J.F. Koster EUR
Co-Promotor:	Dr. W.M. Star
Overige leden:	Prof. Dr. J.H. Wilson EUR
	Prof. Dr. J.E. van Lier, Université de Sherbrooke, Canada
	Prof. Dr. J. van Steveninck, RUL

This study was made possible by a grant of the Dutch Cancer Society (grant DDHK 89-3). Funds for equipment were granted by the "Maurits and Anna de Kock Stichting", the "Nijbakker Morra Stichting" and the "Josephine Nefkens Stichting".

Publication was supported by grants from the Dutch Cancer Society and Lederle Nederland. Their support is greatfully acknowledged.

This study has been prepared at the Department of Clinical Physics of the Dr. Daniel den Hoed Cancer Center, Rotterdam, The Netherlands

Aan Jacqueline

Contents

Voorwoord

Het in dit proefschrift beschreven onderzoek werd verricht op de afdeling Klinische Fysica van de Dr. Daniel den Hoed Kliniek. Vanzelfsprekend kon dit werk slechts uitgevoerd worden met de hulp van velen waarvan ik enkelen speciaal wil bedanken.

Allereerst wil ik mijn promotor Prof. Dr. J.F. Koster en mijn co-promotor Dr. W.M. Star bedanken voor hun begeleiding bij het tot stand komen van dit proefschrift.

Willem je semantische nuchterheid en redactionele virtuositeit hebben in belangrijke mate bijgedragen tot verheldering van de tekst en de vormgeving van dit proefschrift. Ik ben je daarvoor veel dank verschuldigd. Een uitspraak als "dit is, naar ik aanneem, toch nog niet de definitieve versie van je stukje ?!" was voor mij altijd een grote aansporing om de draad weer op te pakken. Je enthousiasme, inzichten, suggesties en retorische vragen zal ik in Buffalo moeten ontberen.

Veel van het praktische werk is uit handen genomen door de analisten en niet alleen veel handen maar ook een goede sfeer maken het werk licht. Jeanne Versteeg wil ik hierbij bedanken omdat ze mij als fotodynamisch groentje heeft ingewijd in de experimentele aspecten van de fotodynamische therapie (PDT). Daarnaast wil ik haar opvolger Otto Speelman bedanken dat hij, wanneer nodig, zich zo gemakkelijk voor mijn karretje liet spannen. Maar mijn dank gaat vooral uit naar Nynke van der Veen, die samen met mij aan het project DDHK 89-3 van de Nederlandse Kankerbestrijding verbonden was. Zonder haar was ik waarschijnlijk nu nog fluorescentie opnames aan het uitwerken. Veel succes de komende vier jaar en bedenk het is gemakkelijker niet te publiceren dan niet te promoveren.....

Hans Marijnissen wil ik hierbij bedanken, voor de morele steun en verbondenheid als lotgenoot, maar vooral om zijn inbreng wat betreft de technische aspecten van het onderzoek. Ik hoop dat ze begrijpen wat ik bedoel als ik daarginds over "verloopbusjes" ga praten. Hugo van Staveren wil ik bedanken als collega en als medeforens met wie ik vele barre tochten naar het, voor amsterdammers, verre Rotterdam heb ondernomen. Als het nodig was zelfs staand in een streekbus.

Anneke van den Berg-Blok wil ik bedanken voor het fabriceren van vele van de kamertjes modellen waarop dit proefschrift steunt en ook voor het overdragen van haar kennis en ervaring aan Nynke. Na een begin van wankelen, vallen en opstaan staan we nu, ook dankzij jou op eigen benen.

Jan Nauta en Max Witjes, twee Groningse lotgenoten, wil ik bedanken voor hun kameraadschap in het onderzoek. Dankzij jullie vele vragen werd ik zelf een stuk wijzer wat betreft de PDT, maar tegelijkertijd ben ik ook een stuk zenuwachtiger geworden voor tandartsen.

Onderzoek doen is vaak improviseren en dat is ook mogelijk geworden door de hulp van ondersteunende diensten zoals de instrumentmakerij, de elektronica afdeling en de dienst computerondersteuning (Beter bekend als Pc & N). Als iets onbetaalbaar was, gewoon niet bestond of niet wilde passen kon ik altijd en als het echt moest onmiddellijk bij jullie terecht. Ik ben jullie: Henk Elderhorst, Aad Melis, Dick van Sluis, Wim Lamprecht, Adrie Bot, Aad van der Heiden en Sylvia Verhoef daarvoor zeer erkentelijk.

Ik wil hierbij ook Hans Vuik, Sten Sliwa, Dennes van der Wal en Majo Polak van de afdeling medische fotografie bedanken voor hun hulp en geduld bij het maken van de mooie opnames die ik heb kunnen gebruiken voor presentaties, artikelen en dit proefschrift.

Het onderzoek is vooral mogelijk geworden doordat nieuwe "stofjes" beschikbaar gesteld werden. Daarvoor ben ik met name Johan van Lier, Hans Schuitmaker, Giullio Jori en Vincenzo Cuomo zeer dankbaar.

Van deze mensen gaat mijn dankbaarheid in het bijzonder uit naar Johan van Lier. Niet alleen omdat hij mijn grootste "dealer" was, maar in het bijzonder omdat ik hem mag beschouwen als de teweegbrenger van mijn buitenlandse avontuur. Ik hoop dat we in de toekomst elkaar nog vaak tegen zullen komen, zowel op het wetenschappelijke als het persoonlijke vlak.

Veel mensen zal ik vergeten zijn met name te noemen, zoals daar zijn alle medewerkers van de afdeling klinische fysica en instrumentatie (die mij als buitenbeentje in hun midden getolereerd hebben), maar ik ben ze daarom niet minder erkentelijk.

Jacqueline, jij haalde me over om te gaan promoveren en om dat te bereiken heb je me telkens weer weten te motiveren door te gaan, met dit boekje als resultaat. Aan jou draag ik dit proefschrift op.

Eric van Leengoed
Amsterdam, 24 februari 1993

Chapter 1

Introduction

A major task for cancer research lies in the development of tumor specific drugs. Usually, toxicity of a drug towards normal tissue is a limiting factor for therapy. In photodynamic therapy (PDT) the situation is different. Here, a photosensitive dye is administered which is retained by the tissue and after an interval of 24-48 h is activated by light of appropriate wavelength and dose. Photosensitizing dyes have the advantage that in contrast to conventional cytostatic drugs they can be selected to be nontoxic in the absence of light. Although certain organs such as liver, kidney and spleen may retain high levels of photosensitive drug, little toxicity is expected as long as these organs remain shielded from light. Another advantage of PDT over conventional types of therapy is its dual selectivity. First, some selectivity is obtained by enhanced localization of the photosensitizer in tumor tissue compared to normal tissue. Secondly, photodynamic damage can be restricted by restricting the irradiated area.

Already at the beginning of the century photodynamic effects on tumor tissue were reported for fluorescent dyes like eosin, acridine orange, and porphyrins. Skin tumors treated topically with eosin and irradiated with a high light dose, sometimes showed tumor regression (von Tappeiner and Jesionek, 1903).

The actual development of PDT was initiated in the sixties by the work of Lipson and Schwarz. During a study to explore the localizing properties of hematoporphyrin in neoplastic tissue, a drug called hematoporphyrin derivative (HPD) was prepared by Schwarz. Lipson (1961) demonstrated that following systemic administration of this preparation, experimental rat tumors could be detected by exciting HPD fluorescence with violet light. However, already in 1913, skin photosensitivity induced by a systemic administration of hematoporphyrin was recognized. Meyer-Betz (1913) became famous as he was the first to describe the effects of skin photosensitivity after he had administered hematoporphyrin to himself. Exposure to sunlight one day later resulted in severe erythema and oedema. This skin photosensitivity lasted for several weeks.

The therapeutical applications of PDT became the main subject of investigation as it appeared impractical to administer HPD and induce long term skin photosensitivity just for tumor localizing purposes.

The development of suitable light sources such as lasers lead to a renewed interest in the therapy. The work of Dougherty et al. (1978) stimulated a

worldwide and still increasing interest in experimental and clinical research on photodynamic therapy. At present many thousands of patients have been treated with encouraging results.

HPD is a complex mixture of porphyrins and contains hematoporphyrin, hydoroxyethylvinyldeuteroporphyrin, protoporphyrin and a hydrophobic fraction that localizes in tumor cells. The preparation procedure of HPD is critical and can be a source of variation in the final composition of the drug (Dougherty, 1982). The hydrophobic fraction, consisting of oligomers linked by ethers and/or esters, appears to be responsible for the therapeutic effect of HPD (Dougherty *et al.*, 1984; Kessel, 1986). Another problem is that light of 630 nm wavelength, which is used clinically to activate the photosensitizer, has only a limited depth of penetration. This restricts the tumor volume that can be effectively treated. Finally, HPD causes temporary skin photosensitivity. These drawbacks of HPD have stimulated a search for better photosensitizers for tumor localization and PDT.

Photodynamic therapy

Photodynamic therapy is based on the dye-sensitized photooxidation of biological matter in the target tissue (Foote, 1990). The dye (sensitizer) is administered to the organism and after a certain time an optimum ratio between photosensitizer concentration in tumor and normal tissue is reached. The tissue containing the dye is then exposed to high dose of light of a wavelength that corresponds with an absorption maximum of that dye. Following the absorption of light, the sensitizer is transformed from its ground state (singlet state) into an electronically excited state (triplet state) via a short-lived excited singlet state. The excited triplet can undergo two kinds of reactions. It can react by electron transfer with a substrate to form radicals and radical ions, which after interaction with oxygen can produce oxidized products (type I reaction). It can also transfer its energy to oxygen directly to form singlet oxygen, a highly reactive, oxidative species (type II reaction) (Foote, 1990; Moan, 1990). These oxidized products can lead to cellular damage and eventually tissue destruction. From the above it is evident that PDT effects are oxygen dependent so that tissue oxygenation levels play a significant role in PDT treatment effectiveness (Bown *et al.*, 1986).

To date patients with a variety of malignancies that are accessible to light application have been treated by PDT. In the beginning, recurrences or metastases in the skin and in easily accessible body cavities (mouth, vagina) were treated by PDT (Forbes *et al.*, 1980; Wile *et al.*, 1984a; Ward *et al.*,

1982). Later, endoscopic applications were developed for PDT of bladder, lung and oesophagus (Benson *et al.,* 1983; Cortese and Kinsey, 1982; Hayata *et al.,* 1984c; McCaughan *et al.,* 1985). A large number of patients, mostly with lung cancer, have been treated by the group of Hayata et al. and they concluded that the best results were obtained in treating small (< 1-2 cm) or superficial tumors (Hayata *et al.,* 1984a; Hayata *et al.,* 1984b; Hayata *et al.,* 1984c). Larger or nonsuperficial tumours probably need to be treated interstitially, using multiple fiber afterloading techniques (Marijnissen *et al.,* 1992). Although in a few cases interstitial PDT has been applied clinically, this approach is still in a developmental stage.

Photosensitizers

First generation

HPD can be regarded as a first generation photosensitizer. It was introduced for clinical therapy in 1976 at Roswell Park Memorial Institute by Dougherty (1978). At present a refined form of HPD is available which has been enriched in the photodynamically active fraction (trade name Photofrin II or simply Photofrin®).

HPD has attractive properties: tumor localization, photodynamic activity and low toxicity. However, as stated above, HPD is not a single compound but a mixture of porphyrins and their aggregates. Porphyrins which are both monomeric and hydrophillic, show high fluorescence upon excitation but do not localize in the tumor cell and appear not to be photodynamically active *in vivo* (Kessel and Chou, 1983). The hydrophobic dimers and oligomers do localize within the tumor cell but fluoresce only weakly. The fact that a fraction of HPD localizes in a tumor therefore does not directly imply that the tumor will also show fluorescence. Specific localization of the drug is not limited to tumor tissue alone. Skin and components of the reticuloendothelial system (e.g. liver, spleen and macrophages) also accumulate significant amounts of the photosensitizer. Experimental tumors growing in liver for example are known to retain less HPD than the surrounding normal tissue (Gomer and Dougherty, 1979; Bugelski *et al.,* 1981)

Therapeutically favourable ratios of porphyrin concentration may be due to several mechanisms:

1. The clearance of hydrophobic porphyrins from the tumor tissues usually occurs at a slower rate than from most healthy tissues, possibly due to a reduced lymphatic drainage (Dougherty, 1987).
2. Increased receptor mediated transport of HPD to the cells. Proliferating cells often have a high expression of low density lipoprotein (LDL) receptors. This

favours the uptake of LDL-bound porphyrins in larger amounts by tumor cells than by normal cells (Jori, 1992).
3. Transfer of porphyrins from plasma to the interstitial space, facilitated by greater permeability of tumor vessels for porphyrin carrying macromolecules.

In order to be activated a photosensitizer must absorb light. The wavelength at which a photosensitizer can be activated is determined by its absorption spectrum. 630 nm is the wavelength commonly used in clinical PDT with porphyrins since this corresponds with the longest wavelength absorption peak of HPD. Although shorter excitation wavelengths can have a higher absorption, the limited depth of penetration at these wavelengths allows only treatment of very superficial lesions. The absorption spectrum does not have to be the same as the action spectrum of a photosensitizer. *In vivo*, it appears that a 5 nm blue shift occurs in the action spectrum of HPD so that the excitation wavelength should actually be 625 nm (Star *et al.*, 1990).

Second generation

The search for second generation photosensitizers is intended to overcome the negative aspects of HPD. Instead of being mixtures like HPD or Photofrin®, second generation photosensitizers should be single compounds. They should show a relatively high uptake or retention in tumor tissue and have a high absorption of light at a wavelength where tissue penetration is high (Fig. 1). This way a maximum tissue volume can be treated. Finally, they should fluoresce in their monomeric state so that fluorescence indicates the presence of dye that is also photodynamically active (MacRobert *et al.*, 1989).

HPD induced skin photosensitivity is caused by the long retention of HPD in the skin in combination with the strong absorption of violet light. When a photosensitizer is used for tumor fluorescence alone, skin photosensitivity should be avoided. This can be realized by choosing a photosensitizer that:
1. Has no photodynamic activity, and/or
2. Is quickly cleared from the body, and/or
3. Has only limited retention in normal skin, and/or
4. Has an absorption spectrum of which the major peaks do not overlap with the solar emission spectrum.

For photodynamic therapy the same possibilities apply except (1) because the quantum yield for photodynamical activity should be high.

The photosensitizers that are discussed in this thesis satisfy one or more of the conditions described above. Conditions 1 and 2 may be satisfied by Uroporphyrin I, for which tumor retention (El-Far and Pimstone, 1986) but no biological activity (Nelson *et al.*, 1986) were reported. Acridine red also belongs

to this category. This dye; which actually is a pyronine and not an acridine (Lillie, 1977) is used for fluorescent labelling of blood platelets in microcirculation research (Star *et al.*, 1985). Conditions 3 and 4 are to a certain extent satisfied by phthalocyanines and bacteriochlorine *a* (Fig. 1). These dyes, however, have a strong tendency to aggregate in an aqueous environment which renders them inactive.

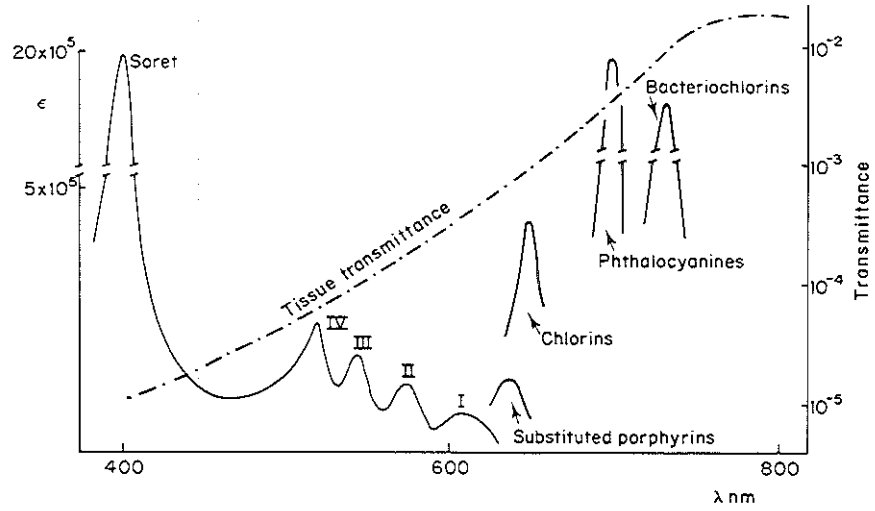

Figure 1. Diagrammatic representation of the absorption spectrum of a typical metal free porphyrin, and of the modifications caused by various structural changes in relation to the transmittance of 1 cm of human tissue (redrawn after Bonnet and Berenbaum (1989))

In order to overcome aggregation and precipitation, the molecule has to be chemically modified, or delivery systems such as liposomes must be used. The consequences of these modifications on fluorescence pharmacokinetics and photodynamic activity will be discussed in this thesis.

A new development in photosensitizer delivery is to administer a precursor that by itself is not a photosensitizer but causes individual (tumor) cells to generate their own photosensitizer. This approach, using an endogenous photosensitizer instead of an exogenous one, is also discussed.

In vivo model system

The studies reported in this thesis were performed *in vivo* on skin fold chambers with a transplantable tumor growing in subcutaneous tissue of the rat. The

model has been developed by Reinhold (1979) for the study of tumor microvasculature. It also proved to be useful for the study of the vascular effects resulting from PDT treatment (Star *et al.*, 1986).

The skin fold chamber contains a 0.5 mm thick layer of subcutaneous tissue of the dorsal skin placed between two transparent covers, one of which can be removed to permit the insertion of tumor tissue (approximately 1 mm^3). Most of the experiments were performed with a transplantable mammary carcinoma.

During the entire experimental procedure the animals were kept in a temperature controlled (32°C) cabinet. The elevated temperature ensures adequate tumor growth in the chamber. The ambient light level inside the cabinet was reduced to less than 30 $\mu W/cm^2$, providing the animals with a proper day/night cycle without causing observable photosensitization.

When the chamber is placed under a microscope, the veins, arteries and the capillary beds of subcutis and tumor tissue can be observed, at low magnification. In this way the fluorescence kinetics in blood vessels, tumor and subcutaneous (normal) tissue of the chamber following i.v. administration of a fluorescent dye can be monitored (van Leengoed *et al.*, 1990). During and after the delivery of a treatment light dose the effect of the therapy on the vasculature can also be determined. A typical sequence of severe vascular effects resulting from PDT starts with arterial spasm followed by ischaemia (blanching of the tumor) and a reduction of the red blood cell column diameter in the larger venules. The tissues of the chamber become hyperaemic due to the dilatation of the capillaries which appear packed with red blood cells. Stasis in the larger vessels, which is usually preceded by thrombus formation will also occur. After treatment extravasation of blood, especially in the tumor area is sometimes observed. If these vascular effects are maintained over a period of more than one day, tissue necrosis can occur. When the vascular effects are less severe, the larger vessels usually remain functional and the capillary bed of the tissues will recover from the effects of therapy.

Fluorescence localization

The advantage of tumor detection by photosensitizer induced fluorescence is the possibility to recognize small occult tumors and/or determine the "extent" of the disease. Especially tumors that progress from carcinoma in situ, like bladder tumors, or which can occur multifocally can be detected using fluorescence (Benson *et al.*, 1982).

When excited with violet light, the salmon red fluorescence of HPD in tumors can be observed with the naked eye. The fluorescence can also be recorded

using a (photo)camera and a filter that blocks the excitation light. Detection methods like these require relatively high levels of excitation light intensity to make the fluorescence observable. Consequently, the excitation light may cause undesired photodynamic damage to tissues under investigation. It is therefore recommended to use intensified video cameras for fluorescence detection.

In order to access body cavities for tumor localization, several types of fluorescence endoscopes have been developed. Non-imaging instruments have been described by Kinsey (1980) and Lin (1984). With these systems the fluorescence signal is detected during white light endoscopy. The tissue is alternately illuminated with white light and with fluorescence excitation light. The intensity of the fluorescence signal of HPD is converted into a sound with a certain pitch. Tissue autofluorescence levels can distort the detection of HPD fluorescence. Autofluorescence is emitted by naturally occurring fluorochromes and its intensity increases with decreasing excitation wavelength. This problem was recognized by Aizawa (1984) who reported on a system that analyzed and displayed the fluorescence spectrum, making it possible to distinguish the characteristic HPD fluorescence emission spectrum from the background autofluorescence spectrum. HPD fluorescence could also be distinguished from autofluorescence by improving the contrast using digital substraction of fluorescence images recorded with different emission wavelengths (Profio *et al.*, 1986), by using multicolor imaging and contrast enhancement (Andersson *et al.*, 1987) and even with the help of intensified colour imaging (Brodbeck *et al.*, 1987). Another technique is based on the fact that autofluorescence does not vary much between two excitation wavelengths provided they are not too far apart. HPD fluorescence on the other hand, has distinct excitation maxima. The image recorded at a wavelength where there is no HPD fluorescence excited can then be subtracted from an image where HPD fluorescence is excited using an excitation wavelength close to the first one. A system like this has been described by Baumgartner (1987) and seems to be very sensitive.

All fluorescence localization systems mentioned above were designed for the excitation and detection of HPD fluorescence using fixed excitation wavelengths around 400 nm. However, HPD also has fluorescence excitation maxima at 500 nm and at 625 nm (Gijsbers, 1986). New photosensitizers that are being developed as alternatives for HPD and Photofrin® have different qualities regarding their fluorescence excitation and emission. The study of the fluorescence properties of fluorescent dyes therefore requires a flexible fluorescence excitation and detection system.

Fluorescence detection system

In order to study the fluorescence pharmacokinetics a fluorescence detection system has been built and currently the fluorescent properties of photosensitizers can be studied on a routine basis. The system that was first used consisted of an expanded low power laser beam exciting the dye in the skin fold chamber (Fig 2A). The resulting fluorescence was then detected through a high pass filter by an intensified charge coupled device (CCD) camera. Currently, the excitation light is obtained from an arc or a halogen lamp and the wavelength can be chosen using a range of filters. Dual wavelength excitation can be performed simply by exchanging filters (Fig. 2(3)). The excitation beam has been coupled into the optical path of the detection system by means of a dichroic mirror (Fig. 2B). In this way excitation light reflected by the chamber or the tissue in the chamber cannot reach the emission filter. This is important because this excitation light may cause fluorescence in the emission filter, which may disturb the tissue fluorescence image. With the aid of image processing, average grey scale values of areas of interest in the image can be calculated.

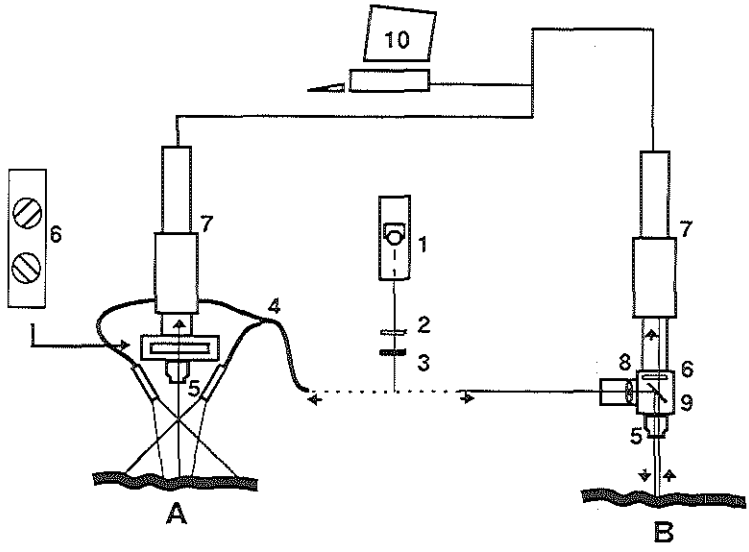

Figure 2. Schematic representation of the first (A) fluorescence detection system and the present one (B) which uses a dichroic mirror and excitation and detection filters. (1) Light source, (2) heat reflecting mirror, (3) revolving filter wheel with excitation filters, (4) Y-fibre, (5) Leitz Photar lens, (6) high pass filter, (7) CCD camera with image intensifier, (8) lens, (9) dichroic mirror, (10) computer with frame grabber and imaging software.

It is even possible to correct these values for fluctuations in the excitation light intensity and for nonuniform spatial response of the optical system using simultaneously recorded reference images made of coloured plastic sheets.

Therapy

Tumor destruction following PDT is a consequence of specific damage by reactive oxygen species resulting in both direct tumor cell death and blood vessel stasis. This blood flow stasis is largely responsible for the definitive tumor destruction after PDT (Star *et al.,* 1986; Fingar *et al.,* 1988; Henderson and Fingar, 1987).

A unique quality of fluorescent dyes that can be exploited during therapy is the fact that porphyrins (Photofrin®) as well as phthalocyanines are photobleached (photodegraded) by their own photochemical reaction (Henderson *et al.,* 1985; Moan, 1986). This phenomenon can be exploited to increase the therapeutic ratio of PDT. The drug dose should be chosen so low that during the irradiation the dye concentration in the normal tissue will rapidly be exhausted. The effect of a longer irradiation will not increase normal tissue damage whereas the higher sensitizer concentration in tumor tissue can still be activated to cause tumor necrosis.

Cellular effects

Direct cell kill as a result of PDT is caused by damage to the plasma membrane (Boegheim *et al.,* 1987) and mitochondria (Hilf *et al.,* 1986), but also other cellular structures such as lysosomes and microsomes can be damaged. Due to the short life-time of singlet oxygen (the main cytotoxic agent of PDT) it probably reacts at the site where it was formed (Bachowski *et al.,* 1991), which follows the dye as it shifts from a membrane localization to a cytoplasmatic localization as a function of time after administration.

The consequence of photodynamic cellular damage is a rapid loss of cell integrity. Associated with such cellular damage is the release of inflammatory and immune mediators (Henderson and Dougherty, 1992). These substances are potent, fast acting and vasoactive and probably relate to the PDT induced vascular damage discussed below.

The role of direct tumor cell kill is of secondary importance. When tumor cells were removed immediately following therapy, cell clonogenicity was not affected by the irradiation (Henderson *et al.,* 1985). Decrease of clonogenicity using the explant technique was only observed when the tumor was left *in situ* for a few hours after therapy.

Vascular effects

PDT mainly acts by destroying (tumor) vasculature (Star *et al.,* 1986; Selman *et al.,* 1984; Fingar *et al.,* 1988; Henderson and Fingar, 1987). After administration photosensitizers are mostly found in the perivascular stroma (Bugelski *et al.,* 1981) and around blood vessels (Carpenter *et al.,* 1977; Peng *et al.,* 1991a) Therefore, it is to be expected that endothelial cells in the vessel walls are damaged by PDT (Berenbaum *et al.,* 1990). The damage which has been directly observed (Star *et al.,* 1986), occurs already early during light treatment and is characterized by vessel constriction and platelet aggregation. These vascular effects will lead to blood flow stasis (Henderson and Fingar, 1987) which causes hypoxia and deprives the tissue of vital nutrients. It is very difficult to distinguish direct and indirect effects resulting from therapy.

PDT leads to mast cell degranulation, release of clotting factors and other mast cell derived mediators (Kerdel *et al.,* 1987). For instance, histamine is released which is a powerful vasodilator which increases the capillary permeability, allowing leakage of fluids and proteins into the tissue. This can explain the edema that is observed after PDT. Histamine also induces the release of von Willebrand Factor from endothelial cells exposed to Photofrin® and sublethal doses of light (Foster *et al.,* 1991). This factor mediates platelet adhesion to the vascular subendothelium. Changes in permeability and vasoconstriction during PDT are caused by serotonin and also cyclooxygenase products including thromboxane (Reed *et al.,* 1989; Fingar *et al.,* 1992).

As was stated before PDT effects are oxygen dependent. The vascular effects determine how much oxygen is available during light treatment and therefore influence the amount of direct killing of tumor cells. In a hypoxic environment cells appear protected from further PDT damage. Tumor oxygenation should be maintained during therapy therefore it is important to understand the mechanisms that causes these vascular effects.

As it appears to be impossible to directly kill all tumor cells with HPD-PDT, nutritional resupply to remaining viable tumor cells should be prevented. It is therefore probably necessary to "sterilize" a margin of normal tissue vasculature about the tumor (Fingar and Henderson, 1987).

Scope of this thesis

Photosensitive dyes have great interest because of the attractive combination of fluorescence imaging and photochemical destruction of tumors. When detected early, tumors are more easy to treat, usually respond better to treatment and there is a reduced risk of spreading of the disease. If a reliable fluorescence

detection technique were available it could be possible to "screen", on a routine basis, people who are at risk for developing a tumor.

Drawbacks of photosensitizers like HPD and Photofrin® such as prolonged skin photosensitivity and low absorption at clinically relevant wavelengths lead to the search of new photosensitizers. A number of fluorescent dyes have been proposed as second generation photosensitizers. In this thesis 13 administered dyes and one endogenously generated dye will be discussed with respect fluorescence pharmacokinetics and photodynamic activity. An *in vivo* skin fold chamber model was used to study these properties.

Chapter 2 discusses aspects of fluorescence pharmacokinetics of 5 fluorescent dyes: HPD, Photofrin II (Ph II), Up I, AR and AlPhcTS. HPD and Ph II are photosensitizers that currently undergo clinical evaluation (presently Ph II is known as Photofrin®). Uroporphyrin I (Up I) and acridine red (AR) are hydrophillic dyes which appear photodynamically inactive but which might have tumor localizing qualities. Finally, aluminum phthalocyanine tetrasulphonate (AlPhcTS), a commercially available phthalocyanine mixture studied as a potential "second generation" photosensitizer. Because of improved photosensitizer qualities with respect to wavelength absorption and skin photosensitivity, phthalocyanines have been investigated more in detail in Chapters 3, 4 and 5. In an aqueous environment phthalocyanines have a tendency to aggregate and become inactive. In order to render them more hydrophillic, sulphonate groups can be added to the molecule. Chapter 3 describes the fluorescence pharmacokinetics of six phthalocyanines differing in central metal ion and degree of sulphonation. The photodynamic activity, especially the vascular effects of these six dyes are investigated in Chapter 4. A different approach in administering hydrophobic dyes is to use liposomes as a delivery system. In Chapter 5 zinc phthalocyanine administered in this way has been studied. In Chapter 6 bacteriochlorine *a* (BCA) is studied for its photosensitizing properties. This dye has an absorption maximum at 760 nm. It therefore can be excited for therapy at a wavelength where tissue penetration of light is about twice that at 630 nm used for porphyrin activation. Theoretically, the treatment volume can thus be increased considerably. Whereas the previous chapters focused on exogenous fluorescent dyes, chapter 7 describes the use of endogenously generated porphyrins for PDT. This is a new approach that uses a photodynamically inactive precursor of heme called 5-aminolevulinic acid (ALA). In (tumor) cells this precursor is converted into the photosensitizer protoporphyrin IX (PpIX).

Chapter 2

TISSUE LOCALIZING PROPERTIES OF SOME PHOTOSENSITIZERS STUDIED BY *IN VIVO* FLUORESCENCE IMAGING.

Journal of Photochemistry and Photobiology, B: Biology, 6 (1990) 111-119

Co-authors
A.A.C. Versteeg[1], N. van der Veen[1], A.E. van den Berg-Blok[2],
J.P.A. Marijnissen[1] and W.M. Star[1]

[1]Dr. Daniel den Hoed Cancer Center, Rotterdam, The Netherlands
[2]Radio Biological Institute, TNO, Rijswijk, The Netherlands

Abstract

Using fluorescence imaging, the tissue localizing properties of five photosensitizers were studied *in vivo* for tumors in "sandwich" observation chambers and for tumors growing on thigh muscle. The preliminary results indicate that of three photodynamically active dyes tested (hematoporphyrin derivative, Photofrin II, and aluminum phthalocyanine tetrasulphonate, the phthalocyanine possesses the best tumor localizing properties. This makes it possible to combine tumor fluorescence detection and photodynamic therapy with reduced skin photosensitivity. The two photodynamically inactive dyes tested (uroporphyrin I and acridine red) may be useful for application in fluorescence imaging to localize superficial tumors without inducing skin photosensitivity. In particular, acridine red has remarkable tumor localizing properties, but is rather toxic.

Introduction

Interest in the use of photosensitizers for tumor localization and tumor therapy is steadily increasing (Dougherty, 1987; Manyak *et al.,* 1988). In clinical photodynamic therapy (PDT), the drugs which are almost exclusively used are hematoporphyrin derivative (HPD) or a purified version (enriched in active material) with the trade name Photofrin II (PhII). Tumor localization using HPD fluorescence was first described by Lipson (1961). This application is particularly interesting because of the potential to detect early cancer (Profio *et al.,* 1983; Benson *et al.,* 1982; Gluckman and Wiessler, 1986). A disadvantage of HPD and Photofrin II is that both cause prolonged skin photosensitivity. This is a major reason for the current search for improved photosensitizers (Dougherty, 1987). In particular, a fluorescent dye that is exclusively used for tumor localization should not make a patient photosensitive over a long period of time. Therefore we have begun a study of the tumor localizing properties of photosensitizers. Some preliminary results are reported in this paper.

Materials and methods

Animal Model

Tumors were transplanted into the subcutis of 18 weeks old female WAG/Rij rats in transparent observation chambers ("skin fold chamber") (Reinhold *et al.,* 1979; Star *et al.,* 1986). The tumors were isogeneic mammary (RMA) carcinoma and incidentally rhabdomyosarcoma (RH). One photosensitizer

(acridine red) was also studied in isogeneic squamous cell carcinoma (SCC) and in a human lung tumor (HLT) in immunosuppressed rats. As selective tumor fluorescence depends on the drug retention in surrounding normal tissue, localization was also documented for tumors (about 3 mm in diameter) growing subcutaneously on thigh muscle in the same animal 24 h post injection (p.i.) of the drug.

Photosensitizers

Five dyes were studied; HPD (Quentron, Adelaide, Australia) and PhII (QLT, Vancouver, British Columbia, Canada) because of their current clinical use. Uroporphyrin I (UpI, Porphyrin Products) is photodynamically inactive (Nelson *et al.*, 1986) and clears quickly from the body. Aluminium phthalocyanine tetrasulfonate (AlPhcTS, Porphyrin Products) belongs to a promising class of new photosensitizers for PDT (Dougherty, 1987). Acridine red (AR, Koch Light) is a pyronine used in microcirculation research to label platelets and leucocytes (Tangelder *et al.*, 1982). No photodynamic activity was noted in observation chambers (10 mg AR/kg, 218 J/cm^2 of light at 514.5 nm).

Excitation light

As an Argon laser was available (Spectra Physics 171) and 514.5 nm is a suitable wavelength, this was used to excite the fluorescence of all dyes except AlPhcTS. For the latter, red light of 608±2 nm was used from a dye laser (Spectra Physics 375B with 4-dicyanomethylene-2-methyl-6-*p*-dimethylaminostyryl-4H-pyran (DCM)), yielding a relatively high emission intensity. Other workers have used a nitrogen laser (Anderson-Engels *et al.*, 1988) at 337 nm for excitation and observed that PhcTS emits less fluorescence light than PhII. The 608±2 nm wavelength is convenient, as it can be used for fluorescence excitation as well as for PDT. Furthermore, a long wavelength is preferred to excite fluorescence, because this reduces autofluorescence, improving the contrast. This wavelength works well with our model system, but may not be suitable for detection of very superficial tumors. An excitation light intensity of 0.1 mW/cm^2 was used. This generated a sufficient fluorescence signal for detection with our system and reduced the risk of unwanted PDT damage to practically zero for all the dyes studied.

Imaging system

An intensified charge coupled device (CCD) video camera (HTH Holland) was used with a Photar macro lens (Leitz) and an OG570 or OG665 long pass filter to block the excitation light. Video signals were processed by a frame grabber

(PC vision plus) and a PC-based image analysis program called TIM.

Experimental Procedure

Animals were anaesthetized using Hypnorm (Janssen Pharmaceutics) and placed on a temperature-controlled holder, fixed to a special stage, allowing exact (re)positioning of the chamber for recording and subtraction of successive images. After recording an autofluorescence image, dye was injected into a tail vein and the fluorescent angiogram was monitored. Fluorescence recordings were measured at a number of intervals up to 2 h and after 24 h p.i. The fluorescence of tumors growing on thigh muscle was observed and recorded after opening and removal of the overlying skin, yielding tumor images with a background signal different from subcutis. Table 1 shows the various dyes tested and the experimental parameters.

Table 1. Summary of the experimental parameters in the tissue fluorescence imaging study using different dyes.

Dye	Dose (mg/kg)	Number of Animals	Fluorescence excitation	
			Wavelength (nm)	Irradiance (mW/cm^2)
Uroporphyrin I	15	5	514.5	0.1
HPD	15	10	514.5	0.1
Photofrin II	15	6	514.5	0.1
AlPhcTS	2.5	20	608 ± 2	0.1
AR	2 or 10	25	514.5	0.1

Different numbers of animals were employed because some drugs were used for fluorescence only, whereas for others the photodynamic activity was also studied (not reported in this paper).

Image scoring

The images were digitized and then evaluated for differences between tumor and normal tissue fluorescence. Tumor selectivity was visually rated positive when the fluorescence of the tumor area significantly exceeded that of the surrounding subcutis (*i.e.* a minimum of 15 "pixel" values out of a maximum value of 256). The rating was performed by at least two observers. For each interval, after subtraction, each observation chamber (animal) was classified in

one of three categories: tumor fluorescence larger (T>Sub), equal to (T=Sub) or less than (T<Sub) fluorescence of subcutis. Changes in fluorescence over time, obtained from subtracted images, are denoted by ΔT and ΔSub.

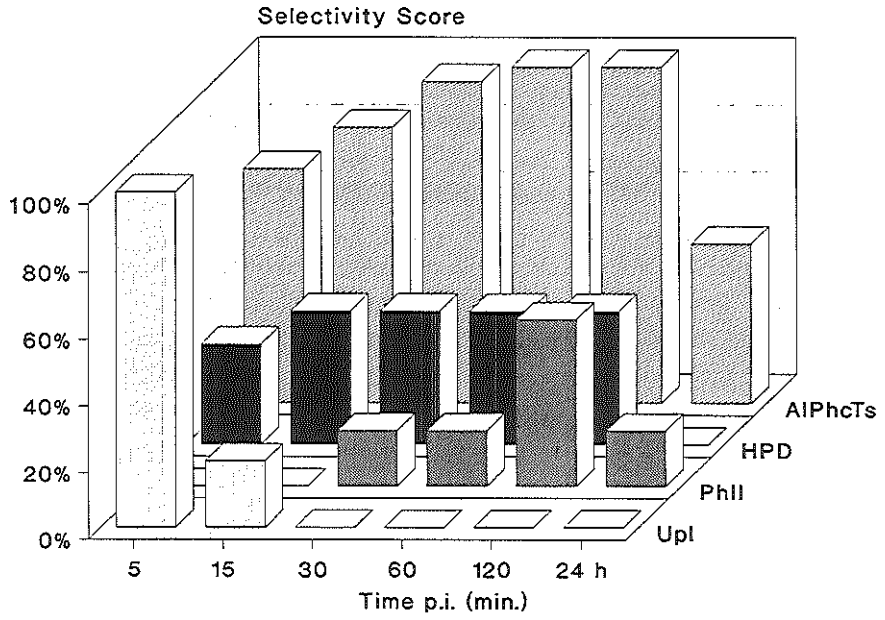

Fig. 1. Selectivity of tumor fluorescence relative to that of the surrounding subcutis in the chamber model for four of the dyes tested. The vertical axis shows the percentage of animals which exhibit tumor fluorescence exceeding subcutis fluorescence (T>Sub).

Results

The excitation light intensity of 0.1 mW/cm^2 does not have observable effects on the (micro)vasculature, even after long periods of continuous observation (1 h). Since the RMA and RH tumors show similar fluorescence kinetics with all five dyes, the data from the two tumor types are pooled for presentation in Fig. 1, where selective tumor fluorescence (T>Sub) is expressed for four of the dyes tested.

After intravenous injection (5 min. p.i.), UpI is selective in all cases. However, after longer intervals, this selectivity is lost and the tumor may even show less fluorescence than the subcutis (60 min.). At 24 h, the tumors are indistinguishable from the subcutis. After injection of PhII, selective fluorescence is observed for the first time after 30 min. and after 120 min. only 50% of

cases show selective fluorescence. At 24 h the tumor is indistinguishable from the subcutis in all cases except one. HPD, unlike PhII, shows selectivity shortly after injection, but never exceeds 40% of cases. The observed selectivity is lost at 24 h. At this time, in 60% of cases the fluorescence of the subcutis exceeds that of the tumor embedded in it. Tumor fluorescence of AlPhcTS gradually increases, reaching 100% selectivity at 60 min. p.i. (Fig 2).

On the following day selectivity is still observed in 50% of cases. Acridine red is 100% selective immediately after injection in all cases (Fig. 3), for all tumor types tested (RH, RMA, SCC and HLT) and for both AR concentrations; it is therefore not included in Fig. 1. AR is rapidly cleared from the circulation. The highest dose (10 mg/kg) causes mortality in some cases. Therefore 2 mg/kg was used in later sessions. The cause of this mortality is under investigation.

Data on the fluorescence dynamics of the dyes up to 120 min. p.i. are presented in Fig. 4. UpI shows a selective increase in tumor fluorescence in all cases during the first interval (5 min. autofluorescence). During the next two intervals the only increase observed is in the subcutis; in the last two intervals there is no difference between the fluorescence increase at the tumor and subcutis sites.

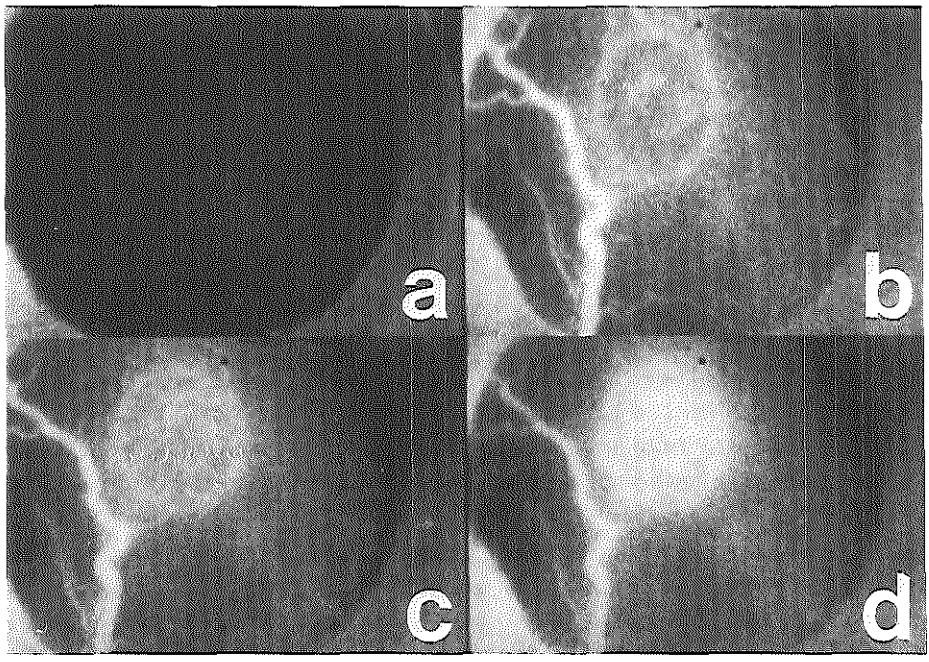

Figure 2.

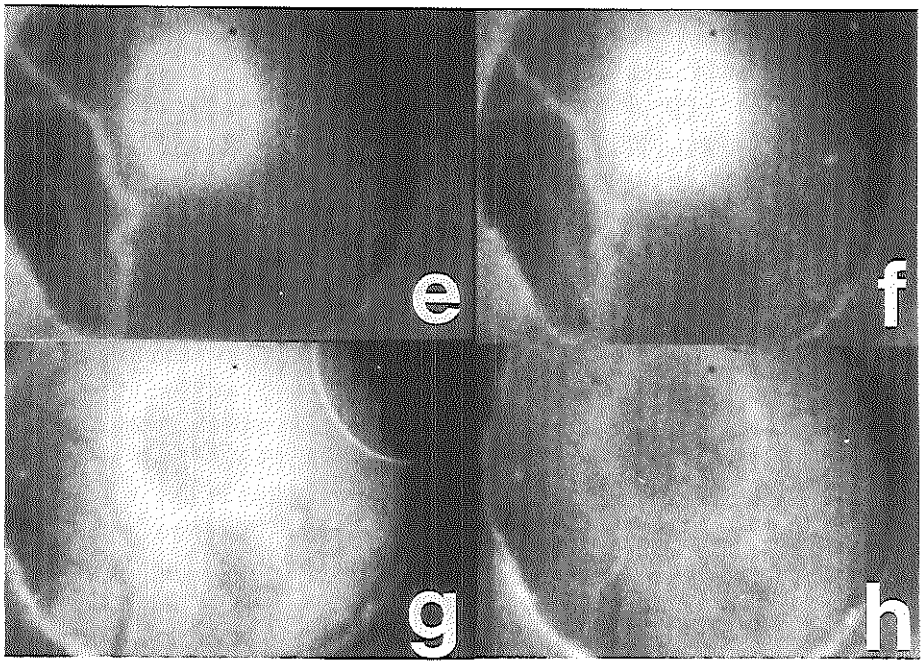

Fig. 2. Sequence of fluorescence images of AlPhcTS (2.5 mg/kg) in the chamber model (diameter, 9.5 mm): (a) autofluorescence; (b) 5 min. p.i., full development of the angiogram; (c) 15 min. p.i.; (d) 30 min. p.i., gradual increase of fluorescence in tumor and decrease in blood vessels; (e) 60 min. p.i.; (f) 120 min. p.i., tumor fluorescence is still increasing, blood vessel fluorescence is decreasing; (g) 24 h p.i., fluorescence intensity is highest at the tumor boundary. Selectivity is decreased due to the fluorescence level in the subcutis, showing a negative fluorescence image of a large blood vessel; (h) 24 h p.i. and after a PDT treatment dose of 450 J at 608 nm. Marked photobleaching can be observed.

The fluorescence of PhII remains almost constant. In most cases no distinction can be made between the fluorescence increase at the tumor and the subcutis sites. In contrast, HPD shows an interesting selective increase in the tumor fluorescence during the first 30 min. p.i., reaching a 100% selective increase between 5 and 15 min. After 30 min. the increase is restricted to the subcutis or becomes equal for the tumor and subcutis sites. AlPhcTS also shows a peak selectivity at the 5-15 min. interval. An increase in selectivity occurs in all intervals but never reaches 100%.

Almost immediately after i.v. injection, the fluorescence of the blood vessels decreases for all dyes except PhII. Both photodynamically inactive dyes (UpI, AR) show an immediate decrease in fluorescence in the blood vessels after the development of the angiogram. At the same time there is a dramatic increase in tumor fluorescence and a dispersion of fluorescence in the subcutis. The fluorescence of HPD and AlPhcTS in the blood vessels decreases more gradually. In contrast, PhII shows an increase in fluorescence in the circulation, in one case even up to 2 h p.i. All photodynamically active dyes show an increase in fluorescence in the subcutis up to 24 h p.i. An interesting observation at this interval is that in 50% of cases for both HPD and AlPhcTS, the fluorescence intensity at the tumor boundary is higher than that in the tumor volume (Fig. 2g). In this context, it should be noted that the observation chamber shows a cross section of the tumor, whereas in clinical practice we usually observe a tumor boundary.

The images taken from the tumors growing on thigh muscle at 24 h p.i. show selective fluorescence for UpI, HPD, PhII, and AlPhcTS. With AR at a dose of 10 mg/kg, selectivity for tumor on muscle is partially lost at day 1 and in some cases the animals do not survive this drug dose. Therefore a lower dose (2 mg/kg) was chosen; at this dose 100% selectivity for tumor on muscle is maintained only during the first 30 min. p.i. At day 1, in 30% of cases, the level of fluorescence from the muscle exceeds the fluorescence of the tumor. This is in contrast with the other dyes where the tumor to muscle ratio at 24 h shows an increase compared with that obtained shortly after injection.

Discussion

There is a striking difference between the selective fluorescence of tumors growing in the subcutis (observation chamber) and tumors growing on thigh muscle. It appears that lipophilic dyes (HPD, PhII, AlPhcTS) are retained more in skin than in muscle (Eckhauser *et al.*, 1987). When a tumor showing less fluorescence than the subcutis in the observation chamber is removed and placed on thigh muscle of the same animal, selective fluorescence is always observed.

Photodynamic therapy is usually performed 24 h after drug administration for murine tumors and 48-72 h for human tumors; these may not be the optimum intervals. The present study shows that the optimum interval for tumor localization using selective tumor fluorescence may be considerably shorter. This has been noted previously by Benson (1982) in their study of HPD fluorescence in human bladder.

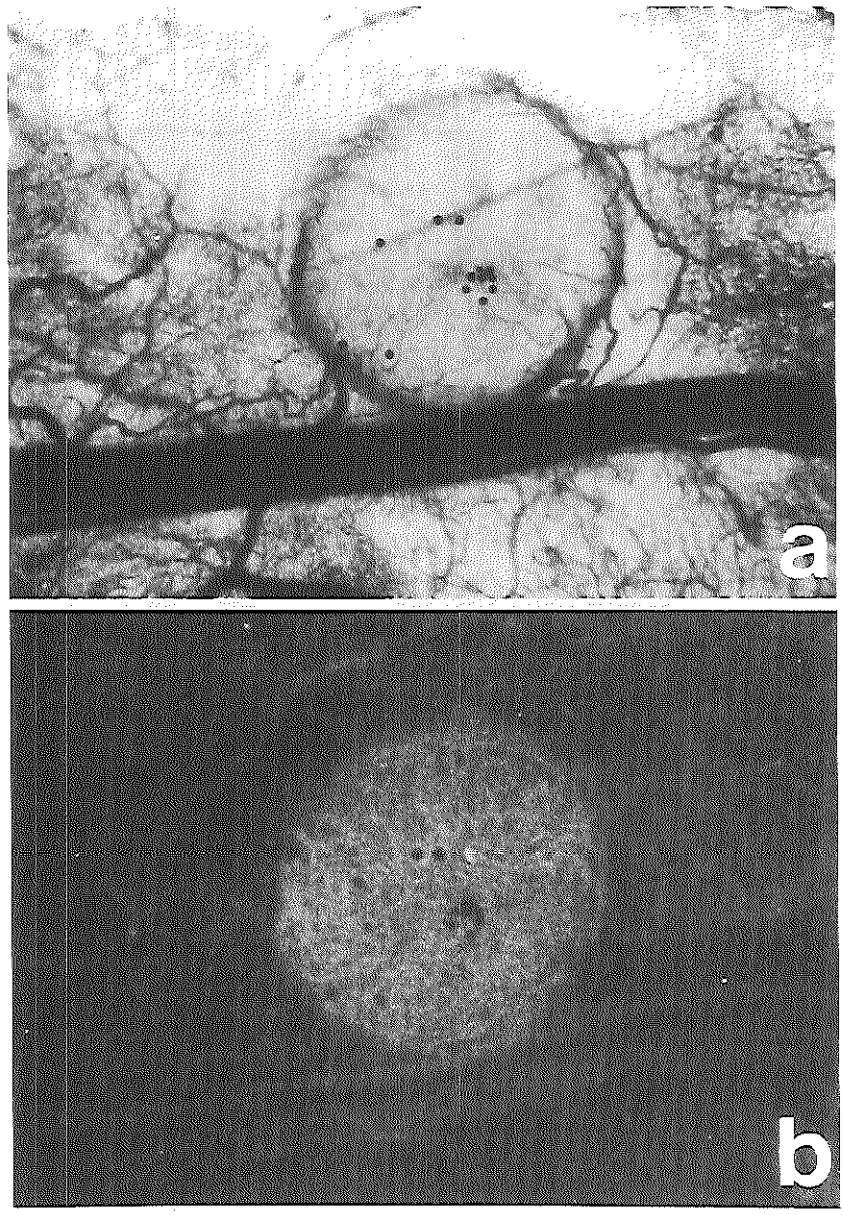

Fig. 3(a). White light photograph of a human lung tumor in an immunosuppressed rat in an observation chamber. The blood vessels surrounding the tumor (diameter, 2.5 mm) can be clearly seen as well as clusters of fat cells to the left and right of the tumor. (b). Fluorescence image of the same tumor a few min. after administration of acridine red (10 mg/kg).

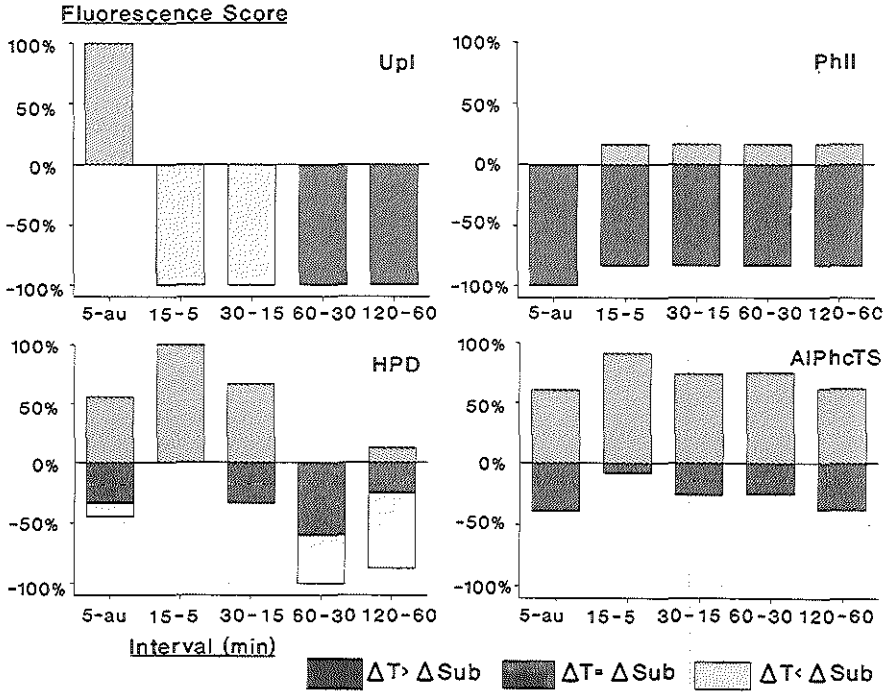

Fig. 4. Fluorescence dynamics of UpI, PhII, HPD and AlPhcTS in the chamber model up to 120 min. p.i. The scores (vertical axes, percentage of animals) are obtained by subtraction of images at given intervals (horizontal axes). Numbers indicate the time (min.) p.i.; au, autofluorescence image before drug injection. A selective increase in tumor fluorescence (ΔT>ΔSub) is given a positive score. An equal increase (ΔT=ΔSub) and a smaller increase in tumor fluorescence than normal tissue fluorescence (ΔT<ΔSub) are given a negative score.

In particular, AlPhcTS appears to be a selective tumor localizing material at relatively short intervals p.i., even in the subcutis. Since this drug causes little skin photosensitivity on exposure to sunlight (Roberts *et al.,* 1989), it seems a promising photosensitizer for PDT and tumor detection.

According to Fig. 1, no real maximum develops for HpD up to 120 min. p.i. and selectivity never exceeds 60%. However, for PhII a maximum score occurs somewhere between 1 h and 24 h. Long-term observations, not included in this paper, indicate that this maximum occurs 3-4 h p.i., in agreement with other workers (Svanberg *et al.,* 1986). A unique phenomenon is the increase in blood vessel fluorescence up to 1 h p.i. of PhII. The dimers and oligomers in PhII do not fluoresce (Dougherty, 1987), but may be broken down in the cells to produce fluorescent species (Kessel, 1986). Does this also occur with PhII in blood?

Chapter 3

IN VIVO FLUORESCENCE KINETICS OF PHTHALOCYANINES IN A SKIN FOLD OBSERVATION CHAMBER MODEL: ROLE OF CENTRAL METAL ION AND DEGREE OF SULPHONATION

Accepted in Photochem. Photobiol.

Co-authors
N. van der Veen[1], A.A.C. Versteeg[1], R. Ouellet[2], J.E. van Lier[2] and W.M. Star[1]

[1]Dr. Daniel den Hoed Cancer Center, Rotterdam, The Netherlands.
[2]MRC Group in the Radiation Sciences, Faculty of Medicine, University of Sherbrooke, Sherbrooke, Québec, Canada.

Abstract

The fluorescence pharmacokinetics of a series of metallosulphophthalocyanines, chelated with either aluminum or zinc and sulphonated to different degree, was studied by fluorescence measurements *in vivo*. Dyes were administered systemically to female WAG/RIJ rats with an isogeneic mammary carcinoma transplanted into the subcutis in a transparent observation chamber located on their backs. Following an i.v. injection of 2.5 μmol/kg of the dye, fluorescence dynamics was observed up to 7 hours post injection. The phthalocyanines were excited at 610 nm with a power-density of 0.1 mW/cm^2 without causing photodynamic damage to the vasculature. Fluorescence was detected above 665 nm using a fluorescence imaging system based on an image intensifier. Dye retention in the blood vessels and tumor tissue was expressed as ratios relative to the fluorescence signal of the surrounding subcutaneous tissue. Phthalocyanines chelated with aluminum gave the highest fluorescence signal with tumor-over-subcutis ratios of up to a value of 4. The zinc complexes exhibited the highest vascular-over-subcutis ratios with maximum values exceeding a value of 6. They also displayed the longest retention times in the vascular system of well over 7 hours. Overall, decreasing the degree of sulphonation of the metallophthalocyanines results in lower tumor-over-normal tissue fluorescence ratios and furthermore aluminum- based dyes seem superior tumor localizers over zinc-based dyes. The advantages of phthalocyanines over porphyrins with respect to tumor localization and photodynamic therapy are discussed.

Introduction

Photodynamic therapy (PDT) is an experimental cancer treatment modality which combines the photosensitizing properties of selected dyes with their tumor retention. Excitation of the dye with light of an appropriate wavelength and dose results in the formation of cytotoxic species and subsequent tumor necrosis.
This excitation of the photosensitizer can also induce fluorescence at a specific wavelength and it is this property of hematoporphyrin derivative (HPD) (Lipson *et al.,* 1961) that resulted in the earliest clinical application of HPD, namely as a tumor localizer. In the following period, however, most of the attention for HPD was drawn to the therapeutical features of the dye. Benson (1982), two decades later, demonstrated that HPD not only displayed fluorescence in malignant tissue but also localized in dysplastic and neoplastic bladder mucosa. From then on attention for HPD expanded again the direction of the diagnostical

properties of the dye. Refinement of the technical aspects of fluorescence detection resulted in the development of a number of sophisticated detection devices (Profio *et al.,* 1986; Andersson *et al.,* 1987; Brodbeck *et al.,* 1987; Rogers *et al.,* 1990). Currently, by combining these detection devices with state of the art endoscopy, clinicians are capable of detecting the very weak coral-red porphyrin fluorescence not only on the exterior but on almost every internal surface of the human body including the aerodigestive tract, intestines and bladder.

Following systemic administration of therapeutical drug doses of HPD, a persistent skin photosensitivity is observed that may last at least up to 4-6 weeks. This is considered one of the major side effects of PDT based on HPD or its purified version Photofrin®, currently under clinical investigation, and this has prompted a worldwide search for new photosensitizers for PDT of malignant disorders (van Lier *et al.,* 1987; Kessel, 1990). Phthalocyanines have received considerable attention as "second generation" photosensitizers for PDT (van Lier, 1990; Ben-Hur and Rosenthal, 1985; Spikes, 1986). They can be modified chemically, thereby altering their photophysical and pharmacological properties in a controllable fashion.

In contrast to the porphyrins currently in use, the dyes can be prepared as single products, they are relatively stable and have strong absorption maxima in the red region of the visible spectrum (650-700 nm) where the tissue penetration of light is relatively high (Brasseur *et al.,* 1987; Bown *et al.,* 1986; Peng *et al.,* 1991b). The phthalocyanines show deep red fluorescence upon excitation and this fluorescence probably correlates with the presence of the photoactive monomers (MacRobert *et al.,* 1989) whereas the fluorescent monomers of hematoporphyrins are not relevant for photodynamic therapy (Kessel, 1982; Kessel, 1986). Several analogues of $MPcS_n$ have a preference for tumor tissue and amphiphilic derivatives have been shown to have a good potential to inflict direct cell kill (Henderson and Bellnier, 1989). Furthermore, skin photosensitivity induced by the dyes is low compared to Photofrin® (Tralau *et al.,* 1989). Unsubstituted phthalocyanines are insoluble in water which makes them unattractive for systemic (i.v.) administration (Berg *et al.,* 1989). Sulphonation of the molecule is one way to overcome this problem.

The effect of the degree of sulphonation of phthalocyanine on their pharmacokinetics has been studied using ^{14}C (Rousseau *et al.,* 1990) and ^{65}Zn radiolabeled analogues (Scasnar personal communication) and structure-activity relationships have been advanced (Paquette and van Lier, 1992). We now report on the fluorescence dynamics and localizing properties, of a series of six differently sulphonated Zn^{2+}- and Al^{3+}- phthalocyanines using an *in vivo* skin fold chamber model.

Materials and Methods

Photosensitizers

Metallosulphophthalocyanines ($MPcS_n$) were prepared via the condensation method using zinc acetate or anhydrous aluminum chloride as the metal source and various proportions of sulphophthalic acid/phthalic acid (Ali *et al.,* 1988). Differently sulphonated fractions were obtained after chromatography on a 30 cm long by 2 cm ID medium pressure column packed with C-18 reverse phase, particle size 25-40 μm (Machery-Nagel, Düren, Germany) eluted with a gradient of methanol and 10 mM acetate buffer, pH = 5. If required, samples were further purified by HPLC on a semi-preparative (25 cm long by 0.94 cm ID) reverse phase C-18 column packed with ODS-2 spherisorb 5 μm (CSC, Montreal) operated at 2 ml min^{-1} with a linear gradient (55 min) of 0-95 % methanol in 10 mM phosphate buffer, pH = 5. The latter system was also used for the analysis of sulphonated fractions in conjunction with an oxidative degradation assay to confirm the degree of sulphonation. The disulphonated $MPcS_2$ were enriched in derivatives with two adjacent sulphonate groups. Cremophor EL (Sigma) was added to the $MPcS_1$ and $MPcS_2$ in order to prevent aggregation and bring them into injectable solutions. Final $MPcS_n$ concentrations were determined spectroscopically after a 1:100 dilution of the sample in DMF, taking $\epsilon = 2.5\ 10^5\ M^{-1}\ cm^{-1}$ at $\lambda_{max} = 675$ nm.

Skin fold chamber animal Model

Twelve weeks old female WAG/Rij Rats, weighing approximately 110-120 g were purchased from ITRI-TNO, Rijswijk, The Netherlands. During a three week preparation period, a layer of subcutaneous tissue from a dorsal skin flap was mounted in a skin fold chamber (Reinhold *et al.,* 1979) also known as the "sandwich chamber". A maintenance dose of antibiotics (Pentrexil: Bristol-Myers, Weesp, Holland and Garamycin, Essex Laboratories, Heyst-op-den-Berg, Belgium) was administered for protection against bacterial infection during this period. The final step in the procedure was the implantation of approximately 0.5 mm^3 of an isogeneic RMA mammary carcinoma into the chamber. Tumor growth, the general condition of the chamber and the circulation were followed using a microscope at low magnification. The animals were kept in a temperature controlled cabinet at 32°C with a 12/12 hour light/dark interval. The elevated environmental air temperature determines the temperature of the chamber and is therefore a prerequisite for tumor growth. After photosensitization the animals were kept under subdued light conditions ($<30\ \mu W/cm^2$). The chamber model enabled *in vivo* observations of the

fluorescence dynamics of an i.v. administered fluorescent dye in subcutis, tumor tissue and blood vessels for the duration of the experiment (up to 24 hours p.i.). Through all procedural steps Hypnorm® (fluanisol/fentanyl mixture, Janssen Pharmaceutics, Beerse, Belgium) was used as a general anaesthetic.

Fluorescence detection

Phthalocyanines were excited at 610 nm with 0.1 mW/cm² of light from an argon-dye laser system (Spectra Physics system 171), with DCM (4-dicyanometyhlene-2-methyl-6(P-dimethylaminostytyl)-4H-pyran) as the lasing dye. Fluorescence was detected through a high-pass filter transmitting light above 665 nm (Schott RG 665).

The imaging system was based on a two stage image intensifier with a 25 mm Photar macrolens (Leitz) coupled to a CCD (Charge Coupled Device) camera. The resulting video images were digitized on a pc-based framegrabber (Pc-Vision Plus), averaged over 16 frames to improve the signal to noise ratio and stored on disk for further processing. The system digitizes 256x256 picture elements (pixels). Average grey scale values of the area of interest, i.e. tumor, vessel or subcutaneous tissue, were calculated using a pixel measurement program of our own design, based on image processing software called TIM (Dífa Measuring Systems B.V., Breda, The Netherlands). In order to determine the level of fluorescence in the circulation, an area of the largest vein in the chamber was chosen.

Experimental procedure

Experiments were performed after the tumors in the skin fold chamber had grown to about 3 mm in diameter and when adequate circulation in both subcutaneous and tumor tissue was observed.

The animals were sedated and placed on a temperature controlled (≃ 30°C) positioning stage, allowing careful positioning of the animal under the camera using a specially designed imaging program. An (auto)-fluorescence recording was made and subsequently the dye, using a dose of 2.5 μmol/kg, was administered via a tail vein of the animal. Fluorescence images of the chamber were recorded at various time intervals from 5 min to 24 h p.i. For each photosensitizer the fluorescence data of 6 animals were collected. At the 24 h interval the animals received a therapeutic light dose. The resulting photodynamic effects will be discussed in a forthcoming paper.

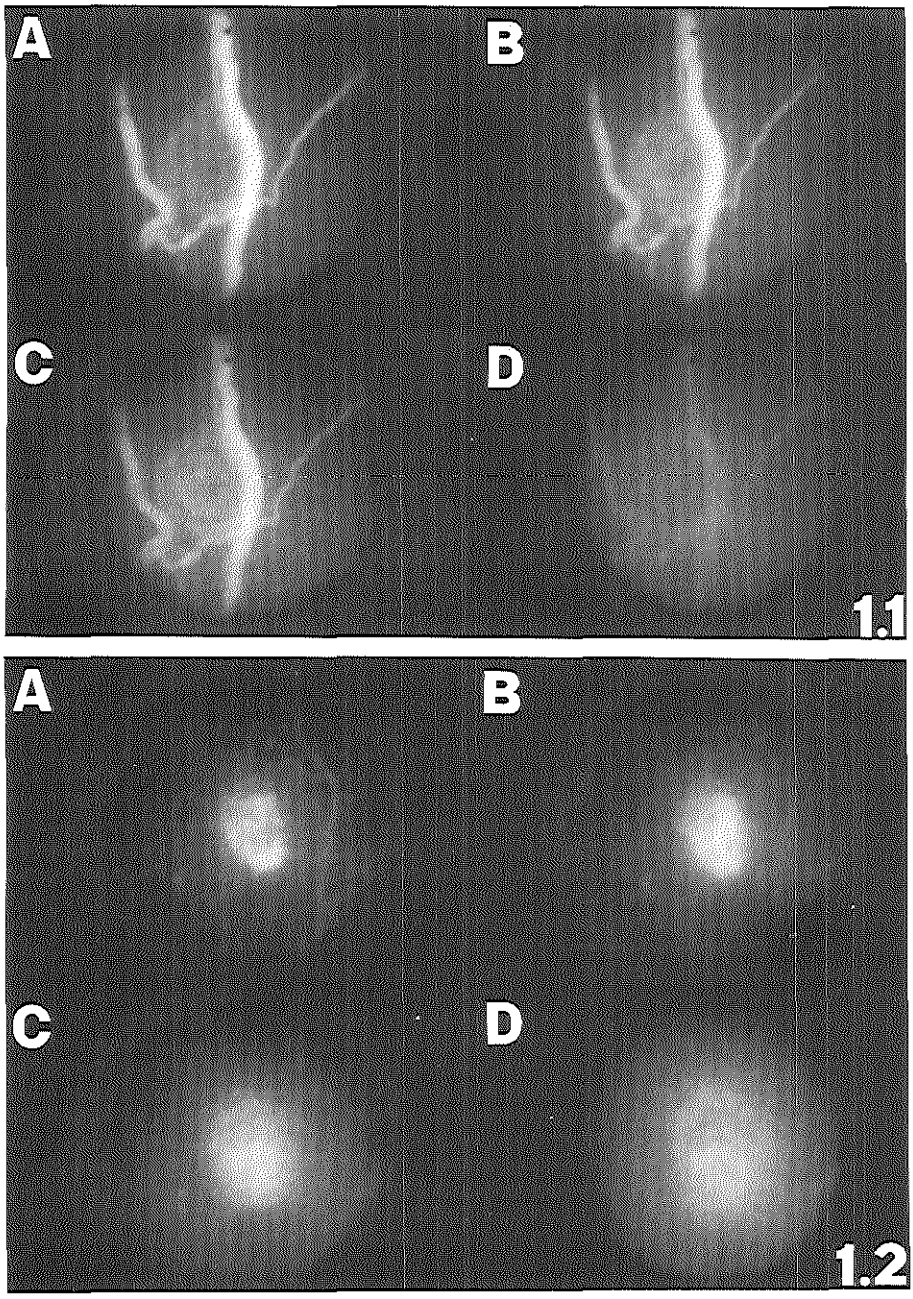

Fig. 1. Digitized fluorescence images of the skin fold chamber containing a mammary carcinoma at 5 (A), 10 (B), 60 (C) and 360 (D) min p.i. of 2.5 µmol/kg phthalocyanine, (1.1) $ZnPcS_2$ (1.2) $AlPCS_4$.

Results

Two extreme fluorescence patterns were observed in the skin fold chamber using the various Pc dyes (Fig. 1.). In the case of the $ZnPcS_2$ (Fig. 1.1) the vessels are clearly delineated immediately post injection (p.i), with the fluorescence intensity slowly decreasing with time. Only moderate increase of fluorescence in the tumor region is observed during the first hour, and little fluorescence remained in either the vessels or the tumor at 6 h p.i. In contrast, the $AlPcS_4$ (Fig. 1.2) showed hardly any fluorescence in the circulation following i.v. administration of the dye whereas immediate fluorescence of the tumor region is evident, persisting at least 6 h p.i. The fluorescence distribution of the remaining dyes was less pronounced, with varying vascular vs tumor fluorescence intensities and the dynamic of all six dyes studies are summarized graphically in Fig. 2. Grey scale values are averaged in an area of interest selected over the tumor, blood vessel and surrounding subcutis, and expressed as ratios relative to the surrounding subcutis i.e. tumor-to-normal tissues (T/NT) and blood vessel-to-normal tissue (BV/NT) ratios. The average fluorescence values of the subcutis alone are also presented on these graphs (grey scale values on right Y-axis) to demonstrate the influence of the fluorescence of the subcutis on the tumor and blood vessel ratios.

The T/NT fluorescence ratio of $ZnPcS_4$ (Fig. 2A) remains higher than 2 up to 420 min p.i. whereas the BV/NT ratio exceeds 6 at 5 min p.i., representing the highest fluorescence signal in the blood vessel observed for any of the dyes tested. The BV/NT value decreases rapidly over the next 3 h while the fluorescence of the subcutis increases only slightly during the same period. Accordingly, the latter can only partly be responsible for the decrease of the BV/NT ratio.

Compared to the $ZnPcS_4$, the $AlPcS_4$ (Fig. 2B) reaches higher T/NT values of almost 4, whereas for $ZnPcS_4$, fluorescence persists for extended periods of up to 360 min. In contrast, the fluorescence peak of the $AlPcS_4$ in the blood vessel is the lowest observed for all six dyes tested with BV/NT values, after a high of 2.2 at 5 min, dropping rapidly to unity over the next 2 h. Judging from the fluorescence of the subcutis the dye has a very short retention time in the circulation. After an initial increase, the BV/NT ratio remains stable, suggesting that tumor tissue accumulates the dye at approximately the same rate as the subcutis. At later time intervals ($t \geq 240$ min) a loss of tumor selectivity is observed, but only at 24 h p.i. can the decrease in T/NT values be attributed to the increasing normal tissue fluorescence.

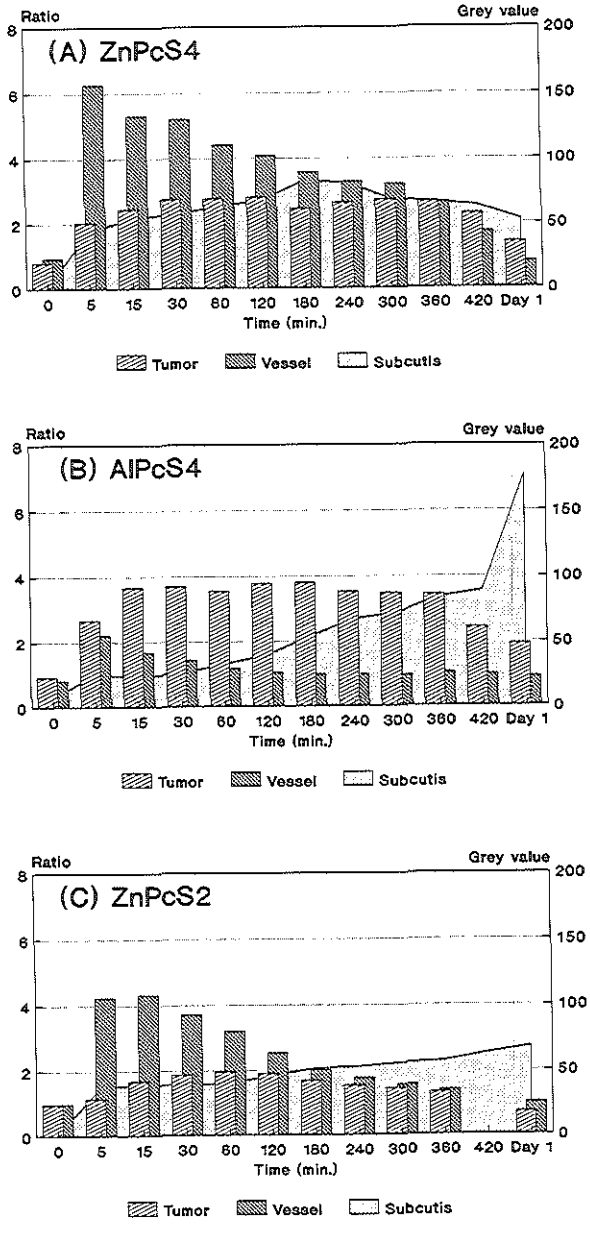
Ratio
Grey value
(A) ZnPcS4
0
2
4
6
8
0
50
100
150
200
0 5 15 30 60 120 180 240 300 360 420 Day 1
Time (min.)
Tumor
Vessel
Subcutis
Ratio
Grey value
(B) AlPcS4
0
2
4
6
8
0
50
100
150
200
0 5 15 30 60 120 180 240 300 360 420 Day 1
Time (min.)
Tumor
Vessel
Subcutis
Ratio
Grey value
(C) ZnPcS2
0
2
4
6
8
0
50
100
150
200
0 5 15 30 60 120 180 240 300 360 420 Day 1
Time (min.)
Tumor
Vessel
Subcutis

Figure 2.

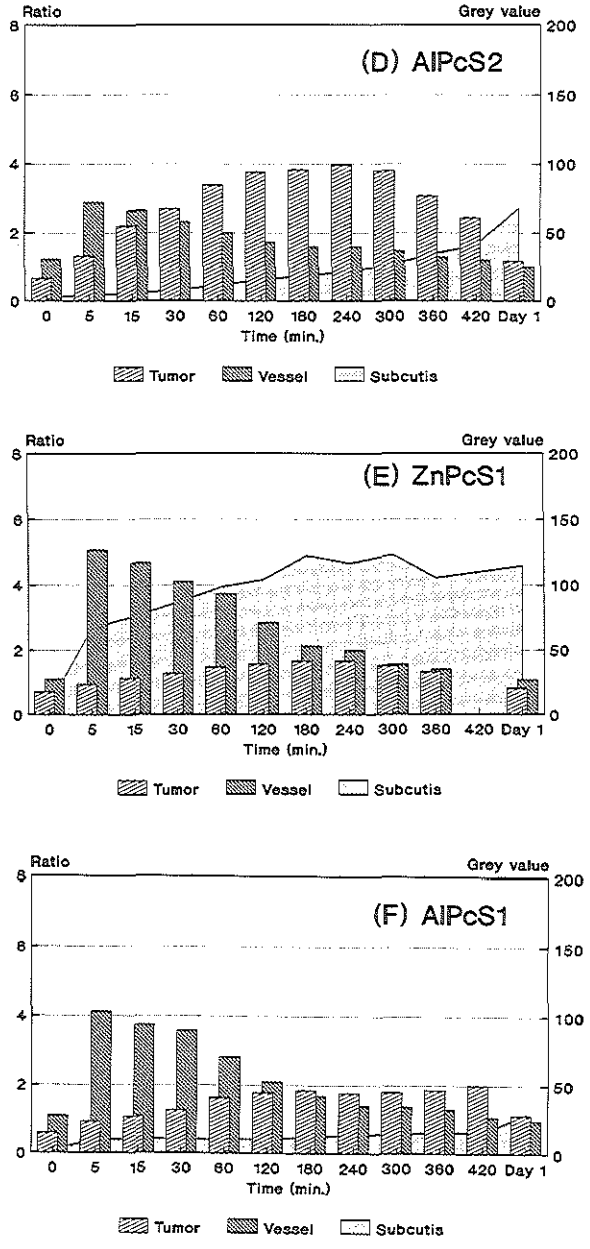

Fig. 2. Fluorescence kinetics in tumor tissue, blood vessel and background (subcutis) as a function of time after i.v. administration of differently sulfonated MPcS$_n$. The left Y-axis refers to the bar plot of tumor-to-background (T/NT) and blood vessel-to-background (BV/NT) ratios. The shaded area represents the fluorescence levels in the subcutis (right Y-axis)

Like the $ZnPcS_4$, the disulphonated $ZnPcS_2$ (Fig. 2C) exhibits strong fluorescence in the blood vessels with BV/NT values of 4.2 at 15 min p.i.
Tumor tissue fluorescence is low, with T/NT ratios reaching a maximum of almost 2 at about 60 min p.i. The changes in background fluorescence are less pronounced than those observed with $ZnPcS_4$ and the increase in grey value can account for the decrease in T/NT and BV/NT ratios.

Similar to the $AlPcS_4$, the disulphonated $AlPcS_2$ (Fig. 2D) exhibits high tumor fluorescence, with T/NT ratios remaining well above BV/NT values. Maximum T/NT ratios of 4 are reached at 240 min p.i., combined with low normal tissue fluorescence. The peak of the BV/NT signal of the $AlPcS_2$ is higher than that observed with $AlPcS_4$. The increase of fluorescence in the subcutis is less striking than that observed with $AlPcS_4$ and this cannot account for the decrease in selectivity of tumor fluorescence at intervals $\geq$ 300 min p.i.

The monosulphonated $ZnPcS_1$ (Fig. 2D) displays the highest normal tissue fluorescence of all Pc's tested. The selectivity of tumor fluorescence is somewhat lower than that observed with the $ZnPcS_2$, and like in the case of the latter, T/NT values remain stable and < 2 during the observation period. Fluorescence in the circulation is high and persistent resembling the profiles observed with the other $ZnPcS_n$.

Finally, tumor fluorescence observed with the monosulphonated $AlPcS_1$ (Fig. 2F) is also low with T/NT values showing some selectivity only after 60 min p.i. Among the $AlPcS_n$ tested, the $AlPcS_1$ is the only dye where the BV/NT maxima exceeded the maximum values of the T/NT ratios, while exhibiting the lowest subcutis fluorescence.

Discussion

In the present study we have evaluated the tumor localizing properties of differently sulphonated zinc and aluminum phthalocyanines through quantification of the fluorescence of the dyes in a skin fold chamber. In contrast to HPD and Photofrin®, where enhanced tumor fluorescence relative to normal tissue could be observed in our model in only 40-60 % of the cases studied (van Leengoed *et al.*, 1990), all phthalocyanines demonstrated consistently good localizing properties. However, the aid of a detection system is needed as the sensitivity of the eye decreases in the red region of the visible spectrum where phthalocyanine fluorescence is emitted.

Marked differences in tissue selectivity related to the chemical structures of the various dyes were observed and both the nature of the central metal as well as the overall hydrophobicity of the Pc structure were found critical factors in

directing the selectivity of the dyes. Our model allowed us to quantify fluorescence in the tumor tissue and blood vessels and in order to permit direct comparison of these data, fluorescence at these sites are presented as ratios to subcutis fluorescence (Fig. 2).

Decreased hydrophobicity, i.e. increasing the number of sulphonate groups, favours tumor localization of the $MPcS_n$ and particularly the tetra and disulphonated aluminum complexes gave high T/NT ratios of up to 4 combined with a low background (subcutis) fluorescence and low BV/NT ratios. Since the background fluorescence of the disulphonated derivative is substantially lower at 0.5 - 1 day p.i. than that observed for the tetrasulphonated derivative, the $AlPcS_2$ provides the most favourable fluorescence ratios for tumor localization. The $ZnPcS_n$ in general gave higher subcutis fluorescence than the AlPcS series combined with higher BV/NT ratios and only the $ZnPcS_4$ scored some tumor selectivity with T/NT ratios > 2. Overall the following T/NT rank order was observed $AlPcS_4 \geq AlPcS_2 > ZnPcS_4 > ZnPcS_2 > AlPcS_1 > ZnPcS_1$. Thus, overall tumor selectivity decreases with decreased levels of dye sulphonation and by changing from a trivalent central metal ion Al^{3+} to the divalent Zn^{2+}. Similar tumor uptake kinetics have been observed using a series of radioactive labelled [^{65}Zn]ZnpcS derivatives (Scasnar personal communication) suggesting that the observed fluorescence distribution patterns represent actual dye dynamics.

A somewhat inverse correlation between Pc structure and fluorescence is observed in the case of the blood vessels. BV/NT ratios diminish in the following order $ZnPcS_4 > ZnPcS_1 > ZnPcS_2 > AlPcS_1 > AlPcS_2 > AlPcS_4$. Again a marked effect of the central ion and degree of sulphonation is observed with the Zn series in general showing higher vessel retention than the corresponding Al derivatives. The large difference in tissue selectivity between the Al^{3+} and Zn^{2+} complexes likely reflects the presence of an axial ligand in the case of the $AlPcS_n$ which affects aggregation and dye association with macromolecules.

The increased tumor specificity of the higher sulphonated $MPcS_n$ is in agreement with earlier studies on radiolabeled gallium sulphophthalocyanines (Rousseau *et al.,* 1990) and contrasts the poor cell uptake properties of these hydrophillic dyes *in vitro*. Under *in vitro* conditions, particularly the amphiphilic di- and monosulphonated derivatives are readily taken up by cells (Berg *et al.,* 1989; Paquette *et al.,* 1988). Therefore, the relationship between the lipophilicity of the dye and cell uptake *in vitro* is the inverse of findings concerning tumor uptake *in vivo* (Chan *et al.,* 1990) These differences likely reflect the dominant role of the extracellular matrix and stroma of the tumor in accumulating the hydrophillic negatively charged, higher sulphonated

phthalocyanines. Since quantifications of the dyes are based on their fluorescence, differences in aggregation and binding to serum components between the various dyes (which diminishes fluorescence yields) should be taken into account for their potential use as tumor localizers. The presence of more than one sulphonated $MPcS_n$ species in a given dye preparation further affects their tendency to aggregate. Thus our earlier report on the fluorescence ratios of $ZnPcS_2$ (van Leengoed *et al.,* 1991) actually involved a mixture of mono- and disulphonated derivatives ($ZnPcS_{1.5}$) resulting in much higher T/NT fluorescence ratios than those observed with the purified mono- and disulphonated $ZnPcS_1$ and $ZnPcS_2$ fractions used in the present study (Fig. 2).

The profiles of the fluorescence kinetics of the blood vessels are similar for the dyes chelated with either Zn^{2+} or Al^{3+}, although the overall BV/NT ratios for the Zn complexes are substantially higher (Fig. 2). Only two of the dye preparations, i.e. the $AlPcS_4$ and $AlPcS_2$, show higher T/NT than BV/NT ratios, even at 5 min p.i. It is possible that changes in fluorescence yields between plasma bound dyes and interstitial bound dye accumulated in the tumor, contribute to such differences.

In conclusion our data suggest that phthalocyanines chelated with Al^{3+} are better tumor fluorescence probes than dyes bearing Zn^{2+} as the central metal ion. Particularly $AlPcS_4$ and $AlPcS_2$ feature the desired *in vivo* fluorescence distribution profile, suitable for tumor imaging and photodynamic therapy.

Chapter 4

IN VIVO PHOTODYNAMIC EFFECTS OF PHTHALOCYANINES IN A SKIN FOLD OBSERVATION CHAMBER MODEL: ROLE OF CENTRAL METAL ION AND DEGREE OF SULPHONATION

Photochemistry and Photobiology (submitted)

Co-authors
N. van der Veen[1], A.A.C. Versteeg[1], R. Ouellet[2] J.E. van Lier[2] and W.M. Star[1].

[1]Dr. Daniel den Hoed Cancer Center, Rotterdam, The Netherlands.
[2]MRC Group in the Radiation Sciences, Faculty of Medicine, University of Sherbrooke, Sherbrooke, Québec, Canada.

Abstract

Six sulphonated metallophthalocyanines, chelated with either aluminum or zinc and sulphonated to different degree, were studied *in vivo* for their photodynamic activity in a rat skin fold chamber model. The chamber, located on the back of female WAG/Rij rats, contained a syngeneic mammary carcinoma implanted into a layer of subcutaneous tissue. Twenty four hours after i.v. adminstration of 2.5 μmol/kg of one of the dyes, the chambers received a treatment light dose of 600 J/cm^2 with monochromatic light of 675 nm at a power density of 100 mW/cm^2. During light delivery and up to a period of 7 days post treatment, vascular effects of tumor and normal tissue were scored. Tumor cell viability was determined by histology and by reinplantation of the chamber contents into the skin of the same animal, either 2 h post treatment or after the seven day observation period. Vascular effects of both tumor and subcutaneous tissue were strongest with dyes with the lowest degree of sulphonation and decreased with increasing degree of sulphonation. Tumor regrowth did not occur with aluminum phthalocyanine mono- and disulphonate and with zinc phthalocyanine monosulphonate. With the protocol that was used, complete necrosis without recovery was only observed when reinplantation took place at the end of the seven day follow-up period. Reinplantation 2 h post treatment always resulted in tumor regrowth. At this interval, the presence of viable tumor cells was confirmed histologically. In general tumor tissue vasculature was more susceptible to photodynamic damage than vasculature of the normal tissue. The effect on the circulation of both tumor and normal tissue increased with decreasing degree of sulphonation. Based on this study, the photodynamic effects using the six sulphonated metallophthalocyanines on the vasculature can be ranked from high to low as: $AlPcS_2 \approx ZnPcS_1 > AlPcS_1 > AlPcS_4 > ZnPcS_2 > ZnPcS_4$.

Introduction

In photodynamic therapy (PDT) of cancer, light of an appropriate wavelength and dose is applied to activate a photosensitive dye, which is retained in (tumor) tissue after systemic administration. The degree of retention of the dye in tumor tissue, the presence of oxygen and the ability to deliver light in an adequate dose determine the chances of a successful therapy with minimal damage to the surrounding normal tissue. To date most of the clinical experience in PDT is accumulated with hematoporphyrin derivative (HPD) or Photofrin®, a commercial preparation enriched in the active fraction of HPD, as the photoactive drug.

Although the results are encouraging, the prolonged skin photosensitivity and low extinction coefficients at clinically relevant wavelengths are regarded as significant drawbacks.

Because of their high extinction coefficient ($\epsilon \approx 10^5$ M^{-1} cm^{-1}) in the red region of the spectrum (between 670-680 nm) phthalocyanines (Pc) have been suggested as "second generation" photosensitizers for PDT (Spikes, 1986). They are structurally similar to porphyrins, are relatively stable, are active as single products and fluoresce in their active form. These qualities, together with their tumor tissue retention, make them ideal for the combination of tumor tissue localization by fluorescence and photodynamic tumor therapy (for recent reviews see van Lier (1990a) and Rosenthal (1991)).

Complexing the phthalocyanine molecule with a diamagnetic metal ion such as Zn^{2+} or Al^{3+} increases its triplet yield and lifetime. On the other hand, their hydrophobicity causes unsubstituted phthalocyanines to aggregate in an aqueous solution, diminishing its usefulness for biological applications. Adding sulphonate groups to the molecule reduces this tendency and results in a dye with suitable photodynamic properties. The number of sulphonate groups attached to the phthalocyanine molecule is inversely correlated with its hydrophobicity.

Sulphonated metallophthalocyanines ($MPcS_n$) are effective photosensitizers both *in vitro* (Ben-Hur and Rosenthal, 1986; Brasseur et al., 1987; Berg *et al.*, 1989; Peng *et al.*, 1990) and *in vivo* (Brasseur *et al.*, 1987; Tralau *et al.*, 1987) and vascular effects are associated with the photodynamic effects (van Leengoed *et al.*, 1991). However, there is a discrepancy between the localizing properties of $MPcS_n$ *in vivo* and *in vitro* (Chan *et al.*, 1990) and it has become clear that the central metal ion and the ring substituents play a predominant role in the photodynamic properties of phthalocyanines. Much of the earlier work on phthalocyanines has been done with aluminum phthalocyanine tetrasulphonated ($AlPcS_4$). However, this commercial preparation is a mixture of molecules with different degrees of sulphonation with an average of three.

In this paper we have compared the photodynamic activity *in vivo* of six phthalocyanines differing in central metal ion and degree of sulphonation. In particular the vascular effects of PDT using phthalocyanines are discussed with respect to tumor tissue necrosis.

Materials and methods

Photosensitizers

The six species of sulphonated metallophthalocyanines ($MPcS_n$), differing in their central metal ion (Al^{3+} or Zn^{2+}) and degree of sulphonation (mono- di- or tetra-sulphonate) were prepared via the condensation method as previously described (Ali *et al.,* 1988). Homogeneity of the dye preparation was verified by reversed phase HPLC and showed that the disulphonated preparations were enriched in isomers with sulphonate groups on adjacent benzo groups. The concentration of the dye was determined by optical absorbance measurement in DMF using $\epsilon = 2.5 \times 10^5\ M^1\ cm^1$ at $\lambda_{max} = 675$ nm.

Cremophor EL (Sigma) was added to the mono sulphonated phthalocyanines to prevent aggregation and precipitation of the photosensitizer and stock solutions of the individual $MPcS_n$ were supplemented with phosphate buffered saline (PBS) to yield an i.v. injectable solution.

The dyes were administered in a concentration of 2.5 μmol/kg via a tail vein 24 h prior to light delivery.

Animal Model

Twelve to fourteen week old female WAG/Rij rats were obtained from ITRI-TNO, Rijswijk, The Netherlands. The skin fold chamber (Reinhold *et al.,* 1979; Star *et al.,* 1986; van Leengoed *et al.,* 1990), is a 0.5 mm thick layer of subcutaneous tissue of the dorsal skin placed between two transparent covers, one of which can be removed to permit the insertion of approximately 1 mm^3 of syngeneic mammary carcinoma tissue. When placed under a microscope at low magnification, the veins, arteries and the capillary beds of subcutis and tumor tissue can be observed.

During the entire experimental procedure the animals were kept in a temperature controlled (32°C) cabinet. The elevated ambient temperature ensures adequate tumor growth in the chamber. The ambient light level inside the cabinet was reduced to less than 30 $\mu W/cm^2$, providing the animals with a day/night cycle without causing observable photosensitization.

During the preparation procedure, for sedation during therapy and during the follow-up procedures, Hypnorm® (fluanisol/fentanyl mixture, Janssen Pharmaceutics, Beerse, Belgium) was used as a general anaesthetic.

Experimental procedure

Each dye was studied in a group of six animals. Twenty four hours before phototherapy the animals received a dose of 2.5 μmol/kg.

Light of 675 nm was obtained from an argon-dye laser (Spectra Physics system 171), with DCM (4-dicyanometyhlene-2-methyl-6(P-dimethylamino-stytyl)-4H-pyran) as the lasing dye. Through an optical fibre and a lens system with diaphragm, the laser light was delivered through the stage of a microscope and directed to the back of the chamber. The circular beam covering the entire chamber (10 mm diameter), had an incident power density of 100 mW/cm^2 at the surface of the chamber as measured by a Spectra Physics 404 power meter. In order to deliver a light dose of 600 J/cm^2, an illumination period of 100 min. was required.

During PDT and up to 7 days after PDT the damage to the vasculature of tumor and normal tissue was rated on a 0-8 scale. A score of 0 corresponds to no observable damage whereas a score of 8 means no observable circulation. Two hours after PDT one chamber of each experimental group was fixed in formaldehyde. The tissue was removed from the chamber, embedded in paraffin, cut in 10 μm sections and stained with Haematoxylin-Eosin. At the same two hour interval after PDT, the chamber of two animals from each group was removed and their content was transplanted into the flank of the same animal. In the remaining three animals the vascular damage score was determined daily until 7 days post treatment. Then, these chambers were also removed and the remainder of the treated tissue transplanted into the flank of the animal. The animal was observed for a 100 days for the occurrence of tumor regrowth.

Results

At different stages during and after light delivery a number of aspects of vascular damage could be distinguished in our model system. A typical sequence of vascular effects that will lead to tissue necrosis may start with spasm of the arteries in the chamber (Fig. 1B). This vascular spasm may be followed by ischaemia (blanching of the tumor) and a reduction of the red blood cell column diameter in the larger venules (Fig. 1C). The capillaries may become dilated and packed with red blood cells. Eventually stasis will occur not only in the capillaries, but also in the larger vessels. Extravasation of blood, especially in the tumor area, may then also be observed. If these severe vascular effects are maintained over a period of more than one day, tissue necrosis occurs. When the vascular effects were less, then the larger vessels remained intact and the recovery of the capillary bed of the tissue was observed.

The circulation damage score ranging from 0 to 8 was assessed separately for tumor and surrounding normal tissue and shown in fig. 2 A-D. Vascular damage was least with $MPcS_4$, a circulation stop occurred only with $AlPcS_4$ (Fig 2B) and

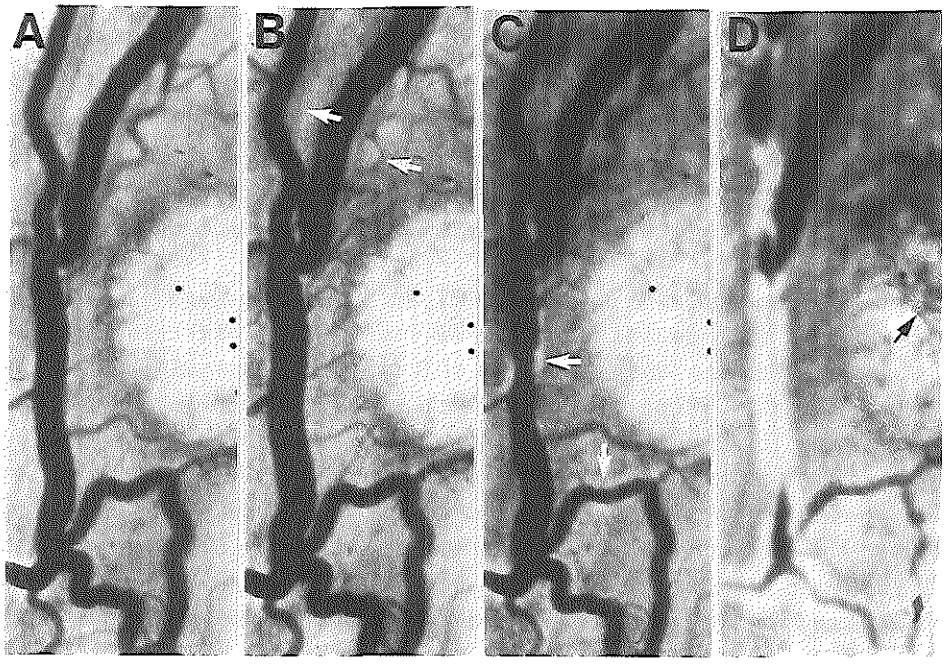

Fig. 1. Observation chamber vasculature before (A) and during illumination at 15 min.(B), 60 min (C) and 2 h after the end of treatment (D). The animal was sensitized with $ZnPcS_2$ and the chamber received a total light dose of 600 J/cm² (100 min. × 100 mW/cm²). Arrows indicate the disappeared artery (b) and the reduced diameter of the vein (C). Reperfusion after treatment (D) often results in extravasation of blood from the capillaries.

this is observed only 2 h post treatment. Tumor regrowth was observed in all cases when reinplantation was performed either 2 h or 7 days post treatment. Stronger vascular effects were observed with $MPcS_2$ where $ZnPcS_2$ as well as $AlPcS_2$ caused maximum circulation damage scores both in tumor as in normal tissue. In one animal that was injected with $ZnPcS_2$ (Fig 2A), thrombi were observed after 60 minutes of light delivery. Two hours post treatment, complete stasis in the tumor tissue was observed, but the circulation started to recover 2 days post treatment. In the normal tissue (Fig. 2C) a complete stop of the circulation was never observed and tumor regrowth occurred in all instances like with $MPcS_4$. In chambers treated with $AlPcS_2$ maximum damage scores were observed not only in tumor tissue but also in normal tissue and this effect persisted during the entire observation period (Fig. 2B-D). Tumor regrowth was observed only when reimplantation was performed two hours post treatment

and not after reinplantation at the end of the 7 day observation period. At this interval the tissue had not yet become necrotic. Vessel constriction, especially of the arteries, was observed with both dyes, but was most striking with $ZnPcS_2$ where it was observed already at 5 min. after the beginning of the light delivery.

In $MPcS_1$, circulation damage patterns similar to those observed with $AlPcS_2$ were seen. Here also viable tumor cells were apparently present 2 h post treatment but reimplantation after the 7 day observation period did not result in tumor regrowth. When comparing the two monosulphonated dyes, vascular spasm of the arteries again was most prominent with the Zn^{2+} dye. In chambers of animals that received $ZnPcS_1$, thrombi in the venules were observed in four animals, already 15 minutes after the start of the light treatment. These thrombi usually did not form a permanent obstruction of the blood vessel as reperfusion was often observed. Of all dyes studied the vascular effects observed in the tumor were always stronger than those observed in the normal tissue.

Discussion

Vascular effects

The mechanism of phthalocyanine induced PDT damage, in terms of vascular damage leading to tumor cell death, as a result of hypoxia and nutritional deficiency, is comparable with damage patterns observed during HPD-PDT (Star *et al.,* 1986). The vascular effects observed range from a small reduction of blood flow with full recovery, to complete stasis sometimes followed by (partial) reperfusion with extravasation of blood from the capillary bed, leading to necrosis of the entire treated area. Stasis can occur due to swelling of erythrocytes in the capillaries or thrombus formation and as a result of endothelial damage (Ben-Hur *et al.,* 1990; Ben-Hur *et al.,* 1988), resulting in vascular occlusion (Star *et al.,* 1986; Reed *et al.,* 1988). Both phenomena have been observed during these experiments.

Focal or total vasoconstriction can be the result of nervous stimulation and could easily be mistaken for thrombi formation along the vessel wall. Edema in the chamber could also lead to compression of vessels, resulting in a similar reduction of the red blood cell column diameter. Although this could be considered an artefact, the reperfusion that is often observed after treatment indicates that edema itself cannot be the only explanation of a reduction in diameter of the red blood cell column. Furthermore, increased interstitial pressure as a result of an increase of vascular permeability e.g. due to inflammation, is a naturally occurring phenomenon in tissue.

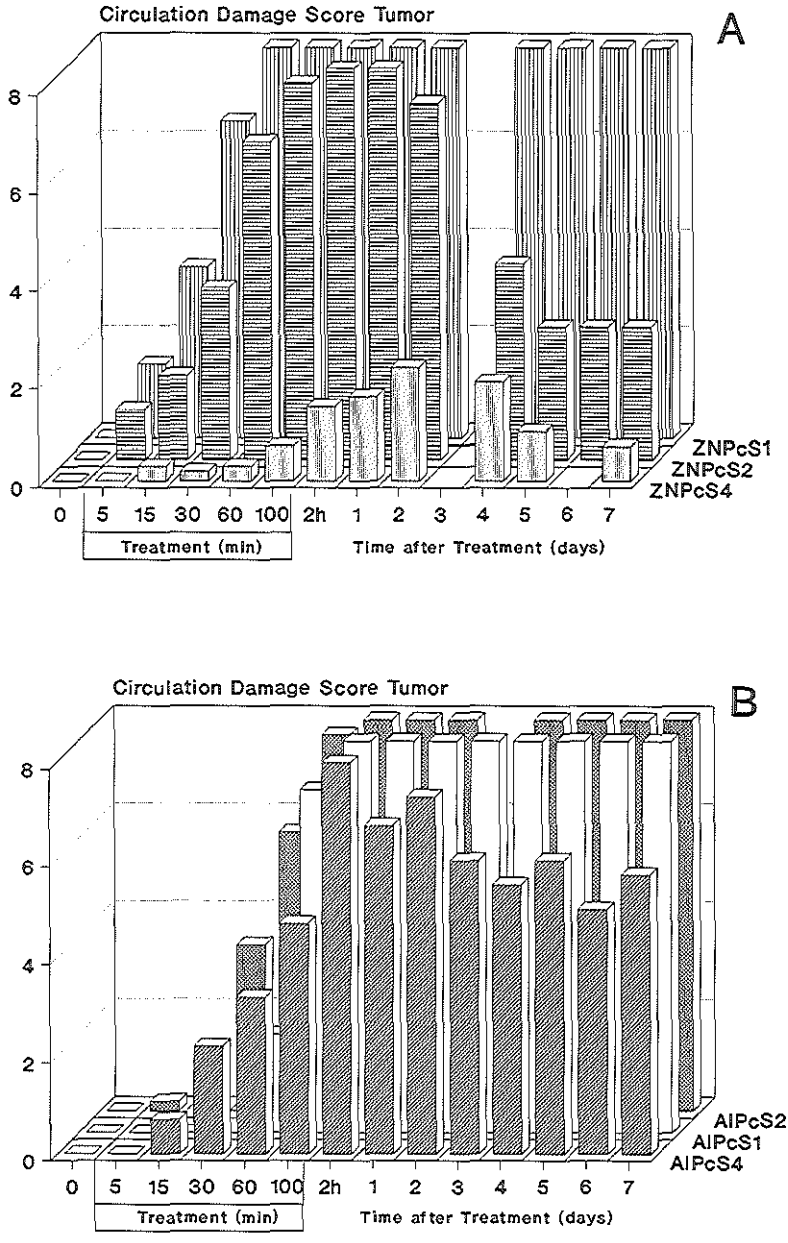
Circulation Damage Score Tumor
A
8
6
4
2
0
0 5 15 30 60 100 2h 1 2 3 4 5 6 7
Treatment (min)
Time after Treatment (days)
ZNPcS1
ZNPcS2
ZNPcS4
Circulation Damage Score Tumor
B
8
6
4
2
0
0 5 15 30 60 100 2h 1 2 3 4 5 6 7
Treatment (min)
Time after Treatment (days)
AlPcS2
AlPcS1
AlPcS4

Figure 2 (A-B)

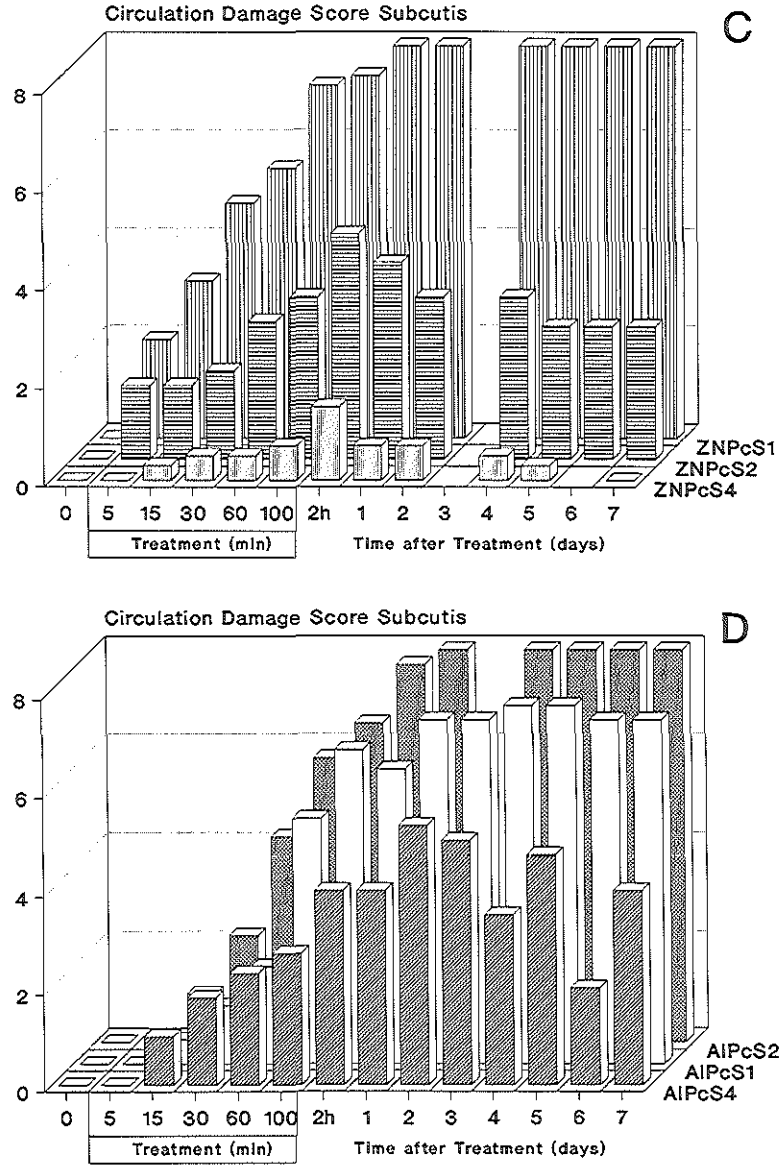

Fig. 2. Circulation damage scores of tumor tissue (2A-B) and normal tissue (2C-D) for the six different dyes in this study during and after a treatment light dose of 600 J/cm^2 (100 × 100 mW/cm^2) 24 h after administration. The values are group averages of 6 animals until 2 h and 3 animals for the remaining time. The damage scores range from 0 (no observable damage) to 8 (no observable circulation). The duration of illumination is expressed in minutes.

Photosensitizer qualities

Photodynamic therapy using the experimental parameters in this study resulted in sufficient vascular damage to induce full necrosis of both tumor and normal tissue in the chamber when the monosulphonated Pc's or $AlPcS_2$ were used as photosensitizer. The lack of recovery of the circulation from the damage caused by the treatment, separates the effects of these three dyes from both tetrasulphonated Pc's and $ZnPcS_2$. These observations agree with what has been found for PDT effects both *in vitro* and *in vivo* by others (Paquette *et al.,* 1988; Brasseur *et al.,* 1988; Berg *et al.,* 1989; Peng *et al.,* 1990). *In vivo* the fluorescence localization of Pc's for tumor tissue is inversely related to the degree of sulphonation (Chan *et al.,* 1990), and was confirmed by our own pharmacokinetics study (van Leengoed *et al.,* 1992).

Tumor, as well as normal tissue vessel damage generated by the six dyes in this study can be ranked from high to low as: $AlPcS_2 \approx ZnPcS_1 > AlPcS_1 > AlPcS_4 > ZnPcS_2 > ZnPcS_4$. Although the vascular effects in the tumor vessels were more predominant than in normal tissue, and extravasation was mostly seen in the tumor area, these effects differed only quantitatively from the normal tissue vascular effects. It is important to note that tumor tissue contains only capillaries, whereas the surrounding normal tissue also includes larger vessels which are less sensitive to PDT damage than capillaries.

Differences in direct killing of tumor cells between the different dyes could not be determined in this *in vivo* model. The reimplantation assay only revealed the presence of sufficient viable tumor cells to give rise to tumor growth, a method not very sensitive to the number of surviving cells. Moreover histology at two hours post treatment was not conclusive in predicting the success of the treatment. Perhaps the interval between the end of the treatment and histology should be increased in order to reveal the cellular and vascular effects leading to success or failure of the treatment. On the other hand both tests revealed that viable tumor cells were present two hours after treatment, for all dyes tested, stressing the importance of the indirect effects in PDT with these dyes.

Light dose

A total light dose of 600 J/cm² is rather high and seems impractical in a clinical setting. In the same chamber model, in order to achieve a similar 100 % tumor necrosis using HPD (15 mg/kg), a light dose of 160 J/cm² (630 nm) was required (Star *et al.,* 1986). Practically tumor necrosis was equivalent to total necrosis of the chamber.

A number of aspects should be taken into consideration with respect to the high light dose that was needed. In the present study the light dose was chosen

high enough to evoke a vascular response even in the higher sulphonated, less photodynamically active Pc's. The sensitizer dose used was relatively low compared to other studies where it varies between 0.2 to 25 mg/kg and with 5 mg/kg as the dose most commonly used drug dose. In spontaneous tumors, complete responses have been reported with Pc using a drug dose of 1 mg/kg and a total light dose of 50-100 J/cm^2 in various animals and a variety of tumors (Roberts *et al.,* 1991). Our drug dose was chosen to accommodate the study of the fluorescence pharmacokinetics of these dyes, the results of which will be published in a separate paper (van Leengoed *et al.,* 1992). Both monosulphonated Pc's and $AlPcS_2$ will probably also be effective at a much lower light dose as they showed maximum damage scores at 600 J/cm^2. At a low photosensitizer dose photobleaching might become a critical factor. Possibly a sixfold increase of the sensitizer dose to 15 μM/kg, to match the dose of HPD described above, probably can lead to a reduction of the treatment light dose by more than a factor of six (less than 100 J/cm^2).

Light source

Using a laser to deliver the treatment light might be another source of variation. In a wavelength range of 670-680 nm, the Pc's have a narrow absorption band. A small shift of this band in a biological environment could result in a dramatic decrease of the light absorption at the wavelength the laser is emitting. Therefore in order to deliver light at the proper wavelength, the *in vivo* absorbance of the Pc's is of vital importance. This information is lacking at present. A study of the *in vivo* action spectrum of HPD-PDT has shown that a shift of 5 nm can considerably reduce the biological effectiveness of PDT (Kessel, 1982). Exciting with a broader wavelength band using a lamp with filters as a light source is much less efficient than laser light. On the other hand when using the broader excitation band, one may still cover the absorbtion maximum of the dye despite possible shifting.

In conclusion, we have shown that *in vivo* PDT effects on the vasculature increase with decreasing degree of sulphonation of $MPcS_n$. Al-based phthalocyanines caused more vascular damage leading to tumor necrosis than Zn-based phthalocyanines and were also more effective in causing tumor necrosis. Our experiments confirm the importance of vascular damage in the PDT effects of Phthalocyanines. By comparing the role of the central metal ion and degree of sulphonation, $AlPcS_2$ emerges as the $MPcS_n$, best suited for photodynamic therapy. From fluorescence pharmacokinetics studies performed on the same $MPcS_n$, $AlPcS_2$ also emerged as a good tumor localizer making the dye an interesting candidate for further study.

Chapter 5

IN VIVO FLUORESCENCE AND PHOTODYNAMIC ACTIVITY OF ZINC-PHTHALOCYANINE LIPOSOME ADMINISTERED

British Journal of Cancer (submitted)

Co-authors
V. Cuomo[2], A.A.C. Versteeg[1], N. van der Veen[1], G. Jori[2] and W.M. Star[1]

[1]Dr. Daniel den Hoed Cancer Center, Rotterdam, The Netherlands.
[2]Dept. of Biology, University of Padova, Padova, Italy.

Abstract

Zinc(II)-phthalocyanine, a hydrophobic photosensitizer dye, was incorporated in unilamellar liposomes and studied *in vivo* for fluorescence kinetics and photodynamic activity. An observation chamber mounted in a dorsal skin fold of female WAG/RIJ rats was used as a model system. In the chamber, an isogeneic mammary carcinoma was transplanted in the subcutaneous tissue. Phthalocyanine fluorescence was excited at 610 nm with a power density of 0.25 mW/cm^2 and was detected above 665 nm through a high pass filter using a two stage image intensifier coupled to a CCD camera. Following i.v. administration of 0.14 mg/kg of the drug, the fluorescence pharmacokinetics of the dye in vasculature, normal tissue and tumor tissue was determined as a function of time. After injection, tumor fluorescence increased slowly to a maximum about 3 h post injection, and remained well above the normal tissue fluorescence till 24 h post injection. Fluorescence in the circulation was always stronger than in the tissues. A treatment light dose at a wavelength of 675 nm was delivered 24 h p.i.. One group of 6 animals received a total light dose of 150 J/cm^2 (100 mW/cm^2). A second group of 6 animals received a total light dose of 450 J/cm^2 at the same dose rate. Vascular damage resulting from treatment was observed only at the final stages of the irradiation, despite the relatively high levels of fluorescence in the circulation. Immediate post treatment (re)transplantation of the content of the chamber into the flank always resulted in tumor regrowth, confirming the presence of viable tumor cells following PDT. When the chamber was left intact, the light dose of 450 J/cm^2 yielded complete tissue necrosis.

Introduction

In photodynamic therapy (PDT) the goal is to achieve tumor necrosis with minimal damage to normal tissue using local activation by light of a photosensitizer that is retained in the target tissue. PDT is currently undergoing clinical evaluation with Photofrin® as photosensitizer, a preparation obtained from hematoporphyrin derivative (HPD) and enriched in the active fraction. At the same time phthalocyanines are being investigated as alternative photosensitizers for PDT (Ben-Hur and Rosenthal, 1986). They are structurally similar to porphyrins but in contrast have a high extinction coefficient in the 670-690 nm range. At this wavelength tissue penetration of light is deeper than at 630 nm where porphyrins are excited.

Phthalocyanines have a strong tendency to aggregate which renders them unsuitable for systemic administration. Adding sulphonic acid groups to the molecule (Brasseur *et al.,* 1987; Tralau *et al.,* 1987) however yields photodynamically active, water soluble derivatives. Their synthesis is relatively easy. The subsequent purification on the other hand can be quite elaborate. Cutaneous photosensitivity resulting from phthalocyanine administration is reported to be much less than from Photofrin® (Tralau *et al.,* 1989). The dye is stable in a biological environment and shows fluorescence in its monomeric, active form. Its fluorescence can therefore be exploited for tumor localizing purposes, but contrary to photofrin®, also gives information on local dye concentration (MacRobert *et al.,* 1989). Phthalocyanines have been shown to photosensitize malignant cells both *in vitro* and *in vivo* (for a recent review see Rosenthal (1991) and van Lier (1990)).

Tumor localization of the sulphonated phthalocyanines is greatly influenced by the lipophilic nature of the drug. From work of others (Chan *et al.,* 1990) and also by our own observations it has been shown that fluorescence based tumor localization of sulphonated phthalocyanines is positively correlated with the degree of sulphonation of the phthalocyanine molecule (van Leengoed *et al.,* 1992). However when photodynamic activity with respect to tumor necrosis is concerned, the degree of sulphonation is inversely related to the effect, favouring lipophilic dyes over hydrophillic dyes (Brasseur *et al.,* 1988; Berg *et al.,* 1989). Instead of adding sulphonate groups to the molecule to increase the water solubility, liposomes can be used as a carrier system making the lipophilic drugs suitable for biological application. *In vivo*, liposomes associate with the lipid core of lipoproteins. Especially low density lipoproteins (LDL) have a high affinity for tumor cells through a receptor mediated transport mechanism (Goldstein *et al.,* 1979). Liposomes have been shown to facilitate efficient targeting *in vivo* by water insoluble porphyrins (Jori *et al.,* 1983) as well as by Zn(II)phthalocyanine (Zn(II)Pc) (Reddi *et al.,* 1987) at very low dosages.

In this paper, we describe the *in vivo* fluorescence kinetics of this drug-carrier complex and determine the *in vivo* effects of subsequent optical irradiation on tumor necrosis using a dorsal skin fold chamber model. The role of the vascular effects resulting from treatment and quenching of photoproducts by the carrier complex of the photosensitizer present in the circulation, will be discussed.

Materials and Methods

Animal model

Female Wag/Rij rats (ITRI-TNO, Rijswijk, The Netherlands) 12-14 weeks of age were used. During a three week preparation period the animals were equipped with a skin fold chamber on their backs. The chamber includes a 0.5 mm layer of subcutaneous tissue, wedged between two transparent covers. Into the subcutaneous tissue of the chamber an isogeneic mammary carcinoma was transplanted. The animal model permits observation of the pharmacokinetics of photosensitizers based on fluorescence and the assessment of vascular effects resulting from photodynamic therapy (Star *et al.*, 1986; van Leengoed *et al.*, 1990). Hypnorm® (Janssen Pharmaceuticals, Beerse, Belgium) was used as a general anaesthetic during all procedures. In accordance with the Dutch law on animal experiments, the protocol was submitted to and approved by the animal experiments committee.

Drug-carrier system

Zn(II)Phthalocyanine (Ciba-Geigy, Basel, Switzerland) incorporated into unilamellar liposomes was prepared as previously described (Valduga *et al.*, 1987). Briefly, a small volume of a mixture of Zn(II)Pc dissolved in pyridine (Janssen pharmaceuticals, Beerse, Belgium) and dipalmitoylphosphatidylcholine (DPPC) dissolved in ethanol was slowly injected into saline of 55° C using a microsyringe. The suspension was dialysed for 3 h against two times 500 ml saline to remove pyridine. The resulting dye concentration was measured by optical absorbance using a Lambda 5 (Perkin Elmer) spectrophotometer ($\epsilon = 2.41 \times 10^5$ M^{-1} cm^{-1} at λ_{max}). A calculated volume of the liposome suspension supplemented with phosphate buffered saline (PBS) was administered via a tail vein of the animals resulting in a dye concentration of 0.14 mg/kg rat.

Fluorescence detection

Fluorescence was excited at 610 nm with a fluence rate of 0.25 mW/cm² and detected above 665 nm using an intensified CCD-camera. Digitized fluorescence images obtained from the fluorescence detection system were used to measure average grey scale values of selected areas of interest of blood vessel, tumor and normal tissue. To minimize individual differences these values were used to express fluorescence of tumor tissue and blood vessels as averaged ratios relative to normal tissue (subcutis) values.

Experimental procedure

In order to establish the optimum dose for fluorescence detection and PDT, the first series of experiments was performed in a pilot study on 14 animals, varying drug dose, light dose and interval between drug administration and treatment. All experiments began when the tumors in the chambers had reached a diameter of 2-3 mm. Two drug doses were compared: 0.14 mg/kg and 0.21 mg/kg. The animals were anaesthetized and following the recording of an autofluorescence image the dye-carrier complex was administered via a tail vein of the animal. At 5 minutes and at 24 h p.i., fluorescence images were recorded.

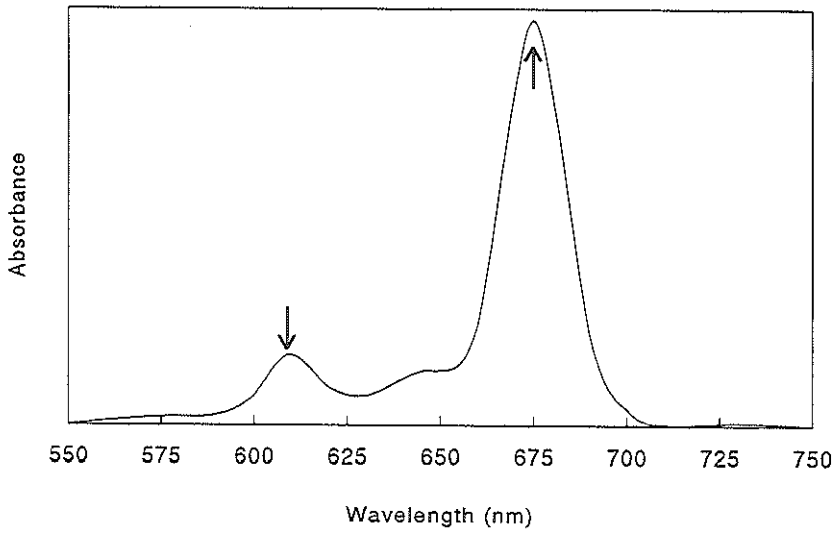

Fig. 1. Absorbtion spectrum of zinc-phthalocyanine in pyridine. The two excitation wavelengths used in this study, 610 and 675 nm, are indicated by arrows.

Twenty four hours after dye administration, a treatment light dose of 450 or 900 J/cm² was delivered to the chamber, using an irradiance of 100 mW/cm² at 610 nm, obtained from an argon ion pumped dye laser system (Spectra Physics 171 + 375). The wavelength of 610 nm is at the fluorescence excitation maximum closest to the fluorescence emission wavelength of 675 nm (Fig. 1).

In this pilot study Rhodamine was used as the lasing dye because fluorescence was the primary objective. With Rhodamine it is not possible to generate light of 675 nm, the wavelength at which ZnPc has maximum light

absorbtion. Therefore, when it was later decided to include PDT, this was performed at 610 nm. In the subsequent series of experiments DCM (4-dicyanometyhlene-2-methyl-6(P-dimethylaminostytyl)-4H-pyran) was used as the lasing dye, because it allows generation of both 610 and 675 nm light (see below).

After treatment the vascular effects were scored for a period of 7 days using a microscope at low magnification. After the observation period the content of the chamber was transplanted subcutaneously into the flank of the same animal to obtain a estimate of tumor cell viability.

All subsequent series of experiments were performed using a drug dose of 0.14 mg/kg (see discussion). In a group of 6 animals, fluorescence pharmacokinetics was observed at 5, 15, 30, 60, 120, 180 240, 300, 360 min. and at 24 h p.i. respectively. Each digitized image was accompanied by a similar image of a piece of reference material (coloured plastic). This enabled correcting the fluorescence image for inhomogenities in the detection system optics and variations in laser output. Twenty four hours p.i. a treatment light dose of 150 J/cm^2 (100 mW/cm^2, 675 nm) was delivered to the chamber. During and after treatment, vascular effects of tumor and normal tissue were scored on a 0 to 8 scale. A score of 0 corresponds to no observable effect on the vasculature whereas a score of 8 indicates no circulation. Two hours after treatment one chamber was prepared for histology and from two animals the content of the chamber was transplanted into the flank of the same animal. In the remaining three animals transplantation was performed at the end of a seven day follow-up period during which the vascular damage was assessed daily. In order to achieve tumor necrosis, in a third group of six animals, the therapeutic light dose was increased to 450 J/cm^2.

Results

In the pilot experiments, both fluorescence excitation and photodynamic therapy were performed using light of 610 nm (see Materials and Methods). The results of these experiments are summarized in Table 1.

Tumor fluorescence (c) showed little selectivity with 0.21 mg/kg and exceeded the background in only 3 out of 10 animals. Complete necrosis (f) was observed at both light dosages using a drug dose of 0.21 mg/kg. A light dose of 900 J/cm^2 was required when a drug dose of 0.14 mg/kg was used. When retransplantation took place immediately following therapy, tumor regrowth was observed with both drug doses.

Figure 2 shows digital fluorescence images of liposome bound phthalocyanine in the chamber model before and at 4 different intervals after i.v. administration of 0.14 mg/kg. Note that the fluorescence of tumor and blood vessel increases following administration and that even at 24 h both tumor and blood vessels fluorescence exceed that of the normal tissue.

Table 1. Results of the pilot experiment comparing: drug dose (a), treatment interval (d) and light dose (e) with the results of tumor fluorescence (c) and treatment effect specifically with respect to complete necrosis of tumor and normal tissue (f) as well as tumor regrowth (g) for a total of 14 animals (b). Treatment light of 610 nm wavelength was delivered to the chamber at an irradiance of 100 mW/cm².

Zn-Pc (mg/kg)	No.	Flu 24 h	Interval p.i. h	Light (J/cm²)	Complete Necrosis	Regrowth
a	b	c	d	e	f	g
	2		24	450	-	2
0,14		4/4				
	2		24	900	1	1
	2 + 2		24 & 48	450	1 + 1	2
0,21		3/10				
	4 + 2		24 & 48	900	1 + 1	4
	14				5 +	9

The fluorescence signals of tumor, blood vessel and normal tissue following i.v. administration of the drug are expressed as averaged grey scale values in Fig. 3. After the dye has been administered, fluorescence in the blood vessels increases slowly, reaching a plateau at 120 min. p.i. Then, the fluorescence signal remains stable but the ratio starts to decline (Fig. 4), due to the slow increase of fluorescence in the normal tissue. Tumor tissue versus normal tissue ratios increase even more slowly, reaching a maximum value approximately 5 h p.i. Two hours p.i. a ratio of two is exceeded and this level is maintained over a three hour period between 2 and 5 h p.i. Interestingly, at 24 h p.i., the fluorescence in both the tumor and the circulation exceed that of the normal tissue.

Twenty four hours p.i., a treatment light dose of 150 J/cm² (100 mW/cm², 675 nm) was administered to the chamber. This light dose was based on a ratio of about 6 between the optical absorbtion of ZnPc at 675 and 610 nm (see also discussion). With this light dose complete necrosis was never observed. Retransplantation, either two hours after treatment or at the end of the observation period, consistently resulted in tumor regrowth. The presence of vital tumor cells was confirmed by histology.

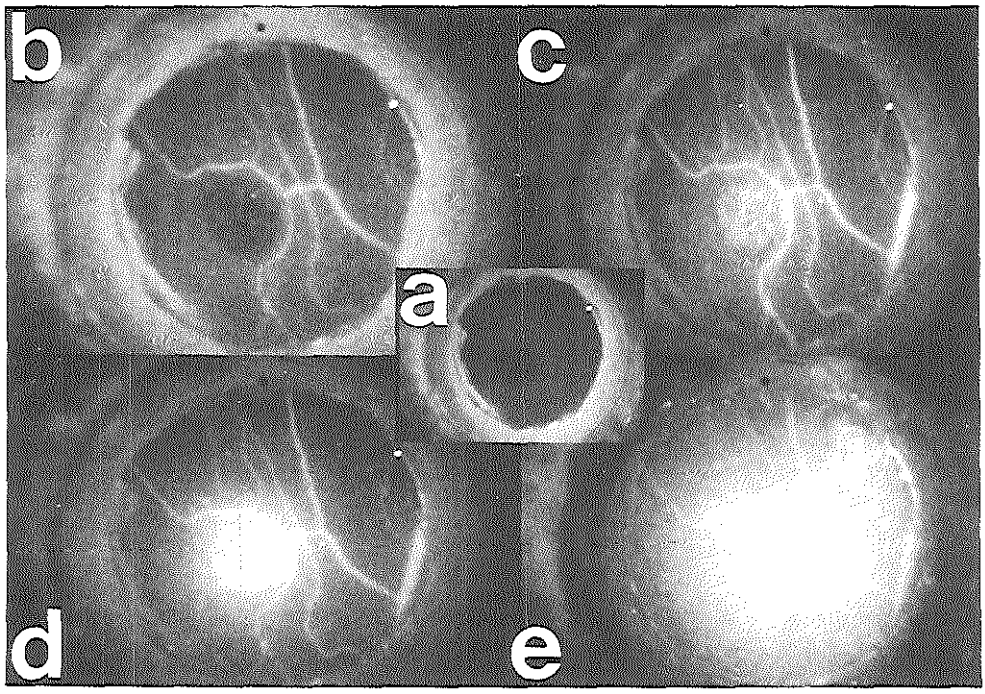

Fig. 2. Digitized fluorescence images of ZnPc-lip taken before (center), 5 (A), 60 (B), 360 min. (C) and at 24 h p.i. (D). Note the tumor fluorescence at 360 min and the persistence of fluorescence in the circulation. In terms of average grey scale values, fluorescecne of the tumor still exceeds values of the normal tissues at 24 h p.i.

In order to achieve tumor necrosis it was decided to increase the dose to 450 J/cm²and the averaged circulation damage scores of the third group of 6 animals are shown in Fig. 5. Using this light dose, maximum damage scores were observed in tumor tissue starting with day one. A small recovery of the circulation in the normal tissue of one animal resulted in the drop of the average damage score below 8 but the damage score in tumor tissue remained maximal

during the observation period. Complete necrosis without recovery was observed in all three cases that were monitored during the whole observation period. When the content of the chamber was retransplanted 2 h after treatment regrowth was observed. Histology performed at the same interval again demonstrated the presence of vital tumor cells. During treatment the vascular effects appeared minimal, increasing only during the last 15 min. of the total treatment time of 75 min.

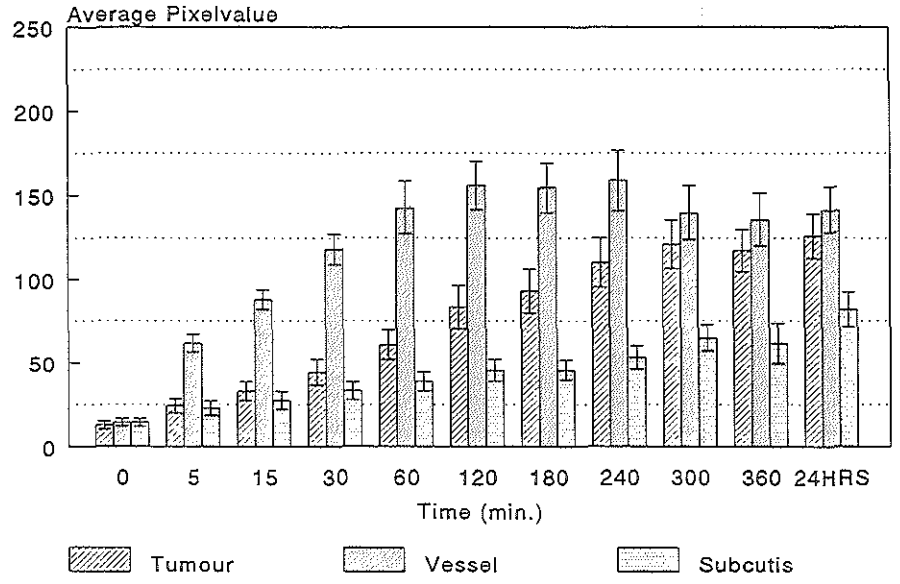

Fig. 3. Fluorescence pharmacokinetics of ZnPc-lip following i.v. administration of 0.14 mg/kg of the drug-carrier complex. Fluorescence was measured as grey scale values and averaged over 6 animals.

Discussion

Hydrophobic photosensitizers like ZnPc, which have excellent photochemical and photophysical properties for PDT, but will aggregate in an aqueous environment, can be incorporated into liposomes and administered systemically. In this way about 30 % of liposome bound photosensitizers can be selectively transferred to LDL (Jori, 1989). These lipoproteins can be endocytosed by neoplastic cells through a specific receptor mediated pathway. Several malignant tissues have an elevated numbers of LDL receptors (Spikes and Jori, 1987). A large amount of drug can thus be accumulated by the tumor tissue in spite of the low injected doses (Reddi *et al.*, 1987).

During the pilot experiment, laser light of 675 nm was not available. The photosensitizer was therefore excited at 610 nm, a local maximum in the absorbtion spectrum (Fig. 1). This wavelength was also used for fluorescence excitation. Based on the results of this pilot study a sensitizer dose of 0.14 mg/kg was selected as optimal to study both fluorescence pharmacokinetics and photodynamic effects of the drug-carrier complex.

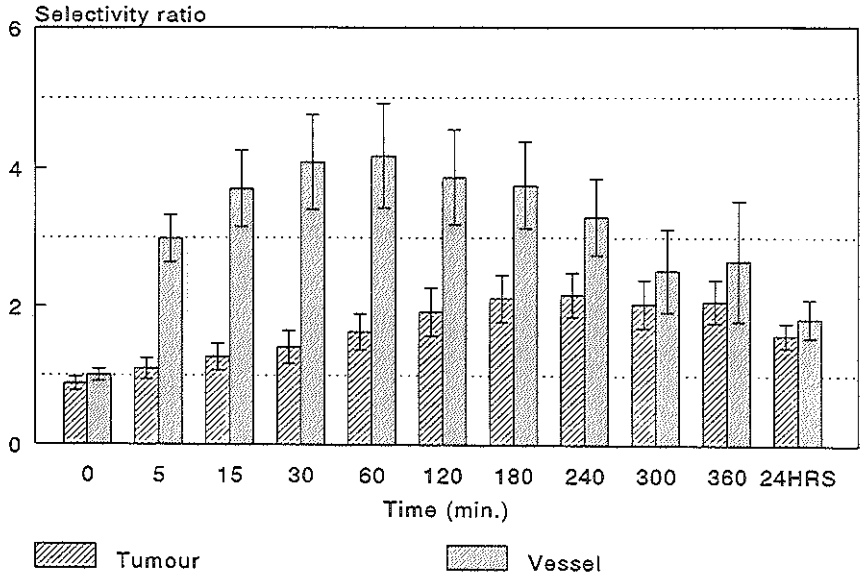

Fig. 4. Averaged ratios ± SEM of tumor tissue fluorescence and blood vessel fluorescence relative to normal tissue (subcutis) fluorescence following dye administration (0.14 mg/kg).

Although a larger photosensitizer dose was expected to result in increased phototoxicity, the increase in normal tissue fluorescence using 0.21 mg/kg had an adverse effect on the tumor over normal tissue fluorescence ratio. This was caused by the increased fluorescence in the normal tissue. The sensitizer dose of 0.14 mg/kg in combination with treatment light of 610 nm and a total light dose of 900 J/cm^2 was sufficient to cause tumor necrosis. This light dose was rather high but should be viewed with regard to the low extinction coefficient of ZnPc at this wavelength (see below for 675 nm).

Phthalocyanine fluorescence can be employed as a diagnostic tool to monitor the presence of the photosensitiser in its monomeric, active state (MacRobert *et al.*, 1989). Detecting HPD or Photofrin® in this way is more complicated because

these drugs contain a number of components with different relationships between fluorescence and photodynamic activity.

After administration of the dye-carrier complex, a gradual accumulation of fluorescence in the circulation as well as in the tumor (Fig. 3) is observed. Interestingly the fluorescence in the circulation reached its peak only 120 min. p.i.. When studying sulphonated phthalocyanines in the same chamber model, usually a fluorescent angiogram with the highest intensity in the circulation is observed immediately p.i., followed by a gradual decrease of the fluorescence in time (van Leengoed *et al.,* 1990). The increase of the fluorescence in the circulation till 120 min. p.i. might be explained by considering the self-quenching of fluorescence due to the relatively high concentration of the photosensitizer in the carrier system.

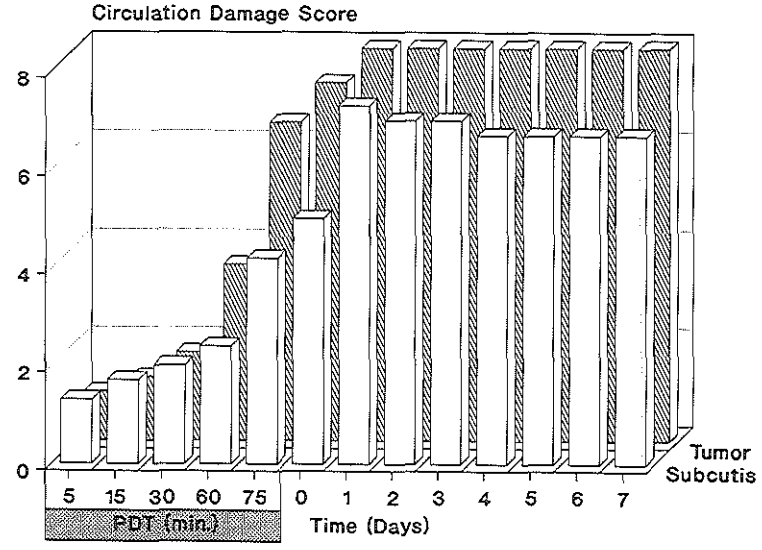

Fig. 5. Circulation damage scores of tumor tissue and normal tissue, during and after a treatment light dose of 450 J/cm² (100 mW/cm²,675 nm) 24 h after i.v. administration of ZnPc-lip. Scores range from 0 (no observable damage) to 8 (no observable circulation). Values are averaged over 6 animals and the duration of the treatment is expressed in minutes.

This increase of fluorescence could represent the release process by the carrier system of the photosensitizer similar to what has been described for fluorescein (Weinstein *et al.,* 1977).

The fluorescence signal in tumor tissue increases even more slowly than the fluorescence in the circulation. This observation probably relates to the fact that the liposome bound ZnPc is taken up by lipoproteins before being accumulated by the tumor cells through an active process. Between 3 and 5 h p.i. the tumor fluorescence exceeds a ratio of 2 (Fig. 4) making it well detectable against the normal tissue fluorescence which hardly increases during this interval. This interval could therefore be utilized for tumor detection. The limited increase of fluorescence in the normal tissue also contributes to the fact that at 24 h p.i. both tumor and blood vessel fluorescence remain detectable. When tested in the same tumor model system at 24 h p.i., HPD and Photofrin® fluorescence usually appeared lower in the tumor than in the normal tissue.

Exciting the photosensitizer at 610 nm with 900 J/cm^2 resulted in tumor necrosis in one out of two animals using a sensitizer dose of 0.14 mg/kg. When the sensitizer was excited at 675 nm, a sixfold reduction of the total light dose was expected to yield similar results. This idea was based on the fact that phthalocyanine absorbtion at 675 nm appeared at least 6 fold larger than at 610 nm (Fig. 1). Actually, one day after treatment the vasculature of the normal tissue was already recovering and tumor regrowth was always observed. On the other hand tumor necrosis was achieved when a light dose of 450 J/cm^2 was used but this light dose also caused a maximal effect on the normal tissue circulation. To explain these observations we propose that *in vivo*, aggregation of the dye may occur and this will result in a reduction of the actual differences in optical absorption.

A drug dose of 0.14 mg/kg can be considered very low compared to the dose of Photofrin® (10 mg/kg) or sulphonated phthalocyanines (2.5-5 mg/kg) used in experiments with rats. The fact that tumor necrosis was observed with this low drug dose suggests that the targeting of the photosensitizer using liposomes as carriers is effective.

Targeting of the photosensitizer towards individual tumor cells is expected to result in more direct cell kill (Zhou *et al.*, 1988). However from our data it appears that the number of tumor cells killed directly is not sufficient for tumor control. Retransplantation immediately after treatment always resulted in tumor regrowth. Moreover, viable tumor cells were confirmed histologically 2 h after treatment. Tumor cell kill cannot be quantified using our method. It only allows the demonstration of the presence or absence of tumor cells capable of causing tumor regrowth. Tumor control by PDT with ZnPc-lip therefore probably requires vascular damage in a margin of normal tissue about the tumor.

During the first 5 min. of illumination, vasospasm of arteries was the most striking vascular effect that was observed. This vasospasm usually disappeared

within the first 30 min. of irradiation. In comparable experiments using sulphonated phthalocyanines similar vasospasm of the arteries was observed. These effects were stronger using dyes chelated with zinc as a central metal ion compared to aluminum. The vasospasms were considered to cause hypoxia and assuming that oxygen is indispensable for Pc-PDT (Bown *et al.,* 1986) thereby negatively influencing the effectiveness of the photochemical reaction. Using liposome bound ZnPc it seems that after the initial response of the artery to the treatment, arterial blood supply is restored till the end of treatment. During the period of illumination no thrombi or vasoconstriction of the larger veins could be observed. By the end of the treatment period stasis was observed predominantly in the capillary bed of both tumor and surrounding normal tissue. However, judging from the initial vasospasms and damage to the capillary bed, the endothelium is likely to be a target for PDT using ZnPc-lip. These findings agree with what has been found by Milanesi (1987) and Evensen (1983). The vascular effects reach their maximum values between 2 h post therapy and day 1 (Fig. 4) and cannot be distinguished from the inflammatory response to the treatment.

Chapter 6

FLUORESCENCE AND PHOTODYNAMIC EFFECTS OF BACTERIOCHLORIN *a* OBSERVED *IN VIVO* IN "SANDWICH" OBSERVATION CHAMBERS.

British Journal of Cancer (accepted)

Co-authors
J.J. Schuitmaker[2], N. van der Veen[1], T.M.A.R. Dubbelman[3] and W.M. Star[1].

[1]Dr. Daniel den Hoed Cancer Center, The Netherlands.
[2]Laboratory of the Dept. of Ophthalmology, Academic Hospital and State University of Leiden, The Netherlands.
[3]Dept. of Medical Biochemistry, State University of Leiden, The Netherlands.

Abstract

Bacteriochlorin *a* (BCA), a derivative of bacteriochlorophyll *a*, is an effective photosensitizer *in vitro* and *in vivo*. BCA has a major absorption peak at 760 nm where tissue penetration is optimal. This property, together with rapid tissue clearance promises minor skin photosensitivity. The tissue localizing and photodynamic properties of BCA were studied using isogeneic RMA mammary tumors, transplanted into subcutaneous tissue in transparent "sandwich" observation chambers on the back of WAG/Rij rats. The fluorescence kinetics following an i.v. administration of 20 mg/kg BCA was assessed in blood vessels, tumor and normal tissue. Subsequently, the development of vascular- and tissue damage after a therapeutic light dose (760 nm, 600 J/cm^2) was observed. Fifteen minutes post injection (p.i.), the fluorescence of BCA in the tumor reached a plateau value of 2.5 times the fluorescence in the normal tissue. From one hour post injection the tumor fluorescence diminished gradually; after 24 h the tumor fluorescence signal did not exceed that of the normal tissue. Following photodynamic therapy (PDT), 24 h p.i., complete vascular stasis was observed 2 h post treatment in the tumor only, with subsequent recovery. The presence of viable tumor cells following PDT was assessed by histology and retransplantation of treated tumor tissue from the chamber into the flank immediately or 7 days after treatment. In both cases tumor regrowth was observed. BCA-PDT (20 mg/kg, 760 nm, 100 J/cm^2) one hour after BCA administration, an interval which gives the optimal differential between tumor and normal tissue, was sufficient to prevent tumor regrowth. However, this only occurred when re-transplantation was performed 7 days after PDT. During PDT, one hour p.i., vascular damage in tumor and normal tissue was considerable. Complete vascular shut-down was observed in the tumor 2 h after therapy and in the surrounding tissues at 24 h. Circulation damage was associated with vascular spasm and occlusion probably due to thrombi formation. Oedema was notable, especially following PDT with 600 J/cm^2 at 24 h p.i.

Introduction

Tumor destruction by photodynamic therapy is achieved through retention of photosensitizing compounds in tissue after injection and the subsequent activation of these compounds by irradiation with light of appropriate wavelength and dose. The photosensitizer currently evaluated in phase III clinical trials is Photofrin®, a derivative of hematoporphyrin, enriched in the photodynamically active fraction. However, Photofrin® has a number of

drawbacks. In particular it induces skin photosensitivity for periods up to 6 weeks and is chemically ill defined. These drawbacks have prompted an intensive worldwide search for new photosensitizers (Kessel, 1990). A good candidate for "second generation" photosensitizer is bacteriochlorin *a* (BCA). BCA is a derivative of bacteriochlorophyll *a* and a potent photosensitizer both *in vitro* and *in vivo* (Schuitmaker *et al.,* 1990). Its lipophilic nature enhances the cellular uptake of the dye (Richter *et al.,* 1991). Effects on mitochondria ex vivo resulting from therapy (Schuitmaker *et al.,* 1991) and *in vivo* tumor fluorescence have been demonstrated (Schuitmaker *et al.,* 1992). This photosensitizer has a major absorption peak at 760 nm, a wavelength where tissue penetration is optimal (Star *et al.,* 1992). With this photosensitizer the penetration depth of the therapeutic light and thus the treated volume may be maximized.

The exact mechanism of tumor necrosis resulting from PDT is still not fully elucidated. Originally it was thought that PDT was effective only through the selective localization of the photosensitizer in the tumor cells. The tumor cells were subsequently killed by singlet oxygen, produced when the dye was irradiated with light of an appropriate wavelength. However, there exists accumulating evidence that an important and immediate effect of PDT is on the vasculature of the tumor and surrounding tissues, depending on the sensitizer used (Henderson and Dougherty, 1992). This results in a decreasing blood flow and eventually vascular stasis (Star *et al.,* 1986; Franken *et al.,* 1988; Schuitmaker *et al.,* 1990). The fluorescence of BCA is of practical interest in PDT as it may be a sensitive non-contact way of detecting otherwise occult cancers and make them accessible for regular biopsy, eventually combining potential tumor tissue identification and photodynamic therapy (Lam *et al.,* 1990).

In the present paper we report on the fluorescence kinetics of BCA and on BCA-PDT induced damage to tumor and normal tissue circulation *in vivo*.

Materials and Methods

Preparation of BCA

Bacteriochlorophyll *a* was obtained by extraction from the photosynthetic anaerobic bacterium *Rhodospirillum rubrum* and purified according to the method of Omata et al. (1983). The purity of the pigment was checked by thin-layer chromatography (TLC). Using an eluent of 93% methanol and 7% phosphate buffer (pH 7, 10 mM), the bacteriochlorophyll *a* yielded a single blue spot (relative mobility approximately 0.5) on Machery-Nagel Nano-Sil C_{18}-100 TLC plates (Düren, Germany). Bacteriochlorophyllin *a* was obtained by saponifying

bacteriochlorophyll *a* as described by Oster et al. (1964). The central magnesium ion of bacteriochlorophyllin *a* was removed with 50 mM sodium acetate (pH 4.5), and the BCA formed was then extracted with ethylacetate. Ethylacetate was evaporated under reduced pressure, and BCA was lyophilized overnight and stored at -20°C in the dark under nitrogen. Throughout the extraction and modification procedures care was taken to work under reduced light and at 4°C as much as possible.

For intravenous administration lyophilized BCA was dissolved in 3 ml methanol; 0.15 ml propane-1:2-diol (BDH, England) and 0.5 ml Cremophor EL (Sigma, St. Louis, USA) were added and the mixture was shaken vigorously. Thereafter the methanol was evaporated under reduced pressure and finally the mixture was diluted with sterile 0.9% NaCl to yield an i.v. injectable suspension with a suitable BCA concentration of 20 mg/kg. For each experiment the suspension was freshly prepared and used within 2 hours.

Animal Model

Female WAG/Rij rats 12-14 weeks of age (ITRI-TNO, Rijswijk, The Netherlands) were equipped with a transparent observation chamber (Reinhold *et al.,* 1979) in a dorsal skin flap. At the end of a three week preparation period, approximately 1 mm^3 of an isogeneic mammary tumor was transplanted into the subcutaneous tissue in the chamber. This *in vivo* model enables monitoring of fluorescence kinetics in blood vessels, tumor and subcutaneous (normal) tissue of the chamber following i.v. administration of a fluorescent dye (van Leengoed *et al.,* 1990). It is also possible to observe the development and recovery of vascular damage in tumor and normal tissue after a therapeutic light dose. Through all procedural steps Hypnorm® (fluanisol/fentanyl mixture, Janssen Pharmaceuticals, Beerse, Belgium) was used as an anaesthetic.

Fluorescence Localization

BCA fluorescence was excited at 514.5 nm using an argon-ion laser (Spectra Physics model 171) at the very low power density of 0.1 mW/cm^2, in order to avoid tissue damage caused by photoactivation of the dye. BCA fluorescence was detected through an RG 665 nm high pass filter using an imaging system capable of detecting very low light levels. The resulting digitized images were subject to image analysis yielding average grey scale values per time interval of selected areas of interest in tumor tissue, normal tissue and a blood vessel.

Photodynamic therapy

Light of 760 nm wavelength was obtained from a dye laser (Spectra Physics 375B, with Styryl 8), pumped by an argon-ion (Spectra Physics 171) laser. Light, at a power density of 100 mW/cm^2, was delivered to the chamber via an optical fibre and a lens system with diaphragm yielding a uniform beam of 10 mm diameter covering the entire window of the chamber (10 mm in diameter). Two groups of six animals were treated. In the first group fluorescence was studied and PDT was performed 24 h p.i. of BCA, with a light dose of 600 J/cm^2. In the second group PDT was performed 1 h p.i. with a light dose of 100 J/cm^2.

Experimental procedure

The experiments were performed on well vascularized chambers and with vital tumors of approximately 3 mm diameter. The animals were immobilized by sedation and placed on a temperature controlled positioning stage (30°C) that enabled positioning of the chamber under the camera. Before i.v. administration of the dye, during the observation period of 2 h and at 24 h p.i., fluorescence recordings were made. Each fluorescence recording was accompanied by an image of a piece of reference material that fitted on top of the chamber. In this way all images could be matched against the reference, enabling correction for any fluctuations in excitation light intensity or spatial variations in the sensitivity of the imaging system.

At 24 h p.i. the chambers received a therapeutic light dose. Before, during and after the irradiation, the status of the circulation was determined under a microscope and scored on a scale from 0 (no observable damage) to 8 (no observable circulation). Tumor and surrounding normal tissue were scored separately. The status of the circulation of three animals from the group of six was determined during a seven day follow-up period. Then, the tumor and a margin of normal tissue (or the necrotic remains) was removed from the chamber and retransplanted into the flank of the same animal. In two animals from each group the tumor and a margin of normal tissue was retransplanted 2 h after therapy to see whether enough damage was inflicted to prevent tumor regrowth. Finally one chamber from each group was prepared for histology. In the second series of six animals a therapeutic light dose of 100 J/cm^2 was delivered at a much shorter interval of 60 min. p.i. Apart from that, a similar protocol was followed. All sensitised animals were kept under reduced light conditions (<30 μW/cm^2) with a 12/12 h day/night cycle.

Results

Digitized fluorescence images of BCA *in vivo* in an observation chamber are shown in Fig. 1. A fluorescence angiogram develops following i.v. administration of BCA. The fluorescence in the blood vessels decreases after 5 min. p.i. whereas the fluorescence in the tumor increases up to 30 min. p.i. Twenty four hours after the administration tumor tissue and blood vessel are undistinguishable from the normal tissue.

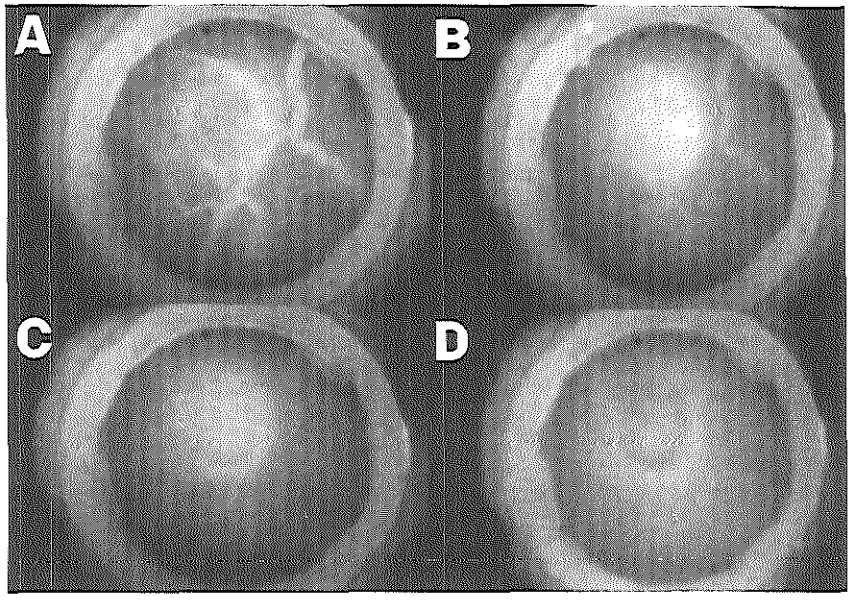

Fig. 1. Digital images of the chamber model (inner diameter of 10 mm), showing the fluorescence of BCA in tumor, blood vessels and normal tissue at 5 (A), 30 (B), 120 min. (C) and at 24 h p.i. (D). Tumor diameter approximately 3 mm. Note the rapid clearance from the circulation and the distinct fluorescence of the tumor. Scale: white bar represents 2 mm.

Also at this interval no signs of vascular or tissue damage could be observed. Therefore the effects of BCA alone and the excitation of fluorescence were considered negligible.

Figure 2 summarizes the results of the fluorescence pharmacokinetics study. Grey scale values measured in selected areas of tumor, blood vessel and normal tissue are presented as a function of time following administration of BCA. Following administration, the fluorescence in the blood vessels decreases whereas tumor fluorescence remains at a constant level until 60 min. p.i. and

then starts to decrease. Note that the fluorescence of the normal tissue hardly changes during the observation period. When expressed as ratios relative to normal tissue, tumor tissue fluorescence increases to a value of 2.5 (interval of 15 min.). This level is maintained up to 60 min. p.i., but at 120 min. it has declined to a ratio of 1.6. At 24 h p.i., the tumor fluorescence ratio has dropped below 1. On average, the fluorescence of the normal tissue then slightly exceeds that of tumor and vasculature. Blood vessel ratios peak immediately post injection and at 5 min. p.i. a level of 2.5 times the fluorescence of the normal tissue is recorded. Gradually this level decreases to become indistinguishable from the normal tissue (a ratio of 1) 2 h p.i.

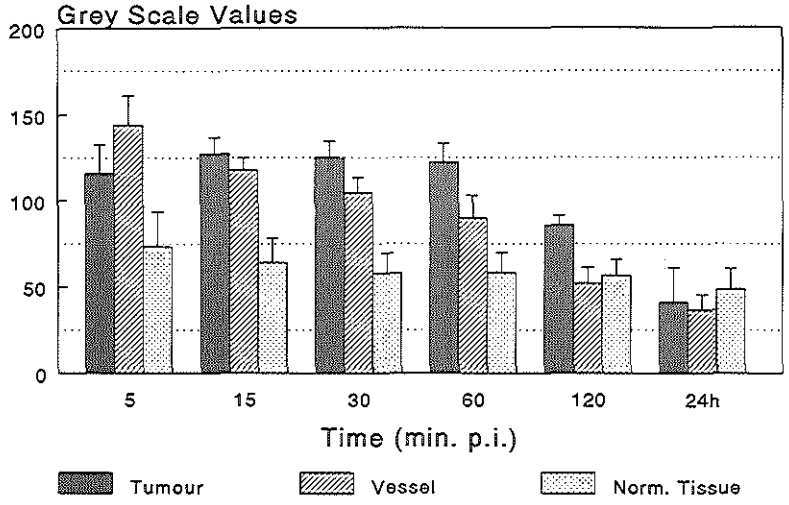

Fig. 2. Fluorescence signal measured as average grey scale values of selected areas of interest of tumor, blood vessel and normal tissue as a function of time following i.v. administration of BCA. The bars represent group averages ± SEM of 6, 6, 6, 5, 3 and 5 animals respectively.

The circulation damage scores during and after a therapeutic treatment with 600 J/cm² at 24 h p.i. are shown in Fig. 3A. Tumor vasculature appears to be damaged to a larger extent than blood vessels in the normal tissue. Only at 2 h after therapy a maximum score of 8 (no circulation observed) is reached for the tumor vasculature. Figure 3A. also shows that, following the protocol with a 24 h interval, the circulation in tumor and normal tissue recovers to a score of about 3-4 within 6-7 days. Usually the larger vessels recover or existing smaller branches increase in diameter. The damaged capillary bed is replaced by new capillaries. Note that during the 100 min. of illumination, vascular damage

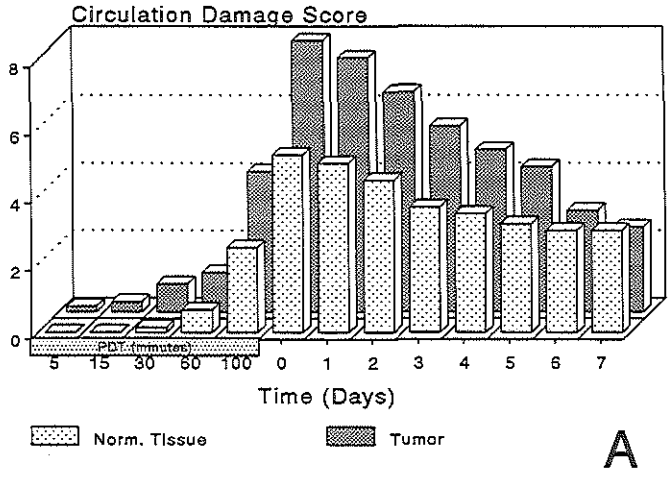

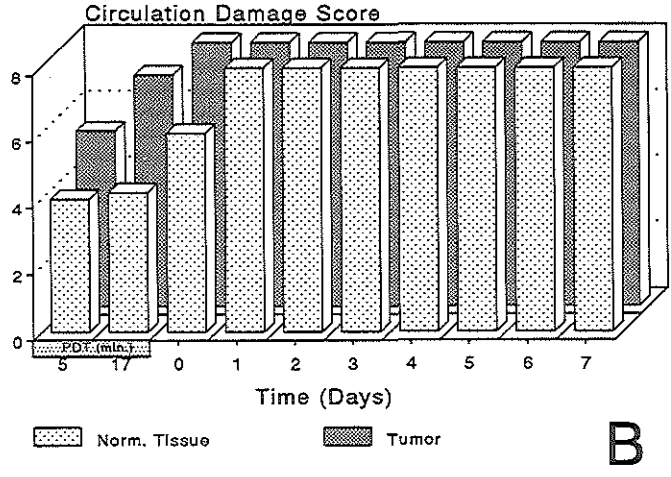

Fig. 3. Circulation damage scores of tumor tissue and normal tissue for the interval between administration of BCA and therapy of 24 h and 600 J/cm² (a) and 1 h and 100 J/cm² (b) respectively. The values are group averages of 6 animals until day 0 and 3 animals for the rest of the experiment. The damage scores range from 0 (no observable damage) to 8 (no observable circulation). PDT (abscissa) marks the duration of illumination which is expressed in minutes. The observations at day 0 were taken 2 h post therapy. Error margins are indicated for two representative observation periods. When a mean score of 8 (maximum) is reported, the error is zero.

developed very slowly reaching a circulation damage score of 3(normal tissue)-5(tumor tissue) at the end of this period. Histology performed 2 h after the treatment light dose demonstrated the presence of viable tumor cells. With this treatment regime, tumor regrowth after reimplantation following therapy was never prevented, not immediately post treatment nor after the 7 day follow up period.

In the second series of PDT treatments an interval of 1 h between i.v. administration of BCA and therapeutic illumination was chosen. This decision was based on the results of the fluorescence kinetics study (Fig. 2). Furthermore the light dose was reduced from 600 J/cm^2 to 100 J/cm^2 in view of the higher photosensitizer concentration present at this interval. The vascular damage scores of these experiments are presented in Fig. 3B. Complete vascular shutdown was observed in the tumor 2 h after therapy, similar to the effects seen following therapy at 24 h p.i. After 24 h post therapy, the normal tissue had no observable circulation either. The vascular effects were already evident after 5 min. of illumination resulting in an ischemic tumor, vascular spasm of the arterioles as well as venules of the normal tissue. Occlusions in the large vessels during and shortly after therapy were possibly caused by the many thrombi that were observed. At the end of the therapeutic irradiation there was still some circulation present in the normal tissue (damage score of 4). Immediate post-treatment retransplantation resulted in tumor regrowth for both treatment regimes. Viability of tumor cells at this interval was again confirmed by histology. Damage scores of tumor and normal tissue remained maximal during the 7 day follow up and retransplantation at this interval did not result in regrowth of the tumor.

Discussion

Depending on the time between i.v. administration of the dye and PDT and on the applied light-dose, BCA-PDT eventually resulted in complete vascular stasis and prevention of tumor tissue regrowth upon reimplantation at the end of a 7 day follow-up period.

In the case of PDT using hematoporphyrin derivative (HPD) or Photofrin® the most common interval between administration of the photosensitizer and illumination of the tumor is 24-48 h. In a first attempt to realize a therapeutic protocol, an interval of 24 h between i.v. administration of BCA and the therapeutic illumination was chosen. Furthermore a BCA dose of 20 mg/kg was selected based on previous experience (Schuitmaker *et al.,* 1990). However, as Fig. 3A demonstrates, using this protocol and despite the relatively high light

dose that was applied, it was not possible to achieve complete and irreversible vascular stasis in the observation chamber model and tumor regrowth always occurred. This observation coincides with the lack of selectivity and reduced fluorescence at 24 h p.i. (Fig. 2).

Table I. Ratios ± SEM of tumor tissue and vessel fluorescence relative to the fluorescence of the normal tissue for different time intervals following administration of BCA.

Time after BCA administration	*Ratios ± SEM*	
	Tumor	*Vessel*
5 min.	1.9 ± 0.3	2.5 ± 0.5
15 min.	2.5 ± 0.5	2.4 ± 0.5
30 min.	2.5 ± 0.4	2.2 ± 0.5
60 min.	2.4 ± 0.4	1.8 ± 0.5
120 min.	1.6 ± 0.2	1.0 ± 0.3
24 h	0.5 ± 0.2	0.8 ± 0.1

Therefore, in the second series of experiments the tumor was treated one hour after administration of the dye. The choice for this one-hour interval was entirely based on the preceding *in vivo* fluorescence kinetics study (see Table I). This study showed that in the window chamber model, tumor selectivity up to 2.5 times the fluorescence signal of the normal tissue can be achieved, during 15 to 60 min. p.i. At 60 minutes p.i. the fluorescence signal ratio of the vessels has decreased by approximately 40% of the highest value whereas this ratio in the tumor had dropped by less than 5% of its highest value. At twenty four hours p.i. tumor and blood vessel ratios become indistinguishable from the normal tissue, similar to what is observed with HPD in the same model (van Leengoed *et al.*, 1990).

A six fold reduction of the light dose to 100 J/cm^2 (100 mW/cm^2) was chosen as a higher overall concentration of the photosensitizer was expected. This light dose resulted in complete and irreparable vascular stasis in the observation chamber. Furthermore, tumor regrowth was prevented in those cases where the tumor was left *in situ* during the 7-day follow up period and was subsequently retransplanted in the flank of the same animal.

The fact that 24 h appears not to be the optimum interval has also been noted for other photosensitizers, e.g. chlorins (Gomer, 1991) and bacteriochlorophyll *a*

(Henderson *et al.,* 1991). As is shown above, the fluorescence kinetics *in vivo* can be used to determine a "therapeutic window" i.e. a suitable time interval between dye administration and PDT. This is different from HPD-PDT, where in this observation chamber model, 2 h p.i., tumor fluorescence could be discriminated from normal tissue in only 40-50% of the cases (van Leengoed *et al.,* 1990). In this model complete necrosis required a light dose of 160 J/cm² at 630 nm applied 24 h p.i. of 15 mg/kg HPD (Star *et al.,* 1986). Although vascular effects are not the primary target of the therapy, the resulting sterilization of the tumor bed will prevent nutritional resupply to still viable tumor cells through diffusion or angiogenesis (Fingar and Henderson, 1987) thereby enhancing the effect of the therapy.

The circulation damage scores (Fig. 3A) of the PDT treatment at 24 h p.i. show a differential effect on the vasculature of the tumor tissue and the normal tissue. This might be partly explained by the fact that in this model, tumor tissue only contains capillaries whereas the normal tissue contains capillaries and larger vessels. A maximum damage score is reached only 2 h after therapy and only in the tumor; from then on the circulation of tumor and normal tissue recovers. As a result, PDT treatment 24 h p.i. of BCA rendered no "cures". At this interval no fluorescence could be detected in the tumor nor in vessels which in this case could indicate that the BCA concentration in the vessels, tumor and normal tissue was too low to be effective. When a 24 h interval between administration and therapy was studied, the blood supply to the tumor was maintained during an illumination time of at least 60 min. (360 J/cm²). This delayed vascular shut down might increase the direct tumor cell kill as this is dependent on the availability of oxygen. Nevertheless, enough tumor cells apparently escaped therapy, causing tumor regrowth in all cases. With only one hour between administration and therapy, where BCA fluorescence was still detectable in the vasculature, 30 J/cm² (=5 min. of illumination) resulted in higher circulation damage scores than 600 J/cm² of light at the 24 h interval. Five minutes after the start of illumination, vascular spasms, circulating and occluding thrombi were observed. These direct vascular effects have also been reported during porphyrin based PDT (Star *et al.,* 1986; Reed *et al.,* 1988).

Following 100 J/cm² of light applied 1 h p.i., the tumor and normal tissue damage was sufficient to prevent tumor regrowth following retransplantation at day 7. Two hours post therapy re-transplantation yielded regrowth of the tumor, demonstrating the presence of viable tumor cells at this time. This observation agrees with the findings of Henderson (1992) that cells removed immediately after PDT can be viable *in vitro*, and stresses the role of tumor bed damage in determining the final outcome of photodynamic therapy. Histology performed

2 h post therapy revealed that individual tumor cells survived following PDT at 1 h as well as at 24 h p.i. Probably the interval at which histology was performed was not optimal with respect to predicting the effectiveness of the therapy since one of the treatment schemes was effective in preventing tumor regrowth.

Summarizing, BCA is useful, not only to induce tumor necrosis in PDT but for tumor detection by fluorescence as well. It induces selective fluorescence from 5 to 120 min. p.i. in mammary tumors in the present model. In this respect and in this model, BCA is a much better tumor localizer than HPD. *In vivo* fluorescence of BCA can be used to determine a suitable time interval between i.v. administration of the dye and the subsequent therapeutic illumination of tumor tissue. The therapeutic ratio of the dye can be increased by making use of the photobleaching properties of the dye. *In vitro*, a 50% decrease of the absorption at 760 nm is observed after 86 J/cm^2 (unpublished data J.J. S.). At the end of the therapeutic treatment viable tumor cells must be present as immediate retransplantation always results in tumor regrowth. Vascular damage appears to be a prerequisite to obtain tumor control with BCA. Determining the optimum sensitizer dose and interval between drug administration and therapy should be the subject of further study.

Chapter 7

PHOTOSENSITIZING PROPERTIES OF PROTOPORPHYRIN IX GENERATED FROM EXOGENOUS 5-AMINOLEVULINIC ACID: PRELIMINARY PRECLINICAL AND CLINICAL EXPERIENCE

Introduction

In recent years a number of fluorescent dyes have been proposed and tested preclinically as photosensitizers for photodynamic therapy (PDT). Compared to porphyrins these "second generation" photosensitizers are often reported to cause less skin photosensitivity and they can be activated with light at wavelengths where tissue penetration is deeper than with the light used for porphyrins so that larger volumes can be treated. For recent reviews see: van Lier (1990a), Gomer (1991), Rosenthal, (1991), Henderson, (1992) and Moan (1992). Following systemic administration exogenous photosensitizers like HPD and Photofrin® also localize in tissues other than the target tissue. Therefore, phototoxic side effects can be expected.

A different approach to photosensitize neoplastic tissue is to administer a specific precursor, stimulating the neoplastic tissue to synthesize its own photosensitizer. In the biosynthetic pathway of heme, 5-aminolevulinic acid (ALA) is a precursor of protoporphyrin IX (PpIX), which in turn is transformed into heme.

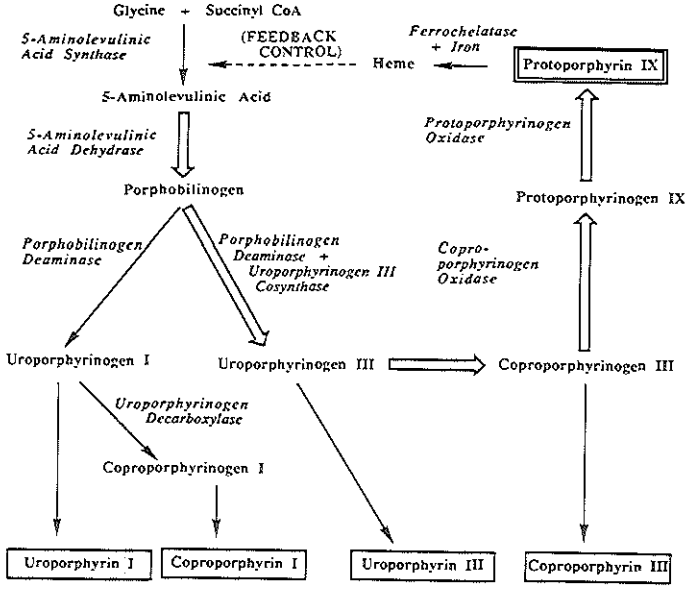

Figure 1. Simplified biosynthetic pathway for heme. Fluorescing and photosensitizing compounds are enclosed in rectangles, with protoporphyrin IX highlighted. The 5-aminolevulinic acid/heme feedback control is indicated by a dotted arrow. The principal biosynthetic route for ALA-induced protoporphyrin IX is indicated by the large arrows. (redrawn from Kennedy and Pottier, 1992)

The accumulation of PpIX in humans is associated with cutaneous photosensitivity seen with protoporphyria. Hence PpIX is an effective photosensitizer. Heme biosynthesis is essential to life and occurs in all aerobic cells (Fig. 1). Different cells however, differ in their heme generating capacity. The synthesized heme inhibits the synthesis of ALA from glycine and succinyl CoA by 5-aminolevulinic acid synthetase. Administering exogenous ALA bypasses this feedback control.

Rate limiting steps such as the conversion of PpIX into heme by ferrochelatase which by itself is a slow process, can then result in an accumulation of PpIX inside cells. In regenerating tissues and in various malignant tissues the porphobilinogen deaminase (PBGD) activity is often increased, whereas the ferrochelatase activity is decreased (Smith, 1987; van Hillegersberg *et al.*, 1992; Leibovici *et al.*, 1988). Therefore, by providing the appropriate precursor, and by the activity status of key enzymes, malignant cells can generate and accumulate their own photosensitizer.

ALA is hydrophillic and is therefore well suited to be administered systemically or to be dissolved in a cream for topical administration. PpIX on the other hand is hydrophobic, has a high affinity for membranes and therefore, once synthesized cannot easily be removed from the cell. Upon illumination and in the presence of molecular oxygen it causes cell death (Malik and Lugaci, 1987). When excited with light of a suitable wavelength it also shows fluorescence, thus combining the properties of a fluorescent tumor localizer and a photosensitizer for PDT.

In vivo, following systemic administration, ALA causes the accumulation of PpIX in tumor tissue. The photosensitizer even accumulates in tumors growing in liver tissue to a higher extent than the host tissue (van Hillegersberg *et al.*, 1992), the reverse of what is seen when HPD or Photofrin® are used as photosensitizers.

This chapter describes preliminary *in vivo* studies of the development and decay of ALA generated protoporphyrin IX fluorescence. Also the effects of a treatment light dose on the normal and tumour tissue vasculature have been investigated. The results are discussed in relation to the clinical experience concerning topical ALA-PDT in our hospital.

PpIX as tumor localizer

The fluorescence kinetics and photodynamic effects of endogenously formed PpIX were studied *in vivo* using the window chamber model. Briefly, a syngeneic mammary carcinoma was transplanted intracutaneously in an observation

chamber mounted on the back of a female WAG/RIJ rat. Following i.v. administration of ALA (100 mg/kg) the fluorescence of the synthesized PpIX was monitored up to 4.5 hours post injection (p.i.). Fluorescence was excited at 514.5 nm, using 0.1 mW/cm^2 of excitation light and detected through a high-pass filter above 665 nm. Fluorescence images were recorded using a two stage light intensified CCD (Charge Coupled Device) camera in combination with a computer based imaging system.

Figure 2 shows the digitized fluorescence images before and at 4 intervals after i.v. administration of 100 mg/kg ALA. This picture differs from what is usually seen in the skin fold chamber. With exogenous photosensitizers (van Leengoed *et al.,* 1990; van Leengoed *et al.,* 1992) a fluorescent angiogram was always observed which also serves as a check for successful drug delivery. No angiogram is observed with ALA which does not fluoresce.

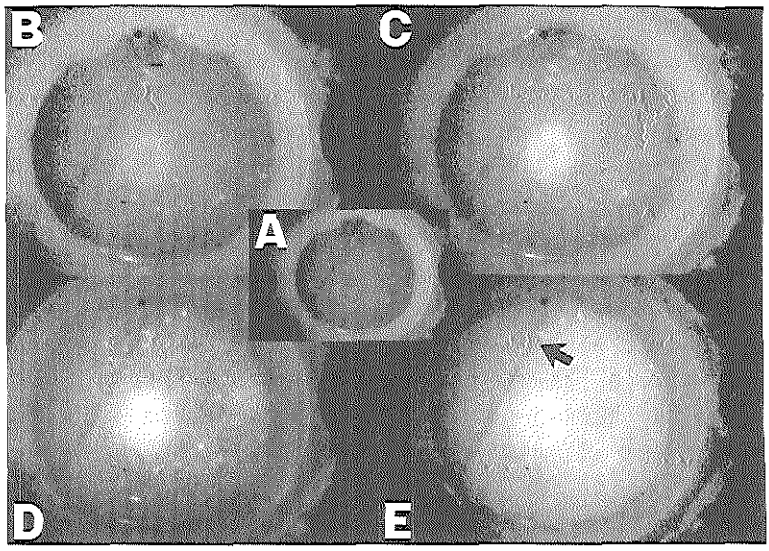

Figure 2. Digitized fluorescence images following i.v. administration 100 mg/kg of ALA before, (A), at 30 min. (B), 60 min. (C), 180 min. (D) and at 270 min. (E) p.i. Fluorescence at the site of the tumor develops while the large vessel (arrow) remains dark.

From selected areas in the image, the average grey scale value can be determined and in Fig. 3 the fluorescence intensity in tumor tissue and normal tissue is shown as a function of time. The data are averages of six animals. Fluorescence in the tumor area becomes observable at 30 min. p.i. and reaches peak values at about 150 min. At 180 min. p.i. the fluorescence starts to

decrease and "selectivity" is lost due to the increase of fluorescence in the normal tissue. Between 60 and 150 min. p.i. the largest differences between tumor and normal tissue are be found. Twenty four hours post injection PpIX fluorescence has disappeared. Interestingly, when ALA was administered intraperitoneally in two animals, the same pattern was found.

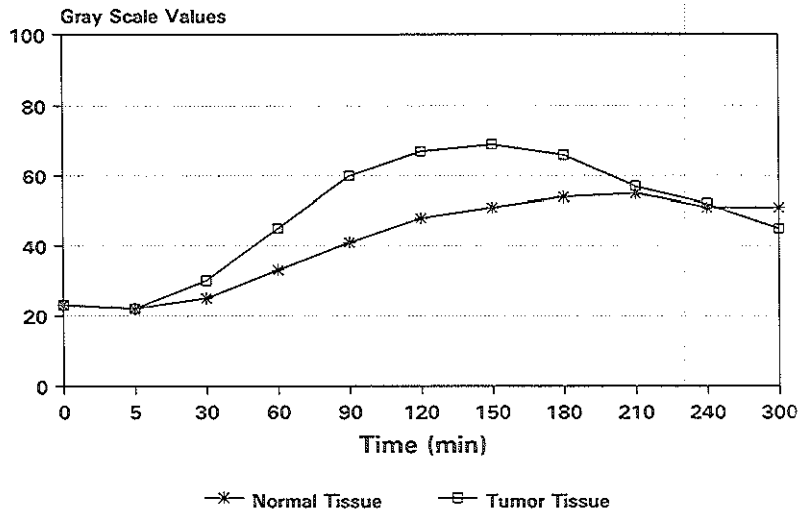

Figure 3. Tissue fluorescence of following i.v. administration of 100 mg/kg b.w. ALA. Values are calculated from the digitized images for areas of tumor and normal tissue and averaged over six animals.

Figure 4 shows the fluorescence of a basal cell carcinoma of a patient with basal cell naevus syndrome, about three hours after topical application of ALA. The photograph was taken at the beginning of the irradiation using the treatment light to excite the fluorescence. ALA was dissolved in a water based cream (25 % w/w) and applied to the lesion which was then covered with thin gauze and subsequently with adhesive plastic foil (Opraflex®). This cover protects the clothing, prevents the undesired removal of the cream and evaporation of the solvent ensuring optimal uptake of ALA. The fluorescence reveals the localization of the protoporphyrin, clearly demarcating the lesions in the irradiated area. The small fluorescent spots mark the hair follicles which are also known to accumulate PpIX following topical ALA application (Goff *et al.,* 1992).

Figure 4. Fluorescence image of PpIX in human basal cell carcinoma following a three hour application period and excitation with 514.5 nm light at 70 mW/cm². The image was recorded at the beginning of the irradiation through an OG 570 high pass filter.

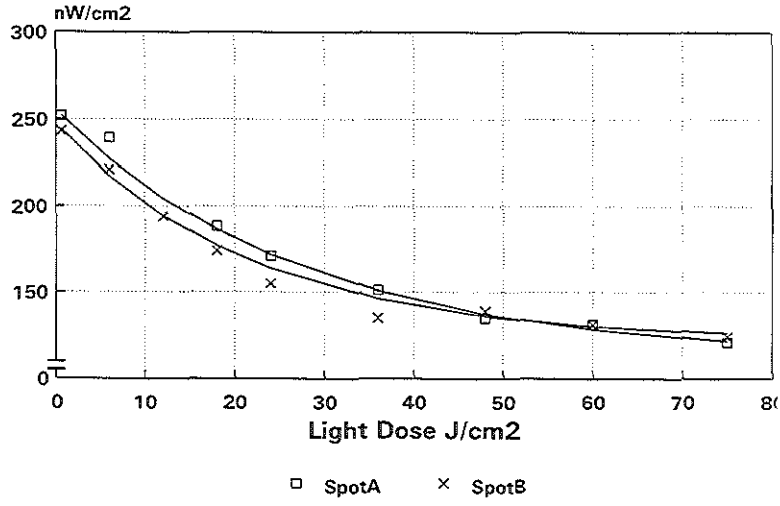

Figure 5. Reduction of fluorescence caused by photobleaching of the photosensitizer due to excitation measured in two different spots. The solid line is a fit of the function A + B exp(-C × D) to the data points, where A, B, C are contstants obtained from the fit and D is the light fluence (J/cm²). It shows the exponential decay of fluorescence as a result of irradiation.

Irradiation causes the destruction of the photosensitizer as a result of the photochemical reaction. The fluorescence that is emitted decreases and this phenomenon might be utilized to monitor the progress of the treatment. If the fluorescence has disappeared, so has the PpIX and further irradiation is useless. Figure 5 shows the decreasing intensity of fluorescence as a result of photobleaching.
Note that there is an exponential decay of fluorescence and that the decreasing levels of fluorescence approaches a background level of about 110 nW/cm², presumably the tissue autofluorescence. Taking this into account already after approximately 24 J/cm² of treatment light, the PpIX fluorescence intensity has decreased to 37% of its starting value.

PpIX as a photosensitizer for PDT

Because the photosensitizer originates in the cell, cellular effects are expected to dominate. However, following systemic ALA administration vascular effects of PDT have been observed in our window chamber model.

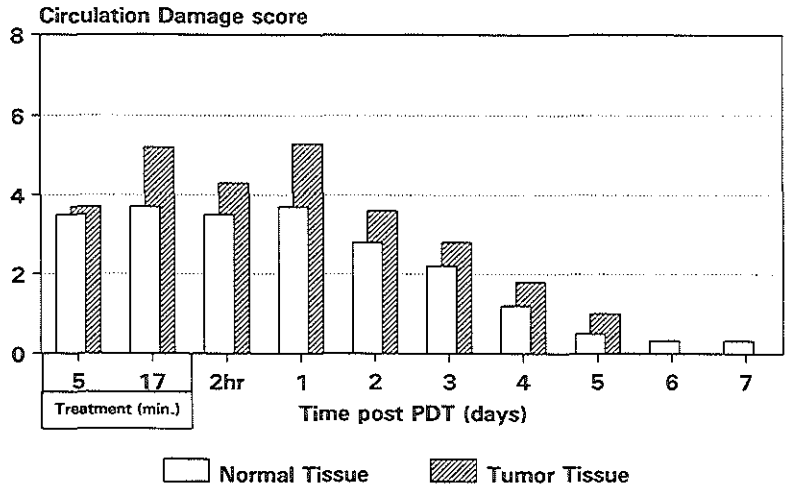

Figure 6. Averaged vascular damage score of six animals following a therapy dose of 100 J/cm² (17 min × 100 mW/cm²), at 514 nm in the in vivo skin fold chamber model, 2 h p.i. of 100 mg/kg b.w. ALA i.v.. A maximum score of 8 corresponds with no observable circulation, whereas a value of 0 means no observable effect.

Endothelial cell damage due to the treatment can therefore not be ruled out. Already during the first 5 min. of irradiation the circulation damage score has

increased to about 50 % of its maximum (Fig. 6). Only minor differences in damage between tumor tissue and normal tissue were observed. Maximum damage scores were not observed and circulation returned to normal during the next few days following treatment. Following a "regular" HPD-PDT treatment with i.v. administered photosensitizer, the vascular effects such as extravasation of blood and stasis can be much more pronounced depending on drug and light dose. In this form of treatment the vasculature is a known target (Star *et al.,* 1986; Selman *et al.,* 1984).

Twenty four hours following ALA-PDT some tissue necrosis of the tumor in the *in vivo* model has been observed. These observations show that PDT using systemically administrated ALA leads to vascular damage but that the combination of ALA dose, light dose and interval between administration and irradiation insufficient to cause tumor necrosis. The effects seem to occur too rapidly to be entirely attributable to an inflammatory response to the treatment.

In patients with superficial lesions, topical ALA-PDT seems to be more effective than in the vivo experiments using i.v. administered ALA, described above. A complete response rate of 79% has been reported for superficial basal cell carcinomas after a single treatment. When partial responders received a second treatment the response rate increased to 95% (Kennedy and Pottier, 1992). The route of administration, the type of tumor and perhaps the degree of vascularisation may play a significant role in the differences between clinical data and *in vivo* experiments. In this respect it should be noted that clinically, 20% ALA was used for topical administration (Kennedy and Pottier, 1992).

In our institute patients receive 25 % w/w ALA in a water based cream and a light dose of 75 J/cm^2 (dose rate between 50-150 mW/cm^2). Often large areas of skin have to be irradiated. Therefore, much light is needed and green light from an argon laser at 514.5 nm is used in such cases. Although tissue penetration of light at this wavelength is limited, the tissue penetration of ALA is believed to be the real limiting factor. Of course only superficial lesions can be effectively treated in this way. Soon after the beginning of the light treatment, the patients report varying levels of discomfort, such as stinging or tingling of the treated area, which usually decreases within minutes during treatment. These sensations vary from patient to patient, and also between treatment sites. When the treatment was finished, edema and erythema were usually observed in the entire area of ALA application, with a histamine "flare" that extended beyond this area. The lesion itself often showed a slightly blue discoloration and there may be some exudate. These findings resemble those reported by Kennedy (1992).

In the period following ALA-PDT the scab that has formed will fall off revealing a normal skin. Sometimes there is hyperpigmentation in the treated area and in the case of basal cell carcinoma it may take several months before the redness of the former lesion fades. The scarring is minimal and even after treating a superficial tumor recurrence in a skin graft the skin healed well.

Concluding remarks

Clinical PDT using topical ALA is currently restricted to the superficial skin lesions because of the limited depth of penetration of ALA. New formulations of ALA might enhance its penetration depth in tissue without interfering with the accumulation of PpIX in tumor cells.

The synthesized photosensitizer disappears within 24 h, independent of the route of administration. When necessary the treatment can therefore be repeated within 48 h. ALA itself is not photodynamically active and not toxic in the concentrations used. ALA can be applied topically and at least *in vivo* it is possible to administer it i.v. and even orally. Topical administration will minimize side effects. When ALA is administered systemically, vascular effects are observed in our *in vivo* model, suggesting that vascular targets (endothelium, leucocytes) do exist for this type of treatment.

Chapter 8

GENERAL DISCUSSION

In this thesis, a number of *in vivo* observations have been reported regarding 14 fluorescent dyes studied for tumor localization and/or photodynamic therapy (PDT). In this chapter the results are summarized and the fluorescence pharmacokinetics and photodynamic properties of these dyes are discussed.

Fluorescence localization

Ideally all photosensitizers eligible for PDT should show fluorescence and generate singlet oxygen. These features, in combination with the retention of the photosensitizer in malignant tissue and the possibility of local activation make PDT a potential new modality for cancer therapy. The localizing properties of photosensitizers can be employed for the detection of tumor tissue and it is evident that early recognition of malignant tissue will increase the success rate of cancer therapies.

Fluorescence localization opens possibilities for such early detection and in principle permits determination of the extent of the disease prior to treatment. The latter can be very useful when dealing with multifocal lesions, areas of field cancerization or invasive processes that need additional treatment after surgical debulking. It should be noted however that when fluorescence localization is considered, false positive and false negative fluorescence are likely to be encountered. Histology should therefore always be performed to ascertain the pathological status of these fluorescent areas.

Hydrophillic dyes

Acridine Red (Chapter 2) is a hydrophillic dye. It has a high fluorescence yield, localizes in tumor tissue and disappears from the circulation within minutes. The cellular site of localization has not yet been elucidated. At the initial dose of 10 mg/kg this dye was sometimes associated with mortality but when the dose was reduced to 2 mg/kg, toxicity or morbidity was never observed. Because of the short half life in the circulation, this dye unfortunately will not localize in areas of the tumor where the circulation is (temporarily) blocked, a phenomenon not rare in larger tumors.

A recently proposed method of photosensitization that is completely different from administering exogenous photosensitizers is to use a water soluble precursor of heme (ALA) and allow the (tumor) cells to generate their own

(hydrophobic) photosensitizer (PpIX, Chapter 7). This strategy results in fluorescence at the site where PpIX is synthesized without causing detectable fluorescence in the vasculature. All other dyes discussed in this thesis are more or less hydrophobic or are mixtures with varying hydrophobic /hydrophillic properties.

Hydrophobic dyes

When brought in an aqueous environment, hydrophobic dyes have a strong tendency to aggregate, making them photodynamically inactive. Three approaches have been used to prevent hydrophobic photosensitizers of becoming inactive.

1. The hydrophillic properties of a dye can be increased by adding sulphonate groups to the macrocycle of the molecules. This approach has been used for AlPhcTS[1] (chapter 2) and the six metallosulphonated phthalocyanines ($MPcS_n$, chapter 3 and 4).
2. Alternatively, before administration hydrophobic dyes can be incorporated into unilamellar liposomes as was done with ZnPc (chapter 5).
3. They can also be administered using an emulsion like cremophor as was done with BCA (chapter 6). Following administration, these hydrophobic dyes tend to interact with serum proteins which can favour cellular uptake through receptor mediated transport. Compared to hydrophillic dyes they are retained in the circulation and therefore available to the tissue for a considerably longer time.

In general, following systemic administration of the fluorescent dyes, a similar pattern of fluorescence kinetics has been observed. Immediately post injection a fluorescent angiogram develops. This is followed by a gradual decrease of fluorescence in the circulation. During this period of decrease, fluorescence at the site of the tumor becomes noticeable. Finally, fluorescence of the surrounding normal tissue starts to increase, usually causing the fluorescence of tumor and blood vessel relative to the normal tissue fluorescence to decrease. Three exceptions to this pattern are formed by:

1. Ph II (Chapter 2): Here, fluorescent monomers are practically absent but fluorescence in the blood vessels increases up to 2 h p.i. This is probably caused by hydrolysis *in vivo* that leads to the formation of monomers.
2. ZnPc incorporated into liposomes (chapter 5): Following administration and like Ph II, fluorescence in the blood vessels increases until 2 h post injection.

[1]Old notation for a commercial preparation, consisting of a mixture of AlPcSn (n = 1-4) with an average degree of sulphonation of 3, which in the literature has been referred to as aluminium phthalocyanine tetrasulphonate.

Twenty four hours after administration fluorescence in the tumor but also in the circulation can be observed. The low levels of fluorescence of the photosensitizer in the normal tissue probably contribute to this degree of selectivity. The dye effectively localizes in the tumor but also becomes strongly associated with serum proteins. 3. ALA (Chapter 7): This precursor of protoporphyrin (PpIX) does not fluoresce and therefore no fluorescence angiogram can be observed upon systemic administration. The fluorescent hydrophobic PpIX becomes only observable at sites where it is being synthesized.

Tumor tissue localization

Photosensitizers should have a certain degree of selectivity towards tumor tissue and therefore should not (or hardly) be retained in normal tissue. In general two factors seem to determine the practical use of photosensitizers for tumor localization.

1. The monomeric form of a photosensitizer has the highest fluorescence yield. Therefore, a photosensitizer should preferably be active in its monomeric form. Fluorescence localization can than be expected to correlate with the site of action of PDT. Because of the opacity that varies between different tissues and because of fluorescence quenching, it will be difficult to asses the actual dye concentration using fluorescence. HPD and Ph II (Photofrin®) are photodynamically active in their dimeric and oligomeric components. Although these dyes are used for fluorescence localization there can probably be no correlation between the therapeutic effect and the presence of fluorescence. HPD fluorescence exists due to its contamination with monomers and fluorescence of Photofrin® is probably caused by conversion or degradation of the dimeric or oligomeric molecule *in vivo*. Theoretically these two dyes should therefore be regarded unsuitable for a combination of localization and treatment.
2. The second factor to consider is that dyes like Up I (Chapter 2) which readily dissolve in water are also "washed" away more easily, reducing their "bioavailability". This implies that the more hydrophillic dyes, which are easy to dissolve and administer, will have to be taken up quickly as they will be available to tissue for only a short period of time. The interval during which localization can take place is therefore limited. Consequently, due to the short exposure, possible side effects could also be expected to be limited.

Except for $AlPcS_2$ and $AlPcS_4$ (Chapter 3) after administration of the dye, fluorescence maxima in the circulation always exceeded the fluorescence maxima in the tumor area. Aggregation of the lower sulphonated dyes upon administration and differences in fluorescence yield between plasma bound and

interstitially bound $AlPcS_n$ are expected to play an important role in these observations. Especially the presence of an extra axial ligand can be of great influence on aggregation. *In vivo* the relation between lipophillicity of the dye and tumor uptake is the inverse of what is found *in vitro*. The extracellular matrix and tumor stroma apparently are important factors in retention of the higher sulphonated phthalocyanines *in vivo*.

The highest tumor tissue to normal tissue ratio (ratio of 4) has been observed with $ALPcS_2$ and $AlPcS_4$. When muscle tissue would have been used as the reference normal tissue these ratios could have been much higher. Muscle tissue hardly retains any photosensitizer which makes it an unsuitable reference to express tumor to normal tissue ratios. In cases where tumors after HPD administration had equal or even lower levels of fluorescence than the subcutis of the skin fold chamber, the tumor fluorescence exceeded that of the background when the tumor was placed on the muscle tissue. (Chapter 2).

The distribution of fluorescence for Up I, AR, HPD, Ph II and AlPhcTs was only rated visually, therefore no tumor to normal tissue ratios could be calculated. These ratios of the remaining 8 photosensitizers can be ranked from high to low as: $AlPcS_2$ > $AlPcS_4$ > $ZnPcS_4$ > BCA > ZnPc-Lip > $AlPcS_1$ > $ZnPcS_1$ > $ZnPcS_2$. In this ranking order HPD en Ph II would probably be placed between $ZnPcS_1$ and $ZnPcS_2$.

Studying the photosensitizing properties of BCA, the concept of using fluorescence kinetics to determine a therapeutical window into which localization and of treatment can take place has been brought into practice in chapter 6. No fluorescence localization could be observed 24 h p.i. and treatment at this interval appeared to be unsuccessful. From the fluorescence pharmacokinetics of the dye a new treatment interval at 1 h p.i. was chosen. At this interval tumor fluorescence was still high, whereas fluorescence in the circulation was already decreasing.

Photodynamic properties

As was stated above an ideal photosensitizer should combine fluorescent and photodynamic properties. Both Up I and AR (Chapter 2) are photodynamically inactive and therefore do not qualify as photosensitizers for PDT. However their tumor localization, especially of dyes with qualities like AR but less toxic, might be utilized for screening purposes. The absence of photodynamic activity could then be regarded favourable. All other dyes discussed here demonstrated photodynamic activity in various degrees.

Comparing these different dyes seems to be almost impossible. Each dye has its own optimum drug dose, its optimum interval between administration and treatment and its optimum excitation wavelength. This thesis shows that each of these three factors can vary between the different photosensitizers.

Activating wavelength

All phthalocyanines and also BCA differ from porphyrins with respect to the maximum wavelength (675 and 760 nm respectively) at which the dye can be activated. The therapeutical benefits of this property, i.e. deeper tissue penetration of the activating light, could not be established in the *in vivo* model which is only 0.5 mm thick. Their photosensitizing properties in terms of fluorescence localization and their ability to cause tumor necrosis however have been demonstrated in chapters 3-6 of this thesis.

Cellular effects

The direct cytotoxic effect of PDT on tumor cells was estimated by histology and by retransplantation, where the treated area was removed from the chamber and implanted subcutaneously in the flank of the same animal. Direct effects on individual tumor cells were never sufficient to prevent tumor regrowth. Two hours post therapy, vital tumor cells were always observed in histology and after retransplantation, tumor regrowth always occurred. This regrowth was only prevented when retransplantation took place at the end of the observation period, 7 days after the treatment light dose. When at the end of this observation period both the tumor and the normal tissue had not become necrotic, tumor regrowth again was observed.

Vascular effects

The mechanism of photodynamic damage to the vasculature that was seen with the photosensitizers mentioned in this thesis, was similar to the photodynamic damage that was observed when HPD or Ph II were used.

Tumor vessel damage seems to occur earlier during treatment than the damage to normal tissue vessels. Part of the difference between the vascular damage score of normal tissue and of tumor tissue might be explained by the fact that the normal tissue score also included damage to larger venules and arteries which were absent in the tumors. These "larger" normal vessels usually show more resistance to PDT induced damage than capillaries. Differences were found with respect to the occurrence of thrombi and the degree of constriction of the larger vessels (chapter 4-6).

Vascular effects were also observed when PpIX was activated after systemic ALA administration (chapter 7). These vascular effects could originate from indirect (inflammatory) effects as a result of treatment. However, they occur within minutes after the start of the irradiation and therefore indicate that possibly also vascular targets exist for this form of treatment. It should be noted that so far in patients ALA is used only topically. The experimental data presented here are based on experiments with systemically administered ALA.

Following treatment and using a specific drug dose, interval to treatment and light dose, tumor necrosis was achieved using ZnPc in liposomes, BCA, $ALPcS_2$ and both $MPcS_1$. Tumor necrosis without in situ recurrence was only observed when also the surrounding normal tissue of the chamber had become necrotic.

Even at the low dose of 0.14 mg/kg, liposome bound ZnPc was effective. This demonstrates that using a delivery system like liposomes allows for a much more efficient administration of a lipophillic photosensitizer. So far it is not known what portion of an administered dose is actually involved in photosensitizing the tissue.

When all $MPcS_n$ are considered, it appears that damage (to the vasculature) increases with increasing degree of lipophilicity (Chapter 4). This is in agreement with what has been found *in vitro* for tumor cells. On the other hand fluorescence localization in the tumor appears to decreases with increasing degree of lipophillicity (Chapter 3). It might therefore be possible to use $MPcS_n$ that have low photodynamic activity for tumor localizing purposes. Only $AlPcS_2$ seems to combine favourable properties for fluorescence localization and photodynamic therapy.

Vascular stasis resulting from PDT is perhaps not the effect that was intended for a therapy based on tumor localization of the photosensitizer. However, the hypoxia that results from the vascular effects can result in additional necrosis of tumor cells unaffected by the primary treatment. Vascular damage originating from PDT should therefore not be regarded as undesired side effects, but should be studied further in order to make maximum use of it. The skin fold chamber model utilized in the previous chapters proved to be ideally suited for studying these vascular effects resulting from therapy as well as fluorescence pharmacokinetics.

Fluorescence pharmacokinetics can provide us with important information about the distribution of the dye over the tissues after administration. This can help to determine the therapeutical window during which localization and therapy can take place. It also appears that for many photosensitizers there is an effective combination of drug dose, light dose, and interval.

References

Aizawa, K., H. Kato, J. Ono, C. Konaka, N. Kawate, H. Yoneyama, M. Otawa, H. Shinohara, M. Saito, H. Takahashi, H. Nakemera, T. Yamada, H. Sakai, and Y. Hayata (1984) A new diagnosis system for malignant tumors using hematoporphyrin derivative, laser photoradiation and a spectroscope. In Porphyrin localization and treatment of tumors. D.R. Doiron and C.J. Gomer, eds., pp. 227-238, Alan Liss, New York.

Ali, H., R. Langlois, R. Wagner, N. Brasseur, B. Paquette, and J.E. van Lier (1988) Biological activities of Phthalocyanines-X synthesis and analyses of sulphonated phthalocyanines. *Photochem. Photobiol.* 47, 713-717.

Anderson-Engels, S., J. Ankerst, J. Johansson, K. Svanberg, and S. Svanberg (1989) Tumor marking properties of different haematoporphyrins and tetrasulphonated phthalocyanine - a comparison. *Lasers Med. Sci.* 4, 115-123.

Andersson, P.S., S. Montan, T. Persson, S. Svanberg, S. Tapper, and S.E. Karlsson (1987a) Fluorescence endoscopy instrumentation for improved tissue characterization. *Med. Phys.* 14, 633-636.

Andersson, P.S., S. Montan, K. Svanberg, and S. Svanberg (1987b) Multispectral system for medical fluorescence imaging. *IEEE J. Quant. Electr.* QE-23, 1798-1805.

Bachowski, G.J., P.J. Pintar, and A.W. Girotti (1991) Photosensitized lipid peroxydation and enzyme inactivation by membrane bound merocyanine 540: Reaction mechanisms in the absence of ascorbate. *Photochem. Photobiol.* 53, 481-491.

Baumgartner, R., H. Fisslinger, D. Jocham, H. Lenz, L. Ruprecht, H. Stepp, and E. Unsöld (1987) A fluorescence imaging device for endoscopic detection of early stage cancer: Instrumental and experimental studies. *Photochem. Photobiol.* 46, 759-763.

Ben-Hur, E., E. Heldman, S.W. Crane, and I. Rosenthal (1988) Release of clotting factors from photosensitized endothelial cells: A possible trigger for blood vessel occlusion by photodynamic therapy. *FEBS Letters.* 236, 105-108.

Ben-Hur, E., A. Orenstein, A. Livine, and I. Rosenthal (1990) Photosensitized oxidation of human red blood cells: Cation effects on volume changes and relevance to blood vessel occlusion. *Lasers Life Sci.* 3, 255-262.

Ben-Hur, E. and I. Rosenthal (1985) The Phthalocyanines: A new class of mammalian cells photosensitizers with a potential for cancer phototherapy. *Int. J. Radiat. Biol.* 47, 145-147.

Ben-Hur, E. and I. Rosenthal (1986a) Photosensitization of chinese hamster cells by water-soluble phthalocyanines. *Photochem. Photobiol.* 43, 615-619.

Ben-Hur, E. and I. Rosenthal (1986b) Action spectrum (600-700 nm) for chloraluminum phthalocyanine induced photoxicity in chinese hamster cells. *Lasers Life Sci.* 1, 79-86.

Benson, R.C., G.M. Farrow, J.H. Kinsey, D.A. Cortese, H. Zincke, and D.C. Utz (1982) Detection and localization of in situ carcinoma of the bladder with hematoporphyrin derivative. *Mayo Clin. Proc.* 57, 548-555.

Benson, R.C., J.H. Kinsey, D.A. Cortese, G.M. Farrow, and D.C: Utz (1983) Treatment of transitional cell carcinoma of the bladder with hematoporphyrin derivative phototherapy. *J. Urol.* **130**, 1090-1095.

Berenbaum, M.C., S.L Akande, F.H. Armstrong, P.K. Bentley, R. Bonnet, R.D. White, and K.C. Lowe (1990) Perflurochemicals and photodynamic therapy in mice. *Adv. Exp. Med. Biol.* **277**, 277-282.

Berg, K., J.C. Bommer, and J. Moan (1989) Evaluation of sulphonated aluminum phthalocyanines for use in photochemotherapy. Cellular uptake studies. *Cancer Lett.* **44**, 7-15.

Boegheim, J.P., H. Scholte, T.M.A.R. Dubbelman, E. Beems, A.K. Raap, and J. van Steveninck (1987) Photodynamic effects of hematoporphyrin derivative on enzyme activities of murine L929 fibroblasts. *J. Photochem. Photobiol. B:Biology* 1, 61-73.

Bonnet, R. and M.C. Berenbaum (1989) Porphyrins as photosensitizers. In Photosensitizing compounds: their chemistry, biology and clinical use. G. Bock and S. Harnett, eds., pp. 40-59, John Wiley and Sons, Chichester (Ciba Foundation Symposium 146).

Bown, S.G., C.J. Tralau, P.D. Coleridge-Smith, D. Akdemir, and T.J. Wieman (1986) Photodynamic therapy with porphyrin and phthalocyanine sensitization: Quantitative studies in normal rat liver. *Br. J. Cancer* **54**, 43-52.

Brasseur, N., H. Ali, R. Langlois, R. Wagner, J. Rousseau, and J.E. van Lier (1987) Biological activities of Phthalocyanines-V. Photodynamic therapy of EMT-6 mammary tumors in mice with sulphonated phthalocyanines. *Photochem. Photobiol.* **45**, 581-586.

Brasseur, N., H. Ali, R. Langlois, and J.E. van Lier (1988) Biological activities of phthalocyanines-IX. Photosensitization of V-79 chinese hamster calls and EMT-6 mouse mammary tumor by selectively sulphonated zinc phthalocyanines. *Photochem. Photobiol.* **47**, 705-711.

Brodbeck, K., A.E. Profio, T. Frewin, and O.J. Balchum (1987) A system for real time fluorescence imaging in colour for tumor diagnosis. *Med. Phys.* 14, 637-639.

Bugelski, P., C. Porter, and T.J. Dougherty (1981) Autoradiographic distribution of haematoporphyrin derivative in normal and tumor tissue of the mouse. *Cancer Res.* 41, 4606-4612.

Candide, C., J. Reyftmann, R. Santus, J.C. Maziere, P. Morliere, and S. Goldstein (1988) Modification of epsilon-amino groups of lysines, cholesterol oxidation and oxidized lipid-apoprotein cross-link formation by porphyrin-photosensitized oxidation of human low density lipoproteins. *Photochem. Photobiol.* 48, 137-146.

Carpenter, R.S., H.G. Neel, R.J. Ryan, and D.R. Sanderson (1977) Tumor fluorescence with hematoporphyrin derivative. *Ann. Otorhinolaryngol.* **86**, 661-666.

Chan, W., J. Marshall, R. Svensen, J. Bedwell, and I.R. Hart (1990) Effect of sulphonation on the cell and tissue distribution of the photosensitizer aluminum phthalocynaine. *Cancer Res.* **50**, 4533-4538.

Cortese, D.A. and J.H. Kinsey (1982) Endoscopic management of lung cancer with hematoporphyrin derivative phototherapy. *Mayo Clin. Proc.* 57, 543-547.

Dougherty, T.J. (1982) Variability in hematoporphyrin derivative preparations. *Cancer Res.* **42**, 1188.

Dougherty, T.J. (1987) Photosensitizers: Therapy and detection of malignant tumors (yearly review). *Photochem. Photobiol.* **45**, 879-889.

Dougherty, T.J., J.E. Kaufman, A. Goldfarb, K.R. Weishaupt, D. Boyle, and A. Mittleman (1978) Photoradiation therapy for the treatment of malignant tumors. *Cancer Res.* **38**, 2628-2635.

Dougherty, T.J., W.R. Potter, and K.R. Weishaupt (1984) The structure of the active component of hematoporphyrin derivative. In Porphyrin localization and treatment of tumors. D.R. Doiron and C.J. Gomer, eds., pp. 301-314, Alan R. Riss, New York.

Eckhauser, M.L., J. Persky, A. Bonaminio, J. Crespin, A.L. Imbembo, and S. Holt (1987) Biodistribution of the photosensitizer dihematoporphyrin ether. *Lasers Med. Sci.* **2**, 101-105.

El-Far, M.A. and N.R. Pimstone (1986) Selective in vivo tumor localization of uroporphyrin isomer I in mouse mammary carcinoma: Superiority over other porphyrins in a comparative study. *Cancer Res.* **46**, 4390-4394.

Evensen, J.F., K.K. Galdal, and E. Nilsen (1983) LDL-induced cytotoxicity and its inhibition by anti-oxidant treatment in cultured endothelial cells and fibroblasts. *Atherosclerosis* **49**, 23-30.

Fingar, V.H. and B.W. Henderson (1987) Drug and light dose dependence of photodynamic therapy: A study of tumor and normal tissue response. *Photochem. Photobiol.* **46**, 837-841.

Fingar, V.H., T.S. Mang, and B.W. Henderson (1988) Modification of photodynamic therapy-induced hypoxia by fluosol-DA (20%) and carbogen breathing in mice. *Cancer Res.* **48**, 3350-3354.

Fingar, V.H., T.J. Wieman, S.A. Wiehle, and P. Cerrito (1992) The role of microvascular damage in photodynamic therapy: The effect of treatment on vessel constriction, permeability and leucocyte adhesion. *Cancer Res.* **52**, 4914-4921.

Foote, C.S. (1990) Chemical mechanism of photodynamic action. *Proc. SPIE Institute "Advanced Optical Technologies on Photodynamic Therapy"* **6**, 115-126.

Forbes, I.J., P.A. Cowled, A.S.Y. Leong, A.D. Ward, R.B. Black, A.J. Blake, and F.J. Jacka (1980) Phototherapy of humane tumours using hematoporphyrin derivative. *Med. J. Aus.* **2**, 489-493.

Foster, T.H., R.S. Murant, R.B. Bryant, R.S: Knox, S.L. Gibson, and R. Hilf (1991) Oxygen consumption and diffusion effect in photodynamic therapy. *Radiat. Res.* **126**, 296-303.

Franken, N.A.P., G.F.J.M. Vrensen, J.L. van Delft, D. de Wolff-Rouendaal, T.M.A.R. Dubbelman, J.A. Oosterhuis, W.M. Star, and J.P.A. Marijnissen (1988) Early morphological changes induced by photodynamic therapy in amelanotic Greene melanoma implanted in the anterior eye chamber of rabbits. *Lasers Med. Sci.* **3**, 27-34.

Gijsbers, G.H.M., D. Breederveld, M.J.C. van Gemert, T.A. Boon, J. Langelaar, and R.P.H. Rettschnick (1986) In vivo fluorescence excitation and emission spectra of hematoporphyrin derivative. *Lasers Life Sci.* 29-48.

Gluckman, J.L. and M.C. Wiessler (1986) The role of photodynamic therapy in the management of early cancers of the upper aerodigestive tract. *Lasers Med. Sci.* **1**, 217-219.

Goff, B.A., R. Bachor, N. Kollias, and T. Hasan (1992) Effects of photodynamic therapy with topical application of 5-aminolevulinic acid on normal skin of hairless guinea pigs. *J. Photochem. Photobiol. B:Biology* **15**, 239-251.

Goldstein, J.L., R.G.W. Anderson, and M.S. Brown (1979) Coated pits, coated vesicles and receptor-mediated endocytosis. *Nature* **279**, 679-685.

Gomer, C.J. (1991) Preclinical examination of first and second generation photosensitizers used in photodynamic therapy. *Photochem. Photobiol.* **54**, 1093-1107.

Gomer, C.J. and T.J. Dougherty (1979) Determination of [3H]- and [14C] hematoporphyrin derivative distribution on malignant and normal tissue. *Cancer Res.* **39**, 146-151.

Hayata, Y., H. Kato, R. Amemiya, and J. Ono (1984a) Indications for photoradiation therapy in early stage lung cancer on the basis of post-PRT histologic findings. In Porphyrin localization and treatment of tumors. D.R. Doiron and C.J. Gomer, eds., pp. 747-758, Alan Liss, New York.

Hayata, Y., H. Kato, C. Konaka, R. Amemiya, J. Ono, Y. Ogawa, K. Kinoshita, H. Sakai, and H. Takahahi (1984b) Photoradiation therapy with hematoporphyrin derivative in early and stage I lung cancer. *Chest* **86**, 169-177.

Hayata, Y., H. Kato, C. Konaka, J. Ono, M. Saito, H. Takahashi, and T. Tomono (1984c) Photoradiation in early stage cancer cases of the lung, oesophagus and stomach. In Porphyrins in tumor phototherapy. A. Andreoni and R. Cubeddu, eds., pp. 405-412, Plenum Press, New York.

Henderson, B.W. and D.A. Bellnier (1989) Tissue localization of photosensitizers and the mechanism of photodynamic tissue destruction. In Photosensitizing compounds: their chemistry, biology and clinical use. G. Bock and S. Harnett, eds., pp. 112-130, John Wiley and Sons, Chichester (Ciba foundation symposium 146).

Henderson, B.W. and T.J. Dougherty (1992) How does photodynamic therapy work? *Photochem. Photobiol.* **55**, 145-157.

Henderson, B.W. and V.H. Fingar (1987) Relationship of tumor hypoxia and response to photodynamic treatment in an experimental mouse tumor. *Cancer Res.* **47**, 3110-3114.

Henderson, B.W., A.B. Sumlin, B.L. Owczarczak, and T.J. Dougherty (1991) Bacteriochlorophyll-a as photosensitizer for photodynamic treatment of transplantable murine tumors. *J. Photochem. Photobiol. B:Biology* **10**, 303-313.

Henderson, B.W., S.M. Waldow, T.S. Mang, W.R. Potter, P.B. Malone, and T.J. Dougherty (1985) Tumor destruction and kinetics of tumor cell death in two experimental mouse tumors following photodynamic therapy. *Cancer Res.* **45**, 572-576.

Hilf, R., R.S. Murant, U. Narayanan, and S.L. Gibson (1986) Relationship of mitochondrial function and cellular adenosine triphosphate levels to hematoporphyrin derivative induced photosensitization in R3230 AC mammary tumors. *Cancer Res.* **46**, 211-217.

Jori, G. (1989) In vivo transport and pharmacokinetic behaviour of tumour photosensitizers. In Photosensitizing compounds: their chemistry, biology and clinical use. G. Bock and S. Harnett, eds., pp. 78-86, John Wiley and Sons, Chichester (Ciba Foundation Symposium 146).

Jori, G. (1992) Low density lipoproteins-liposome delivery systems for tumor photosensitizers in vivo. In Photodynamic therapy: Basic principles and clinical applications. B.W. Henderson and T.J. Dougherty, eds., pp. 173-186, Marcel Dekker, Inc., New York.

Jori, G., L. Tomio, E. Reddi, E. Rossi, L. Corti, P.L. Zorat, and F. Calzavara (1983) Preferential delivery of liposome-incorporated porphyrins to neoplastic cells in tumor-bearing rats. *Br. J. Cancer* 48, 307-309.

Kennedy, J.C. and R.H. Pottier (1992) Endogenous protoporphyrin IX, a clinically useful photosensitizer for photodynamic therapy. *J. Photochem. Photobiol. B:Biology* 14, 275-292.

Kerdel, A.F., N.A. Soter, and H.W. Lim (1987) In vivo mediator release and degranulation of mast cells in hematoporphyrin derivative-induced phototoxicity in mice. *J. Invest. Dermatol.* 88, 277-280.

Kessel, D. (1982) Components of hematoporphyrin derivatives and their tumor-localizing capacity. *Cancer Res.* 42, 1703-1706.

Kessel, D. (1986a) Proposed structure of the tumor localizing fraction of HPD. *Photochem. Photobiol.* 44, 193-196.

Kessel, D. (1986b) In vivo fluorescence of tumors after treatment with derivatives of hematoporphyrin. *Photochem. Photobiol.* 44, 107-108.

Kessel, D. (1990) HPD: Structure and determinants of localisation. In Photodynamic therapy of neoplastic disease, Volume II. D. Kessel, ed., pp. 1-15, CRC Press, Boca Ratow, Florida.

Kessel, D. and T. Chou (1983) Tumor localizing components of the porphyrin preparation hematoporphyrin derivative. *Cancer Res.* 43, 1994-1999.

Kinsey, J.H. and D.A. Cortese (1980) Endoscopic system for simultaneous visual examination and electronic detection of fluorescence. *Rev. Sci. Instrum.* 51, 1403-1406.

Lam, S., B. Palcic, D. McLean, J. Hung, M. Korbelik, and A.E. Profio (1990) Detection of early lung cancer using low dose Photofrin II. *Chest* 97, 333-337.

Leibovici, L., N.I.L.I. Schoenfeld, H.A. Yehoshua, R. Mamet, E. Rakowski, A. Shindel, and A. Atsmon (1988) Activity of porphobilinogen deaminase in peripheral blood mononuclear cells of patients with metastatic cancer. *Cancer* 62, 2297-2300.

Lillie, R.D. (1977) *H.J. Conn's biological stains*, The Williams & Wilkins Company, Baltimore.

Lin, C.W., D.A. Bellnier, G.R. Prout, W.S. Andrus, and R. Prescott (1984) Cystoscopic fluorescence detector for photodetection of bladder carcinoma with hematoporphyrin derivative. *J. Urol.* 131, 587-590.

Lipson, R.L., E.J. Baldes, and A.M Olsen (1961) The use of a derivative of hematoporphyrin in tumor detection. *J. Natl. Cancer Inst.* 26, 1-11.

MacRobert, A.J., S.G. Bown, and D. Phillips (1989) What are the ideal photoproperties for a sensitizer? In Photosensitizing Compounds: their Chemistry, Biology and Clinical Use. G. Bock and S. Harnett, eds., pp. 4-16, John Wiley and Sons, Chichester (Ciba foundation symposium 146).

Malik, Z. and H. Lugaci (1987) Destruction of erytroleukaemic cells by photoactivation of endogenous porphyrins. *Br. J. Cancer* **56**, 589-595.

Manyak, M.J., A. Russo, P.D. Smith, and E. Glatstein (1988) Photodynamic Therapy. *J. Clin. Oncol.* **6**, 380-391.

Marijnissen, J.P.A., A.A.C Versteeg, W.M. Star, and W. van Putten (1992) Tumor and normal tissue response to interstitial photodynamic therapy of the rat R-1 rhabdomyosarcoma. *Int. J. Radiation Oncology Biol. Phys.* **22**, 963-972.

Maziere, J.C., R. Santus, P. Morliere, J. Reyftmann, C. Candide, L. Mora, S. Salmon, C. Maziere, S. Gatt, and L. Dubertret (1990) Cellular uptake and photosensitizing properties of anticancer porphyrins in cell membranes and low and high density lipoproteins. *J. Photochem. Photobiol. B:Biology* **6**, 61-68.

McCaughan, J.S., T.E.N. Williams, and B.H. Bethel (1985) Palliation of esophageal malignancy with photodynamic therapy. *Ann. Thorac. Surg.* **40**, 113-120.

Meyer-Betz, F. (1913) Therapeutische versuche mit fluoreszierenden stoffe. *Dtsch. Arch. Klin. Med.* **112**, 475-481.

Milanesi, C., R. Biolo, E. Reddi, and G. Jori (1987) Ultrastructural studies on the mechanism of the photodynamic therapy of tumors. *Photochem. Photobiol.* **46**, 675-682.

Moan, J. (1986) Effect of bleaching of porphyrin sensitizers during photodynamic therapy. *Cancer Lett.* **33**, 45-53.

Moan, J. (1990) On the diffusion length of singlet oxygen in cells and tissues. *J. Photochem. Photobiol. B:Biology* **6**, 343-344.

Moan, J. and K. Berg (1992) Photochemotherapy of cancer: experimental research. *Photochem. Photobiol.* **55**, 931-948.

Nelson, J.S., C. Chung-Ho, and M. Berns (1986) Study of the in vivo in vitro photosensitizing capabilities of Uroporphyrin I compared to Photofrin II. *Lasers Surg. Med.* **6**, 131-136.

Omata, T. and N. Murata (1983) Preparation of chlorophyll a, chlorophyll b, and bacteriochlorophyll a by column chromatography with DEAE Sepharose Cl-6B and Sepharose Cl-6B. *Plant Cell Physiol.* **25**, 1093-1100.

Oster, G., B. Broyde, and J.S Bellin (1964) Spectral properties of chlorophyllin a. *J. Am. Chem. Soc.* **5**, 1309-1313.

Paquette, B., H. Ali, R. Langlois, and J.E. van-Lier (1988) Biological activities of phthalocyanines-VIII. Cellular distribution in V-79 Chinese hamster cells and phototoxicity of selectively sulphonated aluminum phthalocyanines. *Photochem. Photobiol.* **47**, 215-220.

Paquette, B. and J.E. van Lier (1992) Phthalocyanines and related compounds: Structure-activity relationships. In Photodynamic therapy; Basic principles and clinical applications. B.W. Henderson and T.J. Dougherty, eds., pp. 145-156, Marcel Dekker Inc, New York.

Peng, Q., J. Moan, J.M. Nesland, and C. Rimington (1990) Aluminum phthalocyanines with asymmetrical lower sulphonation and with symmetrical higher sulphonation: a comparison of localizing and photosensitizing mechanism in human LOX xenografts. *Int. J. Cancer* **46**, 972-979.

Peng, Q., J. Moan, G. Farrants, C. Danielsen, and C. Rimington (1991a) Localization of potent photosensitizers in human tumor LOX by means of laser scanning microscopy. *Cancer Lett.* **53**, 129-139.

Peng, Q., J. Moan, M. Kongshaug, J.F. Evensen, H. Anholt, and C. Rimington (1991b) Sensitizer for photodynamic therapy of cancer: A comparison of the tissue distribution of photofrin II and aluminum phthalocyanine tetrasulphonate in nude mice bearing a human malignant tumor. *Int. J. Cancer* **48**, 258-264.

Profio, A.E., O.J. Balchum, and F. Carstens (1986) Digital background subtraction for fluorescence imaging. *Med. Phys.* **13**, 717-721.

Profio, A.E., D. Doiron, O.J. Balchum, and G. Huth (1983) Fluorescence bronchoscopy for localization of carcinoma in situ. *Med. Phys.* **10**, 35-39.

Reddi, E., G. Lo Castro, R. Biolo, and G. Jori (1987) Pharmacokinetics studies with zinc(II)phthalocyanine in tumor bearing mice. *Br. J. Cancer* **56**, 597-600.

Reed, M.W.R., F.N. Miller, T.J. Wieman, M.T. Tseng, and C.G. Pietsch (1988) The effect of photodynamic therapy on the microcirculation. *J. Surg. Res.* **45**, 452-459.

Reed, M.W.R., T.J. Wieman, K.W. Doak, C.G. Pietsch, and D.A. Schuschke (1989) The microvascular effects of photodynamic therapy: evidence for a possible role of cyclooxygenase products. *Photochem. Photobiol.* **50**, 419-423.

Reinhold, H.S., B. Blachiewicz, and A.E. van den Berg-Blok (1979) Reoxygenation of tumors in "sandwich" chambers. *Eur. J. Cancer* **15**, 481-489.

Richter, A.M., E. Waterfield, A.K. Jane, B. Allison, E.D. Sternberg, D. Dolphin, and J.G. Levy (1991) Photosensitizing potency of structural analogues of benzoporphyrin derivative (BPD) in a mouse tumour model. *Br. J. Cancer* **63**, 87-93.

Roberts, W.G., M.K. Klein, M. Loomis, S. Weldy, and M.W. Berns (1991) Photodynamic therapy of spontaneous cancers in felines, canines and snakes with chloro-aluminum sulphonated phthalocyanine. *J. Natl. Cancer Inst.* **83**, 18-23.

Roberts, W.G., K.M. Smith, J.L McCullough, and M.W. Berns (1989) Skin photosensitivity and photodestruction of several potential photosensitizers. *Photochem. Photobiol.* **49**, 431-438.

Rogers, D.W., R.J. Lanzafame, J. Blackman, J.O. Naim, H.R. Herrera, and J.R. Hinshaw (1990) Methods for the endoscopic photographic and visual detection of helium cadmium laser-induced fluorescence of Photofrin II. *Lasers Surg. Med.* **10**, 45-51.

Rosenthal, I. (1991) Phthalocyanines as photodynamic sensitizers. *Photochem. Photobiol.* **53**, 859-870.

Rousseau, J., R. Langlois, H. Ali, and J.E. van Lier (1990) Biological activities of phthalocyanine-XII. Synthesis, tumor uptake and biodistribution of 14C labelled di- and trisulphonated gallium phthalocyanine in C3H mice. *Photochem. Photobiol.* **6**, 121-132.

Schuitmaker, J.J., G.F.J.M. Frensen, J.L. van Delft, D. de Wolff-Rouendaal, T.M.A.R. Dubbelman, and A. de Wolf (1991) Morphologic effects of bacteriochlorin a and light in vivo on intraocular melanoma. *Invest. Ophthalmol. Vis. Sci.* **32**, 2683-2688.

Schuitmaker, J.J., J.A. van Best, J.L. van Delft, T.M.A.R. Dubbelman, J.A. Oosterhuis, and D. de Wolff-Rouendaal (1990) Bacteriochlorin a, a new photosensitizer in photodynamic therapy. In vivo results. *Invest. Ophthalmol. Vis. Sci.* **31**, 1444-1450.

Schuitmaker, J.J., E. van Leengoed, N. van der Veen, T.M.A.R. Dubbelman, and W.M. Star (1992) Laser-induced in vivo fluorescence of bacteriochlorin a: preliminary results. *Lasers Med. Sci.* in press,

Selman, S.H., M. Kreimer-Birnbaum, J.E. Klaunig, P.J. Goldblatt, R.W. Keck, and S.L Britton (1984) Blood low in transplantable bladder tumors treated with hematoporphyrin derivative and light. *Cancer Res.* **44**, 1924-1927.

Smith, A. (1987) Mechanisms of toxicity of photoactivated artificial porphyrins. *Ann. N. Y. Acad. Sci.* **514**, 309-322.

Spikes, J.D. (1986) Phthalocyanines as photosensitizers in biological systems and for the photodynamic therapy of tumors. *Photochem. Photobiol.* **43**, 691-699.

Spikes, J.D. and G. Jori (1987) Photodynamic therapy of tumours and other diseases. *Lasers Med. Sci.* **2**, 3-15.

Star, W.M., J.P.A. Marijnissen, A.E. van den Berg-Blok, A.A.C Versteeg, and H.S. Reinhold (1985) In vivo observation of the effects of HPD-photoradiation on the microcirculation of rat mammary tumor and normal tissue growing in transparent chambers. In Photodynamic therapy of tumors and other diseases. G. Jori and C. Perria, eds., pp. 239-242, libreria Progretto, Padova.

Star, W.M., J.P.A. Marijnissen, A.E. van den Berg-Blok, A.A.C Versteeg, N.A.P. Franken, and H.S. Reinhold (1986) Destruction of rat mammary tumor and normal tissue microcirculation by hematoporphyrin derivative photoradiation observed in vivo in sandwich observation chambers. *Cancer Res.* **46**, 2532-2540.

Star, W.M., A.A.C Versteeg, W. van Putten, and J.P.A. Marijnissen (1990) Wavelength dependence of hematoporphyrin derivative photodynamic treatment effects on rat ears. *Photochem. Photobiol.* **52**, 547-554.

Star, W.M., B.C. Wilson, and M.S. Patterson (1992) Light delivery and optical dosimetry in photodynamic therapy of solid tumors. In Photodynamic Therapy. B.W. Henderson and T.J. Dougherty, eds., pp. 335-368, Marcel Dekker, New York.

Svanberg, K., E. Kjellen, J. Ankerst, S. Montan, E. Sjoholm, and S. Svanberg (1986) Fluorescence studies of hematoporphyrin derivative in normal malignant rat tissue. *Cancer Res.* **46**, 3803-3808.

Tangelder, G.J., D.W. Slaaf, and R.S. Reneman (1982) Fluorescent labelling of blood platelets in vivo. *Thromb. Res,* **28**, 803-820.

Tralau, C.J., A.J. MacRobert, P.D. Coleridge-Smith, H. Barr, and S.G. Bown (1987) Photodynamic therapy with phthalocyanine sensitization: Quantitative studies in a transplantable rat fibrosarcoma. *Br. J. Cancer* **55**, 389-395.

Tralau, C.J., A.r. Young, N.P.J. Walker, D.I. Vernon, A.J. MacRobert, S.B. Brown, and S.G. Bown (1989) Mouse skin photosensitivity with dihaematoporphyrin ether (DHE) and aluminum sulphonated phthalocyanine (AlSPc): A comparative study. *Photochem. Photobiol.* **49**, 305-312.

Valduga, G., E. Reddi, and G. Jori (1987) Spectroscopic studies on Zn(II)-phthalocyanine in homogeneous and microheterogeneous systems. *J. Inorg. Biochem.* **29**, 59-65.

van Hillegersberg, R., J.W.O. van den Berg, W.J. Kort, O.T. Terpstra, and J.H.P. Wilson (1992) Selective accumulation of endogenously produced porphyrins in a liver metastasis model in rats. *Gastroenterology* **103**, 647-651.

van Leengoed, E., A.A.C Versteeg, N. van der Veen, A.E. van den Berg-Blok, J.P.A. Marijnissen, and W. Star (1990) Tissue-localizing properties of some photosensitizers studied by in vivo fluorescence imaging. *J. Photochem. Photobiol. B:Biology* **6**, 111-119.

van Leengoed, H.L.L.M., N. van der Veen, A.A.C Versteeg, A.E. van den Berg-Blok, J.P.A. Marijnissen, and W. Star (1991) Tumor tissue imaging using the localizing properties and fluorescence of some phthalocyanines. *Int. J. Radiat. Biol.* **60**, 121-124.

van Leengoed, H.L.L.M., N. van der Veen, A.A.C Versteeg, R. Ouellet, W. Star, and J.E. van Lier (1993) In vivo fluorescence localization of phthalocyanines in a sandwich observation chamber model: role of central metal ion and degree of sulphonation. *Photochem. Photobiol.* in press,

van Lier, J.E. (1990) Phthalocyanines as sensitizers for PDT of cancer. In Photodynamic therapy of neoplastic disease. D. Kessel, ed., pp. 279-290, CRC press, Boston.

van Lier, J.E., N. Brasseur, B. Paquette, R. Wagner, H. Ali, R. Langlois, and J. Rousseau (1987) Phthalocyanines as sensitizers in photodynamic therapy of cancer. In Photosensitization: Molecular and Medical aspects. G. Moreno, R. Pottier and G. Truscott, eds., pp. 435-444, Springer Verlag, Berlin.

von Tappeiner, H. and A. Jesionek (1903) Therapeutische versuche mit fluoreszierenden stoffen. *Munch. Med. Wochenschr.* **50**, 2042-2051.

Ward, B.G., I.J. Forbes, P.A. Cowled, M.M: McEvoy, and L.W. Cox (1982) The treatment of vaginal recurrences of gynecological malignancy with phototherapy following hematoporphyrin derivative pretreatment. *Am. J. Obstet. Gynecol.* **142**, 357-367.

Weinstein, J.N., S. Yoshikami, P. Henkart, R. Blumenthal, and W.A. Hagins (1977) Liposome cell interaction: Transfer and intracellular release of a trapped fluorescent marker. *Science* **195**, 489-491.

Wile, A.G., J. Coffey, M.Y. Nahabedian, R. Baghdassarian, G.R. Mason, and M.W. Berns (1984) Laser photoradiation therapy of cancer: An update of experience at the University of California, Irvine. *Lasers Surg. Med.* 4, 5-12.

Zhou, C., C. Milanesi, and G. Jori (1988) An ultrastructural comparative evaluation of tumors photosensitized by porphyrins administered in aqueous solution, bound to liposomes or to lipoproteins. *Photochem. Photobiol.* **48**, 487-492.

Samenvatting

Een belangrijke taak van het kankeronderzoek is het ontwikkelen van behandelvormen die tumorspecifiek zijn. Fotodynamische therapie (PDT, afgeleid van "Photodynamic therapy") is zo'n nieuwe behandelingsvorm. Deze maakt gebruik van lichtgevoelige stoffen, fotosensitizers genaamd, die hun toxiciteit ontwikkelen als ze geactiveerd worden door licht.

Bij fotodynamische therapie wordt een lichtgevoelige (kleur)stof meestal via de bloedbaan (systemisch) toegediend. Daarnaast worden lokale toedieningswijzen onderzocht. In het geval van een systemische toediening blijft er na verloop van tijd meer van deze stof in tumor weefsel achter dan in het omgevende normale weefsel. Als na 1 of 2 dagen het tumor weefsel wordt belicht met licht van de juiste golflengte en met een voldoende fluentie tempo (mW/cm^2) en dosis (J/cm^2), leidt dit tot een cytotoxische reactie die uiteindelijk weefsel necrose tot gevolg heeft. Omdat er minder van de lichtgevoelige stof in het omgevende normale weefsel zit en omdat de lichtdosis lokaal wordt toegediend beschikt de therapie als het ware over een tweeledige selectiviteit.

Wanneer een lichtgevoelige stof wordt geactiveerd kan deze ook fluorescentie gaan vertonen. De stof gaat dan zelf licht uitzenden. Deze fluorescentie kan vervolgens worden gebruikt om de lichtgevoelige stoffen op te sporen. Gecombineerd met hun retentie in tumor weefsel, kunnen deze stoffen dus zowel worden gebruikt voor therapie als voor tumor-lokalisatie op basis van fluorescentie.

Hematoporphyrine derivaat (HPD) en Photofrin® (een commercieel preparaat dat verrijkt is in de actieve component van HPD) zijn de fotosensitizers die momenteel klinisch geëvalueerd worden. Deze lichtgevoelige stoffen voldoen echter niet aan de eisen van een ideale fotosensitizer. Zo hebben ze een lage extinctiecoëfficient in het golflengtegebied dat klinisch relevant is. Dit houdt in dat deze stoffen niet efficiënt geactiveerd kunnen worden met licht dat in staat is meer dan enkele millimeters in weefsel door te dringen. Het behandelen van grote volumina is daardoor een probleem. Daarnaast is de tumor-specificiteit van deze stoffen niet groot. Ook gezond weefsel houdt deze stoffen vast en dat geeft vooral problemen met de huid. Na toediening van HPD of Photofrin® moet men rekening houden met gevoeligheid van de huid voor licht die 4 tot 6 weken kan duren. Daarnaast zijn HPD en Photofrin® mengsels van porphyrines waarvan de onderlinge verhoudingen ten gevolge van de bereiding niet constant hoeven te zijn. Tenslotte is de fluorescerende component van HPD of Photofrin® niet dezelfde component die verantwoordelijk lijkt voor de fotodynamische activiteit. De fluorescentie hoeft daardoor niet overeen te komen met de plaats van de

fotodynamisch actieve component. Ten aanzien van al deze aspecten zouden de nieuwe (tweede generatie) fotosensitizers verbeterd moeten worden.

In dit proefschrift worden 14 fluorescerende stoffen onderzocht op hun gebruik voor tumor-lokalisatie met behulp van fluorescentie en op hun fotodynamische activiteit.

Materiaal en methode. Bij het onderzoek is gebruik gemaakt van een *in vivo* model dat bestaat uit een observatiekamertje (circa 10 mm diameter) dat in een huidplooi van een rat is geplaatst. In dit kamertje, waarin een dun laagje subcutaan weefsel zit, kan een stukje transplanteerbaar tumor weefsel geplaatst worden. Onder een microscoop kan dan, met een kleine vergroting, de circulatie in de tumor en het omgevende weefsel bestudeerd worden. Op deze wijze kan, na intraveneuze toediening van een fluorescerende stof, het verloop van de fluorescentie in vaten, tumor en omgevend weefsel worden gevolgd.

Behalve voor het onderzoek naar de fluorescentie-kinetiek is het kamertje ook geschikt om de fotodynamische activiteit van deze stoffen te onderzoeken. Met name het effect van de therapie op de vaten, in de loop van de tijd, is met dit model goed te beoordelen. Na de behandeling kan vervolgens histopathologisch onderzoek of transplantatie van de inhoud van het kamertje in de flank van het dier, uitsluitsel geven over de aanwezigheid van vitale tumor cellen in het weefsel.

Voor het fluorescentie onderzoek is een detectiesysteem gebouwd dat geschikt is om met weinig licht fluorescentie op te wekken en te detecteren. Op deze manier kan worden voorkomen dat de lichtgevoelige stof al tijdens het fluorescentie onderzoek wordt geactiveerd.

Hoofdstuk 2. In dit hoofdstuk worden de lokaliserende eigenschappen van 5 lichtgevoelige stoffen onderzocht. Drie stoffen met fotodynamische activiteit: hematoporphyrine derivaat (HPD), Photofrin II (PhII) en aluminium phthalocyanine tetrasulphonaat (AlPhcTS). Van deze drie heeft de laatste de beste tumor-lokaliserende eigenschappen. In tegenstelling tot deze fotosensitizers zijn de andere twee stoffen hydrofiel, hetgeen betekent dat ze goed in water oplossen. Zowel Acridine Rood (AR) als Uroporphyrine I (UpI) vertonen tumor-lokalisatie en verdwijnen daarbij snel uit de circulatie. UpI wordt echter nauwelijks vastgehouden in tumor weefsel en daarom is de fluorescentie van de tumor maar zeer kort waar te nemen. AR fluorescentie blijft veel langer waarneembaar maar de stof blijkt daarnaast ook giftige eigenschappen te

hebben. Vooral de resultaten met AlPhcTS, dat zowel goede tumor lokaliserende als fotodynamische eigenschappen bezit, gaven aanleiding tot verder onderzoek.

Hoofdstuk 3 en 4. In een waterige omgeving, die nodig is om stoffen intraveneus toe te dienen, hebben phthalocyanines de neiging om te aggregeren. Hierdoor worden ze fotodynamisch inactief. Om deze stoffen meer hydrofiele eigenschappen te geven kan, door middel van het aanbrengen van sulfonzuurgroepen, hun chemische structuur worden gewijzigd. De stoffen kunnen dan ook in water hun eigenschappen als fotosensitizer behouden. In hoofdstuk 3 wordt de fluorescentie farmaco-kinetiek van een zestal phthalocyanines, variërend in hun graad van sulfonering (1, 2 of 4) en centraal metaalion (Al^{3+} of Zn^{2+}), onderzocht. Het blijkt dat tumor-lokalisatie op basis van fluorescentie toeneemt als het aantal sulfonzuurgroepen ook toeneemt. Phthalocyanines met aluminium als centraal metaal ion blijken betere lokaliserende eigenschappen te hebben dan die met zink.

De fotodynamische activiteit van deze zes stoffen is beschreven in hoofdstuk 4. Wat deze eigenschap betreft blijkt dat laag gesulfoneerde phthalocyanines meer (vaat)schade veroorzaken dan hoger gesulfoneerde phthalocyanines. Ook nu hebben phthalocyanines met aluminium als centraal metaalion meer effect.

Hoofdstuk 5. Een andere manier om hydrofobe stoffen toe te dienen is ze op te lossen in de lipidenlaag van liposomen. De liposomen worden vooral opgenomen door low density lipoproteins (LDL), waarvan de opname in tumor cellen hoog is. Op deze wijze blijkt zink-phthalocyanine (ZnPc) al in een lage concentratie als fotosensitizer effectief te zijn. Daarnaast was het ook met deze lage concentratie mogelijk de tumor met behulp van fluorescentie te lokaliseren. In tegenstelling tot de andere lichtgevoelige stoffen die onderzocht werden was ook na 24 uur nog fluorescentie in de circulatie waarneembaar.

Hoofdstuk 6. Een derde manier om hydrofiele stoffen toe te dienen is door ze in een emulsie op te nemen. Deze methode is toegepast voor bacteriochlorine *a* (BCA). Deze lichtgevoelige stof heeft als gunstige eigenschap dat het absorptie maximum van deze stof bij 760 nm ligt. Ten opzichte van de andere fotosensitizers is deze golflengte hoog waardoor het theoretisch mogelijk is met het activeringslicht dieper in het weefsel door te dringen. In dit hoofdstuk worden de eigenschappen van BCA als fotosensitizer met betrekking tot fluorescentie en fotodynamische activiteit beschreven. De fluorescentie-kinetiek

is gebruikt om een geschikt tijdsinterval te vinden tussen toediening van de fotosensitizer en de behandeling met licht.

Hoofdstuk 7. In tegenstelling tot (exogene) fotosensitizers die in het lichaam gebracht moeten worden kan fotodynamische therapie ook met een endogene fotosensitizer uitgevoerd worden. Protoporphyrine IX (PpIX) is een tussenprodukt van de haem synthese dat zowel fotodynamische als fluorescerende eigenschappen bezit. Wanneer een "precursor" van haem, 5-aminolevuline zuur (ALA) in een overmaat aan (tumor) cellen wordt aangeboden, vindt er een ophoping van PpIX in de cel plaats. ALA is hydrofiel en kan daardoor gemakkelijk worden toegediend. Dit kan zowel systemisch als met een crème (lokaal) gebeuren. In dit hoofdstuk worden de voorlopige resultaten beschreven van *in vivo* onderzoek naar de fluorescentie-kinetiek van PpIX fluorescentie. Ook worden de vasculaire effecten van een therapeutische belichting onderzocht. Deze *in vivo* resultaten worden besproken in relatie tot de klinische ervaringen van lokaal ALA-PDT in ons ziekenhuis.

Hoofdstuk 8. In dit hoofdstuk worden de resultaten van het onderzoek samengevat. De lichtgevoelige stoffen worden besproken met betrekking tot hun fluorescentie farmaco-kinetiek en fotodynamische activiteit.

De fluorescentie farmaco-kinetiek kan ons belangrijke informatie geven over de verdeling van de lichtgevoelige stof over de weefsels als functie van de tijd. Op basis van deze informatie kan een raamwerk worden gedefinieerd waarbinnen diagnostiek op basis van fluorescentie en therapie plaats kan vinden.

De vaateffecten blijken nog steeds doorslaggevend te zijn bij het bepalen van het uiteindelijke succes van de therapie. Het onderzoek naar de vaateffecten blijft daardoor van groot belang. Het lijkt er op dat er voor veel fotosensitizers een effectieve combinatie bestaat van de dosis van de stof, het interval tussen toediening en behandeling en de lichtdosis.

Curriculum Vitae

12 Dec. 1956	Geboren te Roosendaal.
1970 - 1974	Mavo 4. St. Joan Berchmans Mavo, Roosendaal.
1974 - 1977	MBO (Chemisch Analist). IHBO, West Brabant, Breda.
1977 - 1980	HBO-A (Zoölogisch Analist). Ir. W. v/d Broek Instituut, Amsterdam.
1980 - 1986	WO (Biologie). Universiteit van Amsterdam. Hoofdvak: Neurobiologie. Onderzoekstage aan het Nederlands Instituut voor Hersenonderzoek (Prof. Dr. D.F. Swaab). Bijvak: Neurofysiologie. Onderzoekstage aan de vakgroep dierfysiologie van de Universiteit van Amsterdam (Prof. Dr. F.H Lopes da Silva). Bijvak; Psychologie. Cursorisch bijvak aan de Faculteit Psychologie van de Universiteit van Amsterdam.
1987 - 1992	Research medewerker verbonden aan de afdeling Klinische Fysica van de Dr. Daniël den Hoed Kliniek, Rotterdam. Vanaf 1989 tot 1993 aangesteld als onderzoeker op een project van de Nederlandse Kankerbestrijding getiteld: "Photosensitizers for tumor fluorescence and photodynamic therapy" (DDHK 89-3).
1993 -	Post-doc aanstelling aan het Roswell Park Cancer Institute, Buffalo NY, USA (Dept. of Dermatology).

List of abbreviations

ALA	5-Aminolaevulinic acid
$AlPcS_n$	Aluminum $_n$sulphonated phthalocyanine
BCA	Bacteriochlorin *a*
DPPC	Dipalmitoyl-phosphatidylcholine
HDE	Dihaematoporphyrin ether/ester
HDL	High density lipoproteins
HP	Haematoporphyrin
HPD	Haematoporphyrin derivative
i.v.	intravenous
LDL	Low density lipoproteins
$MPcS_n$	Metallo $_n$sulphonated phthalocyanine
PDT	Photodynamic therapy
Ph	Photofrin®
PhII	Photofrin II
PpIX	Protoporphyrin IX
PBS	Phosphate buffered saline
Pc	Phthalocyanine
p.i.	post injection
RH	Rhabdomyosarcome
RMA	Mammary carcinoma
UpI	Uroporphyrine I
ZnPc	Zinc phthalocyanine